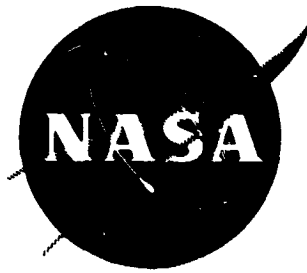


N O T I C E

THIS DOCUMENT HAS BEEN REPRODUCED FROM
MICROFICHE. ALTHOUGH IT IS RECOGNIZED THAT
CERTAIN PORTIONS ARE ILLEGIBLE, IT IS BEING RELEASED
IN THE INTEREST OF MAKING AVAILABLE AS MUCH
INFORMATION AS POSSIBLE



Single-Stage Experimental Evaluation of Boundary Layer Blowing Techniques for High Lift Stator Blades

IV - Data and Performance of Double-Slotted 0.75 Hub Diffusion Factor Stator

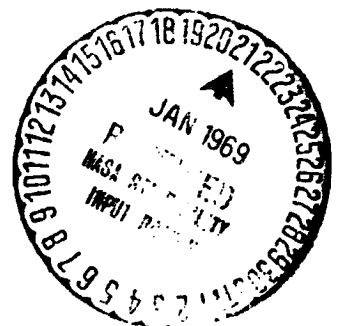
Prepared for
NATIONAL AERONAUTICS AND SPACE ADMINISTRATION

Contract NAS3-7619

FACILITY FORM 602

ND9-74856
(ACCESSION NUMBER) (THRU)
130
(PAGES) (CODE)
NPSP-001-54567
(NASA CR OR TMX OR AD NUMBER) (CATEGORY)

Allison Division • General Motors
Indianapolis, Indiana



NOTICE

This report was prepared as an account of Government sponsored work. Neither the United States, nor the National Aeronautics and Space Administration (NASA), nor any person acting on behalf of NASA:

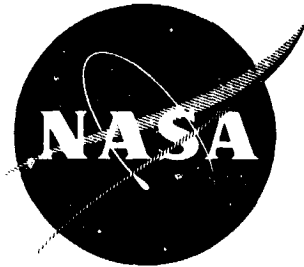
- A.) Makes any warranty or representation, expressed or implied, with respect to the accuracy, completeness, or usefulness of the information contained in this report, or that the use of any information, apparatus, method, or process disclosed in this report may not infringe privately owned rights; or
- B.) Assumes any liabilities with respect to the use of, or for damages resulting from the use of any information, apparatus, method or process disclosed in this report.

As used above, "person acting on behalf of NASA" includes any employee or contractor of NASA, or employee of such contractor, to the extent that such employee or contractor of NASA, or employee of such contractor prepares, disseminates, or provides access to, any information pursuant to his employment or contract with NASA, or his employment with such contractor.

Requests for copies of this report should be referred to

National Aeronautics and Space Administration
Office of Scientific and Technical Information
Attention: AFSS-A
Washington, D.C. 20546

NASA CR-54567
AUGUST 1968
Allison EDR-5861



**Single-Stage Experimental Evaluation of
Boundary Layer Blowing Techniques
for High Lift Stator Blades**

**IV - Data and Performance of Double-Slotted
0.75 Hub Diffusion Factor Stator**

by

R. H. Carmody and G. Seren

Prepared for

NATIONAL AERONAUTICS AND SPACE ADMINISTRATION

Contract NAS3-7619

Technical Management
NASA-Lewis Research Center
Cleveland, Ohio

Lewis Project Manager: William L. Beede
Lewis Research Advisor: L. Joseph Herrig

Allison Division • General Motors

Indianapolis, Indiana

PRECEDING PAGE BLANK NOT FILMED.

ABSTRACT

The test described in this report is part of an overall program to establish experimentally the extent to which it is feasible to increase compressor stator loading and stall-free flow margin by employing suction surface boundary layer blowing techniques. A secondary objective was to obtain blade element data for design use.

In this test, overall and blade element performance of a row of 0.75 hub diffusion factor double slotted stators with self-energized blowing boundary layer control was measured. In addition the vane static pressure distribution was obtained at three radial locations. Overall and blade element performance was also obtained for the rotor and compared to data previously obtained for this rotor without stator vanes. Preliminary discussion of test results and correlations of data are presented.

PRECEDING PAGE BLANK NOT FILMED.

TABLE OF CONTENTS

<u>Title</u>	<u>Page</u>
Summary	1
Introduction	3
Symbols	4
Apparatus and Procedures	6
Test Facility	6
Compressor Test Rig	6
Blading	6
Instrumentation	7
Determination of Annulus Wall Bleed Flow for Stator Vane Tests	8
Hysteresis Test with Slotted 0.75 Hub Diffusion Factor Stator . .	9
Overall and Blade Element Performance Data	9
Data Reduction	10
Presentation of Results	12
Overall Performance of Flow Generation Rotor and Stage	12
Blade Element Performance	12
Discussion of Results	14
Overall Performance	14
Flow Generation Rotor	14
Double-Slotted Stator Stage	15
Annulus Wall Bleed for Stator Test	16
Hysteresis and Rotating Stall Results—Slotted Stator Stage .	16
Blade Element Performance	17
Rotor	17
Stator	18
Stator Static Pressure Distributions	19
Stator Slot Blowing Flow	20
Concluding Remarks	21
References	22
Appendix: Performance Equations	23

LIST OF ILLUSTRATIONS

<u>Figure</u>	<u>Title</u>	<u>Page</u>
1	Compressor test facility	27
2	Layout of compressor test rig	28
3	Double slotted 0.75 hub diffusion factor stator slot configuration	29
4	Test rig flow path	30
5	Circumferential location of instrumentation viewed downstream	31
6	Radial location of streamlines for instrumentation positions	32
7	Schematics of survey instrumentation	33-34
8	Slotted stator vane static pressure tap locations at 10, 50 and 90% streamlines.	35
9	Flow generation rotor overall performance in stage test-pressure ratio.	36
10	Flow generation rotor overall performance in stage test-adiabatic efficiency	37
11	Stage overall performance-pressure ratio	38
12	Stage overall performance-adiabatic efficiency	39
13	Rotor blade element performance-stage test	40-44
14	Radial variation of rotor blade element performance	45
15	Rotor out radial mass flux distribution at design speed	46
16	Rotor loss parameter versus diffusion factor	47
17	Slotted stator blade element performance	48-52
18	Variation of wall bleed flows with stage pressure ratio	53
19	Stator slot blowing flow versus stage pressure ratio	54
20	Stator slot blowing flow spanwise distribution	55-56
21	Radial variation of 0.75 D_f slotted stator blade element performance	57
22	Stator loss parameter versus diffusion factor	58
23	Slotted stator static pressure distribution at 60% speed	59-63
24	Slotted stator static pressure distribution at 80% speed	64-68
25	Slotted stator static pressure distribution at 90% speed	69-73
26	Slotted stator static pressure distribution at 100% speed	74-79
27	Slotted stator static pressure distribution at 110% speed	80-86
28	Double slotted stator wake surveys.	87-92
29	Variation in stator wake at 10, 50, and 90% streamlines from tip during wall bleed optimization	93

LIST OF TABLES

<u>Table</u>	<u>Title</u>	<u>Page</u>
I	Blade and vane geometry summary	94
II	Rotor incidence at minimum and maximum flow for flow generation rotor and slotted stator stage tests.	95
III	Rotating stall results for double slotted stator stage test . .	96
IV	Blade element performance—slotted stator stage	97-124

SINGLE-STAGE EXPERIMENTAL EVALUATION OF BOUNDARY LAYER BLOWING TECHNIQUES FOR HIGH LIFT STATOR BLADES

IV—DATA AND PERFORMANCE OF DOUBLE-SLOTTED 0.75 HUB DIFFUSION FACTOR STATOR

By

R. H. Carmody and G. Seren
Allison Division, GMC

SUMMARY

To establish the feasibility of increasing compressor stator loading and stall-free flow margin by the use of a boundary layer blowing technique and to determine the extent to which such concepts may be employed, an investigation was made of a single-stage compressor provided with a double-slotted stator row. The stator was designed with NACA 65-series airfoils and a hub diffusion factor of 0.75.

The two blowing slots were designed to re-energize the boundary layer air on the suction surface with the slots located at 40 and 70% chord. For this purpose, the air is inducted into the vane core through a full-span slot near the leading edge of the vane pressure surface and is discharged through the two full-span blowing slots. The front slot is located upstream of the point on the suction surface where flow separation is estimated to take place on the unslotted vane, and the rear slot is located upstream of the point, on the suction surface, where flow separation is estimated to take place if only the front slot were provided. The orientation of the blowing slots relative to the suction surface is as nearly tangential as mechanically feasible. To ensure an attached stator end wall boundary layer and to minimize secondary flows, annulus wall bleeding was employed during all stator testing from a point forward of to a point behind the stator. The flow into this stator row was generated by a state-of-the-art flow generation rotor with prewhirl established by a row of inlet guide vanes.

Overall performance of the rotor and inlet guide vanes was evaluated separately for this stage test. Compared with rotor design values of 1.37 pressure ratio, 88.2 lb/sec inlet flow, and 88.8% overall adiabatic efficiency at design pressure ratio, the corrected inlet flow was 94.9 lb/sec with an adiabatic efficiency of 92.2%. In general, this performance agreed well with the flow generation rotor performance without stators reported in Reference 2. Overall performance for the slotted stator stage indicated a pressure ratio of 1.33 at the 94.9 lb/sec airflow corresponding to the flow generation rotor design pressure ratio. Stage design values are a 1.35 pressure ratio at 88.2 lb/sec flow rate.

Blade element performance was measured for the rotor blade and stator vane row. Experimental values are presented in terms of diffusion factor, deviation angle and loss coefficient as a function of incidence for various annulus heights with rotative speed as a parameter. Minimum loss values are determined and compared with the NACA loss parameter versus diffusion factor correlation curves. Radial variations of the experimental rotor and stator blade element performance near their design inlet flow conditions are also compared with the design values.

A hysteresis test with acquisition of rotating stall characteristics was also obtained at 60% corrected speed for the slotted stator stage. Recorded data did not indicate a definite hysteresis effect for the slotted stator stage although differences, in terms of flow rate and pressure ratio, were observed between points going into and recovering from stall. Onset of stall was found to be abrupt at speeds up to and including 90% with stall cells first appearing in the hub region. However, at higher speeds, 100 and 110% of design, stall occurred gradually with intermittent stall zones appearing at the hub and tip with decreasing airflow. The stresses experienced at these points exceeded the steady state limit and approached the transient limit.

The double-slotted blowing 0.75 diffusion factor stator performance apparently met the design flow turning values over the entire vane span with acceptable total pressure losses at these high loadings. Blade element performance loss correlations for these stators at the tip were above an extension of the existing NACA correlations. For all other radial positions they agreed with or were less than the NACA correlations.

Surface pressure distributions and wake surveys were obtained for the double-slotted stator.

Suction surface pressure distributions indicated separation of the boundary layer occurring at 65 to 85% chord throughout the range of the test. However, the existence of flow separation was not evident in the wake patterns or deviation angle.

The experimental flow rates through the blowing slots at the suction surface of the slotted stator, at design speed, were found to be approximately 107% of the design values at the first slot and approximately 142% of the design value at the second slot.

INTRODUCTION

Advanced airbreathing propulsion systems require lightweight compact compressors capable of high levels of performance. These compressors should have a broad range of operation and a large stall margin. High reliability and relative insensitivity to inlet flow distortion are generally required of all compressors. In meeting the more demanding compressor design requirements, compromises must be made that are strongly dependant on the particular application. New applications are steadily increasing the range of requirements which the compressor must meet.

Compressor technology has been advanced continuously by extending, among other parameters, the usable rotational speeds; increasing stage loadings or diffusion factors; and reducing stage length through the use of high blade aspect ratios. Whereas further advancements can be made through optimizations and improved combinations of these parameters, severe aerodynamic limitations such as increasing losses and decreased stall margin, are being encountered. Significant advancements in compressor technology require the application of advanced concepts in terms of improved blading for high flow Mach numbers and application of high lift devices to extend the stall-free flow range for compressor rotors and stators. Advanced concepts in these areas may result in sizable reductions in the number of compressor stages and improved compressor performance.

Airfoils, designed to provide high lift, experience steep blade surface pressure gradients which become steeper as the angle of incidence is increased. As a result, the suction surface boundary layer separates and high total pressure losses and a decrease in stall-free flow margin result. To some extent, however, separation of the suction surface boundary layer can be delayed by energizing it with high energy air. In view of these considerations, an experimental single-stage compressor rig was designed and constructed to test highly loaded stators using internal blowing concepts to reduce losses and to improve stall-free flow margin.

The objectives of this program are to establish experimentally the feasibility of increasing blade loading and stall-free flow margin by boundary layer blowing and the extent to which it may be employed. A secondary objective is to obtain blade element data for design use. The stator designs were to be representative of those for middle and latter stages of highly loaded axial-flow compressors. Stator inlet flow is generated by a state-of-the-art flow generation rotor. This report presents the test results for the double-slotted 0.75 hub diffusion factor stator. Previous test results on the flow generation rotor performance, the mid-span suction surface pressure distribution for an unslotted 0.75 hub diffusion factor stator, and the single-slotted 0.75 hub diffusion factor stator performance are presented in Reference 2. The test results of a single-slotted 0.65 hub diffuser factor stator, also employing blowing techniques, are presented in Reference 1.

SYMBOLS

A_a	Annulus area, ft ²
c	Airfoil chord, in.
C_W	Flow coefficient
D_f	Diffusion factor
g	Gravitational constant, 32.2 ft-lb _m /lb _f -sec ²
H	Hysteresis loop data point
h	Height of blowing slot, in.
i	Incidence angle based on mean camber line, degrees
L	Net slot length, in.
M	Mach number
\dot{m}	Blowing mass flow rate in blowing slot per blade, lb _m /sec
n	Number of blades per row
N	Rotational speed, rpm
P_t	Total pressure, psia
p	Static pressure, psia
q	Dynamic pressure, psia
R	Radius, in.
\mathcal{R}	Gas constant, 53.35 lb _f -ft/lb _m -°R
R_c	Pressure ratio
S	Airfoil surface pressure coefficient, (Equation A13)
T_t	Total temperature, °R
t	Static temperature, °R
t/c	Thickness-to-chord ratio
V	Air velocity, ft/sec
W_a	Compressor airflow, lb _m /sec
W_{BL}	Annulus wall bleed flow, lb _m /sec
x	Distance from blade leading edge, in.
Greek	
β	Air angle measured from axial direction, degrees
γ	Ratio of specific heats
γ°	Blade chord angle, degrees
δ	Ratio of total pressure to standard sea level pressure of 14.7 psia
δ°	Deviation angle, degrees
Δ	Incremental value

η	Efficiency
θ	Ratio of total temperature to standard sea level temperature of 518.6°R
κ	Blade metal angle measured from axial direction, degrees
ρ	Density, lb _m /ft ³
ψ	Slot angle with respect to chord
σ	Blade row solidity
ϕ	Camber angle, degrees
ω	Angular velocity of rotor, radians/sec
$\bar{\omega}$	Total pressure loss coefficient
$\frac{\bar{\omega} \cos \beta}{2\sigma}$	Loss parameter

Subscripts

0	Guide vane inlet
1	Rotor inlet
2	Stator inlet or rotor exit
3	Stator exit
θ	Tangential direction
ma	Mass averaged
ad	Adiabatic
m	Mean or 50% streamline
z	Axial direction

Superscripts

'	Relative value, rotor property
---	--------------------------------

APPARATUS AND PROCEDURES

TEST FACILITY

A general arrangement of the test facility is shown in Figure 1. Air enters the test compressor after passing through the test facility filter house, an inlet duct, plenum, and bellmouth and is exhausted to the atmosphere through a diffuser. Provisions exist for maintaining compressor inlet pressures above or below atmospheric if necessary.

Two power units can be used simultaneously to drive the test compressor. One is a T56 power turbine with combustors which burn fuel mixed with high pressure air from test facility compressors; the other is a complete T56 power section. The two units are coupled by a primary gearbox whose output shaft drives a secondary gearbox which in turn drives the test compressor. Control of the test compressor speed is effected by throttling the turbine air supply with a hydraulically operated valve and by independent fuel controls for each unit.

COMPRESSOR TEST RIG

The mechanical arrangement of the test compressor is shown in Figure 2. It consists of a cylindrical inlet section, the test compressor section, and an exhaust diffuser. The single-stage rotor is supported on two bearings whose housings are linked by a vertically split compressor case. The compressor case houses the inlet guide vanes, the rotor tip abrasible coating, the stator vanes, and the case and hub bleed manifolds. The design of the rig allows the rapid exchange of inlet guide vanes, if necessary, without dismantling the remainder of the compressor, and the exchange of stator vanes without disassembly of the entire test rig.

Airflow rate and pressure ratio are varied by throttle plates located in the exhaust diffuser. The throttles are linked by a ring and operated by a common actuator.

Provision is made in the rig for bleeding the wall boundary layers at stator tip and hub. This is accomplished by fabricating the stator flow passage walls from perforated sheet metal. Manifolds behind the perforated metal surfaces are connected by multiple tubes to separate vacuum headers for tip and hub wall bleeds.

BLADING

The design of the stator vanes, rotor blades and design inlet guide vanes is described in detail in Reference 3. Selected types of airfoil sections are:

(1) 63-006 series for the inlet guide vanes, (2) double-circular arc for the rotor blades, and (3) 65-series thickness distribution with circular arc meanline for the stator vanes. For convenience however, the principal geometric details of these components are repeated in Table I. Only the design inlet guide vanes (Ref 3) were used in this test. Basic details of the slot configuration of the double slotted 0.75 diffusion factor stator are shown in Figure 3.

INSTRUMENTATION

Instrumentation was provided to obtain blade element performance for the rotor and stator row and to measure overall performance. The locations of instrumentation planes are shown in Figure 4. Figure 5 shows, schematically, the circumferential location of the instruments installed at each plane. The radial element locations at each plane were selected along streamlines passing through the 10, 30, 50, 70, and 90% annulus height stations from the tip at the stator inlet measurement plane. The streamline locations are shown in Figure 6. Instrumentation was distributed so as to minimize area blockages and prevent immersion in upstream instrument wakes. Duplicate instrumentation was distributed so as to average out any inlet guide vane effects. Dimensional sketches of the probes are shown in Figure 7.

Compressor Inlet Conditions

Weight flow was measured with an ASME thin plate orifice located in each branch of the triple inlet header. Six total pressure probes and two 6-element temperature rakes were located in the cylindrical section approximately three feet upstream of the test compressor inlet for measurement of inlet total pressure and temperature (see Figure 5a). Inlet static pressure was measured at the same axial station by two static taps in the inlet wall.

Rotor Inlet—Station 1

Four approximately equally spaced static pressure taps were located on both the inner and outer walls as shown in Figure 5b. An 8-degree wedge static pressure traverse probe was also installed to measure the radial static pressure distribution. Three radial traverse combination total pressure and yaw angle probes were used to measure the distribution of these parameters across the annulus. Total temperature was obtained from plenum thermocouples.

Stator Inlet or Rotor Exit—Station 2

Four approximately equally spaced static pressure taps were located on both the inner and outer walls; the radial distribution of static pressure was measured by two 8-degree wedge static pressure traverse probes as shown in Figure 5c. Three radial traverse combination probes were installed at this station to measure the radial distribution of total pressure, total temperature, and flow angle.

Stator Exit—Station 3

Four approximately equally spaced static pressure taps were located on both inner and outer walls; two 8-degree wedge traverse probes were installed for measurement of the radial static pressure distribution as shown in Figure 5d. One traverse combination total pressure, total temperature, and yaw probe was installed primarily to measure flow angle. A 16-element total pressure circumferential rake, shown in Figure 7d, was installed at this station to measure discharge total pressure and stator vane wake. This rake spanned 1.08 vane spaces at the 10% streamline and 1.43 vane spaces at the 90% streamline. Total temperature was measured by four 5-element radial rakes. Inner and outer wall boundary layers were surveyed by fixed 5-element total pressure probes. All taps, probes, and radial rakes were located on extensions of mid-channel streamlines.

Special Instrumentation

In addition to the instrumentation already enumerated for blade element and overall performance, the following special instrumentation was installed. At the rotor exit, two fixed and one traverse hot wire anemometers were installed to signal the onset of compressor stall and to provide rotating stall data. Shaft whip was monitored by means of a whip pickup, mounted in the plane of the rotor blades; strain gages were mounted on eight rotor blades to monitor blade stresses.

The 10, 50, and 90% streamline sections of the slotted vanes were each provided with 10 suction surface and 7 pressure surface static pressure taps as indicated in Figure 8. Two blowing discharge slot static taps and one core static pressure tap were provided at each section to measure blowing flow rate. The 20 static pressure taps for each streamline section were distributed among 4 vanes.

DETERMINATION OF ANNULUS WALL BLEED FLOW FOR STATOR VANE TESTS

With the compressor operating at design speed and stage pressure ratio, the circumferential total pressure rake at the stator exit was set at the streamline station 10% from the tip. Hub and tip wall bleeds were set at a

nominal flow of less than 1% of compressor flow. The stator wake pattern at this bleed flow was noted, and the tip wall bleed was then increased until no further improvement in wake pattern was visually observed on a manometer bank. This bleed flow rate was defined as the "optimum" bleed rate. One limiting consideration set as a reasonable upper value, however, was to extract no more than 2.5% of compressor inlet flow per wall at design conditions.

The circumferential rake was then set at the streamline station 90% from the tip. The tip wall bleed flow rate was reset at its original low value, and the procedure described was repeated for the hub bleed.

After hub and outer wall bleed flows had been optimized, the circumferential rake was moved to the mean position. Hub and outer wall bleeds were varied simultaneously in increments from the original nominal flow rate to optimum flow. The effects on the stator wake at mean depth were studied to check that optimum hub and tip wall bleeds coincided with an optimum wake at mid-span. The valve settings for these optimum bleed flow rates were left unchanged for all subsequent speed and flow conditions.

HYSTERESIS TEST WITH SLOTTED 0.75 HUB DIFFUSION FACTOR STATOR

The following method was employed to determine the characteristics of this stage at entry to, and when recovering from stall. With corrected speed set at 60%, the throttle was closed until stall cells were indicated by the three hot-wire anemometers (two of which were at the 10% and one at the 90% station from the tip) thus signaling the onset of stall. At this stalled condition, taken as the first hysteresis data point setting, a partial data recording, which consists of data required for airflow and pressure ratio calculation, was obtained. The throttle was then closed further and a second partial data recording was made at an intermediate point. After further throttle closure, a third partial data recording was obtained. The throttle was then gradually opened in steps and when indications of stall, as signalled by the hot-wire anemometers, disappeared a fourth short data cycle was recorded.

Rotor blade stresses were monitored continuously during the hysteresis test to ensure that excessive vibratory stresses were not encountered.

OVERALL AND BLADE ELEMENT PERFORMANCE DATA

Overall and blade element performance data were obtained at a sufficient number of points per speed line to define rotor or stage performance between choke and stall. The stage stall point is defined as the onset of a steady stall cell indication on the hot wire anemometers. The near-stall test point was taken as close to the rotating stall condition as could be set without actually being in rotating stall. This type of near-stall setting permitted a full data point recording. At each full data point, fixed and traverse

pressure and temperature data were recorded at five radial locations corresponding to streamlines passing through the 10, 30, 50, 70, and 90% span stations at the stator inlet measurement plane.

DATA REDUCTION

Overall performance and blade element data reduction is accomplished in one program. A second program is used to calculate pressure coefficients and slot blowing flow rates for the stator vanes.

In the first program, raw data from the test stand is read in and printed. The program converts wedge probe static pressure transducer readings to inches of mercury absolute and applies a Mach number correction. All yaw units are converted to degrees. Data recording system, wire calibration, and Mach number corrections are applied to all temperatures. Pressures recorded on the data recording system are corrected to standard inlet total pressure. The corrected data is then printed.

Circumferential arithmetic averages of total pressures, static pressures, total temperatures, and yaw angles are calculated and printed. Individual data readings are compared with the averages to validate the data. Any individual reading which differs from its respective average by more than the prescribed deviation (0.5 in. Hg for all the pressures, 3° for the yaw angles, 1.5°R, 2°R, and 3°R, respectively, for the reference inlet, and all other temperatures) is not used in the final calculations. Mass-averaged values required for performance calculations are determined.

The program provides a choice of two radial distributions of static pressure: (1) distributions measured by the wedge probes and (2) a linear distribution across the flow annulus calculated from the arithmetically-averaged hub and case wall static pressure taps. Overall and blade element performance are calculated and printed using the two static pressure distributions mentioned. If a continuity check at any data measurement station is not satisfied within 5%, a simple radial equilibrium solution is provided to give an indication of the problem.

Overall performance values are calculated for the inlet guide vanes and rotor and for the complete stage. The following operations were performed to determine these values.

At the inlet plenum station two total temperatures are arithmetically averaged at each radial station. Mass flow is integrated radially, assuming that averaged wall static pressure exits over the entire cross section. Total pressure and temperature are then mass-averaged. Behind the rotor, all total pressures, total temperatures, and wall static pressures are arithmetically averaged circumferentially at each radial station. Mass flow is radially integrated and total pressures and temperatures are mass averaged.

At the stator exit, four total temperatures are arithmetically averaged circumferentially at each radial station. Mass flow is computed using an arithmetic average of the circumferential rake total pressure readings spanning a stator vane passage at each radial station. A radial integration is made for weight flow. For performance calculations, the total pressures at each radial station are mass averaged circumferentially and the total pressures and temperatures are mass averaged radially. The overall pressure ratio and adiabatic efficiencies are obtained using the radially mass averaged values of total pressure and temperature.

The calculation of performance variables, as programmed in the data reduction programs, are delineated in the Appendix.

PRESENTATION OF RESULTS

Experimental results obtained in the test program are summarized for the double-slotted 0.75 hub diffusion factor stator vane and flow generation rotor with the design inlet guide vane set. The reduced data presented were based on a linear static pressure distribution across the annulus at each axial survey station rather than on the static wedge survey values. Comparison of results using both linear and wedge static data (Reference 2) showed that, when the wedge data were considered reliable, differences in reduced data were small; there was a tendency, however, for the wedge static data to be erratic for some test points. Use of the linear static data gives a consistent basis for comparison over the test range and with the data from other tests.

OVERALL PERFORMANCE OF FLOW GENERATION ROTOR AND STAGE

Overall pressure ratio and adiabatic efficiency are each plotted versus corrected inlet flow with corrected speed as a parameter. These plots are presented in Figures 10 and 11 of Reference 1 for the flow generation rotor test; Figures 9 and 10 present data for the flow generation rotor during this stage test, and Figures 11 and 12 present data for the stage.

To indicate whether the rotor or the double-slotted stator caused the stage to choke or stall, rotor incidence range is summarized in Table II for the flow generation rotor test of Reference 2 and the flow generation rotor of the double-slotted 0.75 D_f stator stage test. Stage rotating stall characteristics at the double slotted stator stall points and hysteresis points are summarized in Table III.

BLADE ELEMENT PERFORMANCE

Rotor blade and stator vane blade element characteristics were computed at the five streamline positions previously defined. The blade element characteristics chosen to present the detailed performance of each blade row are as follows.

Blade element parameter

Incidence angle, i
Total pressure loss coefficient, $\bar{\omega}'$ or $\bar{\omega}$
Diffusion factor, D_f
Deviation angle, δ°
Inlet flow angle, β' or β
Flow turning $\Delta\beta'$ or $\Delta\beta$
Inlet axial velocity, V_z
Inlet Mach number, M' or M

Rotor blade element data are plotted as a function of incidence with corrected speed as a parameter for each of the streamline stations. The blade element data obtained during the stage test are shown in Figure 13. For comparison and to aid the analysis of the rotor blade performance, blade element data for the rotor blade are plotted versus percent annulus height in Figure 14 for the flow providing the best approximation of the design incidence angle at design speed. Design values are also plotted for comparison. Mass flux distribution out of the rotor corresponding to the design flow rate is plotted and compared with the design flow distribution in Figure 15. Rotor blade element performance is evaluated, in Figure 16, by comparing the loss parameter versus diffusion factor curves at the 10, 50, and 90% streamline stations from the tip with the NACA correlation curve from Reference 4.

Stator vane blade element data are also plotted as a function of incidence angle with corrected speed as a parameter for each streamline station. The blade element data for the double-slotted stator are plotted in Figure 17. Also presented are the annulus wall bleed rates and the double-slotted stator slot blowing flow rates in Figures 18 through 20. Blade element data of the slotted stator vane for conditions nearest to the design incidence angle are plotted against the percent annulus height in Figure 21 to aid stator vane performance analysis and comparison. Stator vane blade element performance is also presented in Figure 22 where the loss parameter versus diffusion factor for 10, 50, and 90% streamline stations from tip, is compared with the NACA correlation curve from Reference 4.

The static pressure distributions, along the 10, 50, and 90% streamlines from the tip, of the double-slotted stator suction and pressure surfaces are presented in Figures 23 through 27 for all the speed lines tested.

The stator wakes and the variation of the stator wakes during the optimization of the wall bleeds are plotted in Figures 28 and 29, respectively.

To enable compressor designers to evaluate and apply the results of this test, a detailed summary of vector diagrams, blade element characteristics and loss data at each streamline station is provided. These summaries are listed in Table IV.

DISCUSSION OF RESULTS

The method of presentation using the overall and blade element parameters for evaluating the performance has been described in detail. Since the figures and tables are self explanatory, only general observations are made.

OVERALL PERFORMANCE

Flow Generation Rotor

Flow generation rotor pressure ratio and adiabatic efficiency with the design inlet guide vanes is shown in Figures 9 and 10. The adiabatic efficiency was based on the mass averaged temperature measured by the stator vane exit station radial temperature rakes.

A review of the test data on Figures 10 and 12 shows minor discrepancies the most apparent of which are the points on the 60% characteristic. The normal method of computing efficiency reveals this discrepancy may be due to small differences of two large numbers. Using standard inlet conditions the temperature rise across the rotor at the 60% speed points is of the order of 24°F. A 1-degree change in the measured temperature rise for these two test points will result in the three percent change in efficiency required to position the points on the curve. Conversely for the measured temperature rise minute differences in rotor exit pressure (≈ 0.2 in. Hg) will result in the same three point decrement. The actual discrepancy could be either a pressure or temperature error but is well within experimental accuracy.

In general, the performance data for the flow generation rotor from this stage test agreed favorably with the data obtained from the flow generation rotor test of Reference 2. The design point pressure ratio and efficiency are 1.37 and 88.3%, respectively, at a design flow rate of 88.2 lb/sec with the design inlet guide vanes. At the design equivalent rotor speed, maximum efficiency was 96.5% with corresponding pressure ratio of 1.455 and flow rate of 90 lb/sec. At the design pressure ratio of 1.37 the flow rate was 7.6% higher than design at 94.9 lb/sec with an adiabatic efficiency of 92.2%. The excess flow was attributed to the effective overcambering of the blades as evidenced by the fact that the measured deviation angles were less than the design values. The difference between measured and design deviation angles for this test tended to be greater than those of References 1 and 2, particularly in the hub region.

Flow generation rotor pressure ratio and adiabatic efficiency with the design inlet guide vanes and no stators are shown in Figures 10 and 11 of Reference 2. The pressure ratio results are in good agreement with the rotor test results without stator vanes. When the maximum value of the adiabatic efficiencies are examined at 100% corrected speed, however, a value of 96.5% is obtained from the results of the stage test, Figure 10, as opposed to 92.5% from the flow generation rotor test, both at the same measured airflow rate. Since the accuracy of the thermocouple is $\pm 0.75^\circ\text{F}$, the

possible error in the adiabatic efficiency, corresponding to a pressure ratio of 1.4 would be $\pm 1.2\%$. The values of the adiabatic efficiencies are not, therefore, considered within the limits of experimental accuracy. The discrepancy observed in the value of the efficiency may be due to an additional error in the readout or the calibration.

A prime concern during the design phase of the flow generation rotor, discussed in Reference 3, was that sufficient flow range would be available to avoid excessive limitations on the stator operating range by the rotor or facility. In this report, Table II gives a summary of rotor incidence angles near stall and choke, at hub, mean, and tip streamlines. The stall incidence angles correspond to the minimum flow rate due to either rotor or stator stall. The choke incidence angles correspond to the maximum flow rate due either to rotor choke, stator choke, or facility pressure loss limitations. Rotor incidence angle differences at stall observed between slotted stator test and flow generation rotor test of Reference 2 are small, and stage stall may be due to rotor stall rather than stator stall.

The comparison of the incidence angles at maximum flows indicates that the stator limited the maximum flow at 60 and 80% corrected speed. At 100% corrected speed, the approximately equal rotor incidence angles for both tests indicate that either the rotor or stator are choked at nearly the same flow or the facility pressure loss was controlling. It is believed that the facility exit duct pressure loss was controlling at these relatively low pressure ratios with high flow rate conditions.

Double-Slotted Stator Stage

The overall stage pressure ratio and adiabatic efficiency are shown in Figures 11 and 12, respectively. During these tests only the design inlet guide vanes were employed.

Stage design pressure ratio and adiabatic efficiency are (as indicated in Reference 3) 1.35 and 85.5% at a design flow rate of 88.2 lb/sec. At the design equivalent rotor speed a maximum stage adiabatic efficiency of 87.6% was obtained with a pressure ratio of 1.395 and a flow rate of 91.0 lb/sec. At the flow generation rotor condition of 94.9 lb/sec corrected flow rate the stage pressure ratio was 1.33 and adiabatic efficiency was 84.9%. For simplicity, the stage adiabatic efficiency, presented herein, is not penalized by the case and hub wall bleed flows. Inasmuch as the rotor loading is not compatible with the stator loading, the stage efficiency is of secondary interest.

The design average total pressure recovery of the slotted stator is 0.986 (1.35/1.37) and the measured "design" total pressure recovery is 0.971 (1.33/1.37). Since the stator inlet flow conditions are equivalent to approximately a 1.6 pressure ratio rotor without inlet guide vanes, the stage efficiency of 84.9% would be increased by 1.5 to 2.0 points due to the additional work with the same average pressure recovery of 0.971 and rotor efficiency of 92.2%.

Annulus Wall Bleed for Stator Test

Annulus wall bleed over the stator row at tip and hub surface was defined at 100% corrected speed and rotor pressure ratio of 1.37 by monitoring visually the circumferential rake and boundary layer total pressure rakes at tip and hub. Except at very low wall bleed flows of about 0.5% where stator wakes were still relatively large, the boundary layer total pressure rakes indicated an attached boundary layer. That is, total pressures increased away from the wall. Once the wall boundary layer attached, additional wall bleed essentially affected only the blade end regions. When the stator wake reduction showed negligible improvement with increased wall bleeds, the tip and hub bleed valves were held fixed throughout all remaining test points. The optimized hub and tip bleed values at the reference operating point were 2.06 and 1.70%, respectively. The tip and hub wall bleed rates experienced throughout this test with the fixed bleed line valve settings are summarized in Figure 18.

Hysteresis and Rotating Stall Results—Slotted Stator Stage

This test was made to determine whether the stall of this stage was gradual or abrupt, and whether the stall would disappear and the stage recover smoothly. The onset of rotating stall at each corrected speed is indicated by the hot wire anemometer located at the 90% streamline. Rotor stall was abrupt at all speeds below 100% as indicated by the stall zone progression to the tip of the rotor with only a slight increase in backpressure. The onset of stall at the higher speeds, 100 and 110% of design, occurred gradually with stall zones appearing intermittently at the hub and tip. Despite the high rotor blade stresses observed, partial data readings were obtained.

At 60% corrected speed, a four-point hysteresis loop test was conducted. The pressure ratio-flow rate points are shown in Figure 11. The existence of a definite hysteresis effect, in terms of pressure ratio and flow rate, was not indicated by the measurements defining the path from point H_1 to H_4 . The value obtained for the pressure ratio at the data point H_4 is significantly different from the value obtained at the point H_1 , the first hysteresis point, going into stall. The mass flow rates at these two points, however, are approximately equal; therefore, they cannot be considered to be out of stall. The maximum transient blade stresses encountered during the hysteresis test were 13,600 psi.

There were indications, from the frequent recurrence of stress peaks, that these maximum transient stresses prevailed for a significant period during the hysteresis test. These blade stresses were considered to be at a potentially damaging level, since their magnitudes were appreciably higher than the stress limit which was 11,250 psi.

Rotating stall results in terms of rotative speed, frequency, and number of stall zones are summarized in Table III. Following the onset of stall, a

single stall cell was recorded in both hub and tip regions. The rotative speeds of the cells ranged from 27 to 43% rotor speed in the direction of rotation with frequencies varying from 23 to 50 cps for single-stall zones and 100 cps for two-stall zones, depending on the corrected speeds run. In deep stall, at 100% design speed, the stall cell rotative speed was approximately 36% rotor speed in the direction of rotation and the frequency was 100 cps. High rotor blade transient stresses prevented radial traversing of the hot wire probe. It appears, however, that the stall zone extended across the blade span.

BLADE ELEMENT PERFORMANCE

An extensive study of the inlet guide vanes, both at design and off design conditions, was made as reported in Reference 2. Investigation into the possible persistence of the inlet guide vane wakes through the rotor, at the design flow rate condition, indicated the attenuation of these wakes before entering the stator rows. In view of these results, repeated study of the inlet guide vane flow for each test was found unnecessary.

Rotor

Diffusion factor, deviation angle, and loss coefficient data throughout the rotor operating range for the slotted stator stage test are summarized in Figure 13. In general the measured loss coefficients are found to be less than design values at the 0° design incidence angle at the 10 and 30% streamline stations and about equal to the design values at the 50, 70, and 90% streamline stations.

Primary rotor blade element performance for the double-circular arc blade during the stator test is shown in Figure 14. Rotor blade measured data for both the flow generation rotor and slotted stator stage tests, operating near the design incidence angle at 100% design speed, are compared with the design values. The selection of measured data was based on the best agreement with the design incidence angle values, since the rotor exceeded its design pressure ratio. In general, the measured and design values of incidence angle compare favorably.

Values of deviation angle and diffusion factor differing significantly from the design values were observed as also evidenced in Reference 2. The lower than design deviation angles result in an effective overcambering of the rotor blades producing an excessive amount of work on the flow. The combination of higher work input and lower axial exit velocity results in the higher than design values of diffusion factors.

The radial distribution of mass flux at the rotor outlet, for the flow generation rotor and slotted stator stage test, are compared with the design values in Figure 15. A flow shift to the tip occurred experimentally with respect to the design distribution. This can be attributed to the low deviation angles in the tip region of the rotor. An additional mass flow shift was observed between the measured test values of the flow generation rotor test, Reference 2, and the test of Reference 1 for the 0.65 diffusion factor slotted stator stage. This additional mass flow shift at the rotor outlet could be due to an effective blockage in the hub region caused by the separation of the boundary layer at the stator suction surface inducing a secondary flow and end wall effects. The stator exit hub wall boundary layer rake, however, did not indicate any wall boundary layer separation.

Rotor loss parameter data at the 10, 50, and 90% streamlines are shown in Figure 16. Minimum loss coefficient values are indicated as filled symbols when they could be defined. The minimum values are selected as the data point nearest to the minimum value of the curve drawn through data points in Figure 13. Minimum loss data for the tip region or 10% streamline are found to lie on the lower band of the data scatter. Loss data for the mid-span and hub region are found to agree well with the NACA correlation curves in the test diffusion factor range. The comparison between the correlation curves obtained for the flow generation rotor in this report and those of Reference 2 shows favorable agreement. The data reported herein indicate an improvement in the rotor performance, with lower loss parameters at higher diffusion factors, particularly in the hub region, compared with Figure 25 of Reference 2.

Stator

Measured results of higher flow turning and greater losses than design values are shown in Figure 17 representing diffusion factor, deviation angle, and loss coefficient over the entire test operating range for a given annulus height. A study of these results also indicates that the choke or minimum incidence angle limit may not be clearly defined except at the 90% streamline. Further study also shows that the loss coefficient versus incidence angle curve is quite flat over a wide range except at the 90% streamline height. It is indicated, therefore, that the operating range of this stator with self energized boundary layer control agrees favorably with the ranges obtained for the stators of References 1 and 2.

The radial variation of blade element data for the slotted stator at a point where the values of the incidence angle provided the best approximation to design incidence are compared with the design values in Figure 21. Inlet axial velocity and incidence angle variations from design trends of Figure 21 result from a mass flow shift with respect to the design value for the flow generation rotor. Other significant results shown in Figure 21 are that

flow turning was greater than expected or deviation angles were much less than design values at the tip region. Figure 17e shows similar results for the flow turning and deviation angles at the hub region. This deviation angle result agrees with the measured deviation angles for the single-slot 0.75 diffusion factor stator of Reference 2. Measured losses were found to be greater than the design values, particularly at the tip.

Loss parameter values calculated from the data of Figure 17 are compared with the NACA loss parameter versus diffusion factor correlation (Reference 4) in Figure 22 for the 10, 50, and 90% streamlines from the tip. The minimum loss values (filled symbols) for the 0.75 diffusion factor slotted stator for the 10% streamline are generally greater than the values on an extension of the NACA correlation curve; for the 50% streamline, the minimum loss values are less than those of the curve, while the 90% streamline has the majority of its values less than those of the extended curve. Comparing these data with the 0.75 diffusion factor single-slotted blowing stator results indicates that possibly all of the data are within experimental accuracy and that the present correlation curves are satisfactory. The minimum losses obtained for the double-slotted stator appear to be lower than the values obtained for the single-slotted 0.75 diffusion factor stator. The flow turning and loss performance of these stators are not significantly better than the performance of the single-slotted 0.75 diffusion factor stators, reported in Reference 2.

Typical slotted stator wake distributions are shown in Figure 28. Selected cases nearest to -3-degree incidence, which show the increasing wake size as inlet Mach number increases, are given in Figures 28a, b, c, and e. Figures 28f through 28i illustrate the effects of incidence angle at an inlet Mach number near 0.7. The wake surveys at high positive incidence angles in Figures 28h and 28i show that the hub region is experiencing a strong secondary flow or wall effect. That is, the peak total pressure at rake elements 7 and 8 are considerably lower than the inlet values for the test conditions of Figures 28h and 28i.

Wake survey data were recorded during the wall bleed optimization runs at the design stage pressure ratio of 1.35 and 100% corrected speed. The effect of reduced stator losses with increasing wall bleed rate is shown in Figure 29. It is evident in Figure 29 that increased wall bleed reduced the end region flow disturbances and stator losses. Higher wall bleed rates above the 30 and 29 in. H₂O orifice pressure differential at tip and hub, respectively, had little effect on increasing wake total pressure at the 10 and 90% radial stations.

Stator Static Pressure Distributions

Suction surface static pressure distributions for the slotted stator indicate the possibility of boundary layer separation at 65 to 85% chord throughout

the entire range of tests as shown in Figures 23 through 27. The blowing slots were located at 40 and 70% chords. The possible existence of separation displayed by the static pressure distributions is not consistent with the wake surveys and loss coefficients. Therefore, the apparent separation may not be as severe as displayed by the static pressure distributions. The static pressure distributions given in this report also bear close resemblance to those given in Reference 2.

Stator Slot Blowing Flow

The variation of combined and individual slot blowing with pressure ratio is presented in Figure 19. The variation of slot blowing flow along the span of the stator is given in Figure 20. The test point representing design incidence angle at each corrected speed was selected to give the best approximation over the blade span. Experimental flow rates are found to be about 107 and 142% of the design values at 100% corrected speed for the first and second slots, respectively. The flow rates were estimated from a measured static pressure in the core of the stator, which was assumed equal to core total pressure, and a static tap located in the slot. Design values for the hub, mean, and tip section slots (i. e., separated by slot bridges) taken as an average for each slot section are: 0.00475, 0.00446, and 0.00421 lb_m/sec-in. at the front slots, and 0.00639, 0.00600, and 0.00480 lb_m/sec-in. at the rear slots, respectively. Experimental blowing flow spanwise gradients were greater than experienced on the 0.75 diffusion factor single-slotted stator test presented in Reference 2. Figure 20b shows the variation in blowing rates from the value at design incidence to either test extreme on the speed line characteristics was within 30% of the value at design incidence.

CONCLUDING REMARKS

Discussion of the experimental results has been based on analysis work completed to date. In addition to the beneficial experience to be obtained on continuing stator tests, considerably more effort is required before final conclusions can be drawn. Analysis of the data, however, indicates the following points.

1. The overall performance of the flow generation rotor in this stage test agreed well with the performance of the flow generation rotor without stators, reported in Reference 2. At the flow rate corresponding to the flow generation rotor design pressure ratio the stage pressure ratio was lower than the design value.
2. The blade element performance of the double-slotted 0.75 hub diffusion factor stator in flow turning and total pressure loss was somewhat better than that of the single-slotted 0.75 hub diffusion factor stator. This difference was apparently due to the improved effectiveness of a double blowing slot configuration over one employing a single slot, with respect to distributing the blowing flow and re-energizing the boundary layer.
3. A hysteresis effect, in terms of pressure ratio and mass flow rate, was not definitely established at 60% corrected speed where different mass flow rates and pressure ratios were obtained going into and coming out of stall.
4. Rotor blade stresses exceeded the prescribed steady state limits approaching the transient limit during the hysteresis test at 60% of design speed and the stall point tests below 100% design speed. The transient stress limit was exceeded during the stall point tests at 100 and 110% design speeds.
5. The results of the stator loss parameter versus diffusion factor curves were in good agreement with the extension of the NACA correlation curves.
6. The blade suction surface static pressure distributions indicated the possibility of flow separation occurring at 65 to 85% chord. Flow turning and pressure loss levels do not indicate severe flow separation.

REFERENCES

1. Miller, M. L., and Seren, G. Single-Stage Experimental Evaluation of Boundary Layer Blowing Techniques for High Lift Stator Blades, III - Data and Performance of Single Slotted 0.65 Hub Diffusion Factor. NASA CR-54566, Allison Division, GMC, EDR 5759, June 1968.
2. Miller, M. L., and Beck, T. E. Single-Stage Experimental Evaluation of Boundary Layer Blowing Techniques for High Lift Stator Blades, II - Data and Performance of Flow Generation Rotor and Single Slotted 0.75 Hub Diffusion Factor Stator. NASA CR-54565, Allison Division, GMC, EDR 5691, February 1968.
3. Chapman, D. C., and Miller, M. L. Single-Stage Experimental Evaluation of Boundary Layer Blowing Techniques for High Lift Stator Blades, I - Compressor Design. NASA CR-54564, Allison Division, GMC, EDR 5636, February 1968.
4. Aerodynamic Design of Axial Flow Compressors, NASA SP-36, 1965.

APPENDIX

PERFORMANCE EQUATIONS

The following overall and blade element performance parameters were calculated for the analysis of test data and the evaluation of the slotted stator performance.

WEIGHT FLOW

Overall performance is presented as a function of corrected weight flow, defined as

$$\frac{W_a \sqrt{\theta}}{\delta} \quad (A1)$$

ADIABATIC EFFICIENCY

Adiabatic efficiency for the inlet guide vane and rotor combination is

$$\eta_{ad2} = \frac{\left(\frac{P_{t2, ma}}{P_{t0}} \right)^{\gamma-1/\gamma} - 1}{\frac{T_{t3, ma}}{T_{t0}} - 1} \quad (A2)$$

and for the guide vane rotor and stator is

$$\eta_{ad3} = \frac{\left(\frac{P_{t3, ma}}{P_{t0}} \right)^{\gamma-1/\gamma} - 1}{\frac{T_{t3, ma}}{T_{t0}} - 1} \quad (A3)$$

DIFFUSION FACTOR

For the rotor, diffusion factor is defined as

$$D_{f2} = 1 - \frac{V_2'}{V_1'} + \frac{V_{\theta 1}' - V_{\theta 2}'}{2\sigma V_1'} \quad (A4)$$

and for the stator as

$$D_{f3} = 1 - \frac{V_3}{V_2} + \frac{V_{\theta 2} - V_{\theta 3}}{2 \sigma V_2} \quad (A5)$$

These quantities are calculated using the appropriate velocity triangle values previously computed by the program.

DEVIATION ANGLE

Rotor blade deviation is defined as

$$\delta_2^\circ = \beta_2' - \kappa_2' \quad (A6)$$

and stator deviation as

$$\delta_3^\circ = \beta_3 - \kappa_3 \quad (A7)$$

where κ_2' is the rotor blade exit metal angle based on the mean camber line for a double-circular arc airfoil and κ_3 is the stator vane exit metal angle based on the circular arc camber line used with the 65-series thickness distribution.

INCIDENCE ANGLE

Rotor blade incidence is defined as

$$i_1' = \beta_1' - \kappa_1' \quad (A8)$$

and stator incidence as

$$i_2 = \beta_2 - \kappa_2 \quad (A9)$$

where κ_1' is the rotor blade inlet metal angle based on the mean camber line for a double-circular arc airfoil and κ_2 is the stator vane inlet metal angle based on the circular arc camber line.

TOTAL PRESSURE LOSS COEFFICIENT

Total pressure loss coefficient for the rotor is defined as

$$\bar{\omega} = \frac{\left[1 + \frac{\gamma-1}{2} \frac{(\omega R_2)^2}{\gamma g R T_{t1}'} \left(1 - \frac{R_1^2}{R_2^2} \right) \right]^{\gamma/(\gamma-1)} \left[1 - \frac{P_{t2}/P_{t1}}{(T_{t2}/T_{t1}')^{\gamma/(\gamma-1)}} \right]}{1 - \left[1 + \frac{\gamma-1}{2} (M_1')^2 \right]^{\gamma/(\gamma-1)}} \quad (A10)$$

and for the inlet guide vanes as

$$\bar{\omega} = \frac{1 - \frac{P_{t1}}{P_{t0}}}{1 - \left[1 + \frac{\gamma-1}{2} (M_0)^2 \right]^{-\gamma/(\gamma-1)}} \quad (\text{A11})$$

and stator as

$$\bar{\omega} = \frac{1 - \frac{P_{t3}}{P_{t2}}}{1 - \left[1 + \frac{\gamma-1}{2} (M_2)^2 \right]^{-\gamma/(\gamma-1)}} \quad (\text{A12})$$

Pressure Coefficient

Pressure coefficient (S) is defined by

$$S = \frac{P_{t2} - p}{q_2} \quad (\text{A13})$$

where:

P_{t2} = total pressure at stator inlet

p = static pressure at a given point on the vane surface

$$q_2 = \frac{\gamma p_2 M_2^2}{2} = \text{dynamic pressure at stator inlet}$$

Vane Blowing Flow

Vane blowing flow per unit slot length is first calculated at each station at which surface static pressure taps exist and is defined as

$$\dot{m} = C_W \rho_{\text{slot}} h V_{\text{slot}} \quad (\text{A14})$$

where

C_W = slot flow coefficient = 0.82

$$\rho_{\text{slot}} = \frac{P_{\text{slot}}}{R_{t\text{slot}}}$$

Slot static conditions were based on stator inlet free stream total temperature, the core measured pressure taken as total pressure at the streamline in question, and the measured slot static pressure. The values thus obtained are used to calculate blowing flow through each segment of the slot and thence total blowing flow taking account of the blockage introduced by the interruption between slot segments.

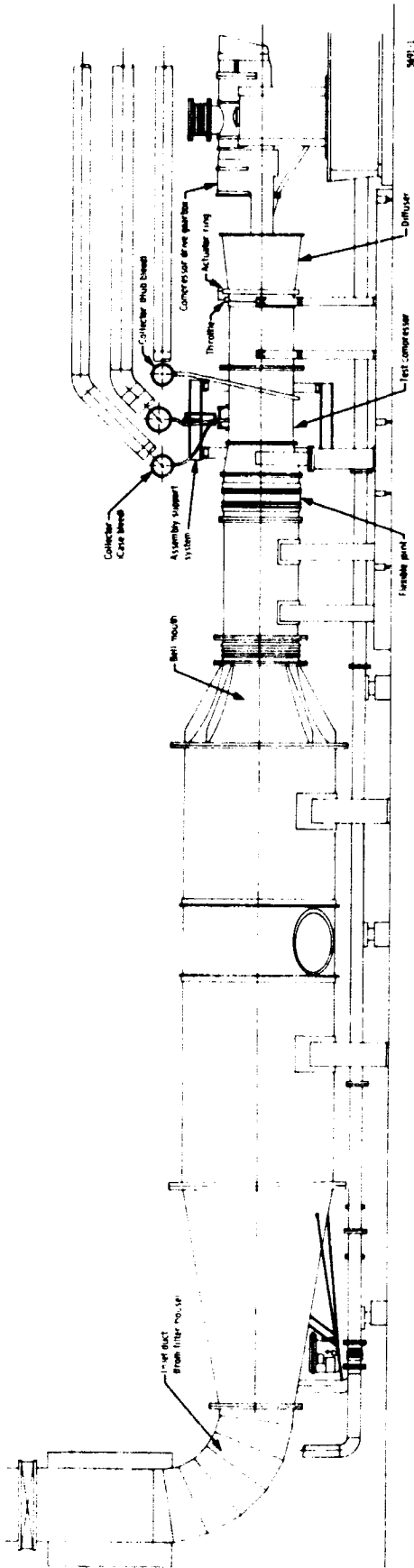
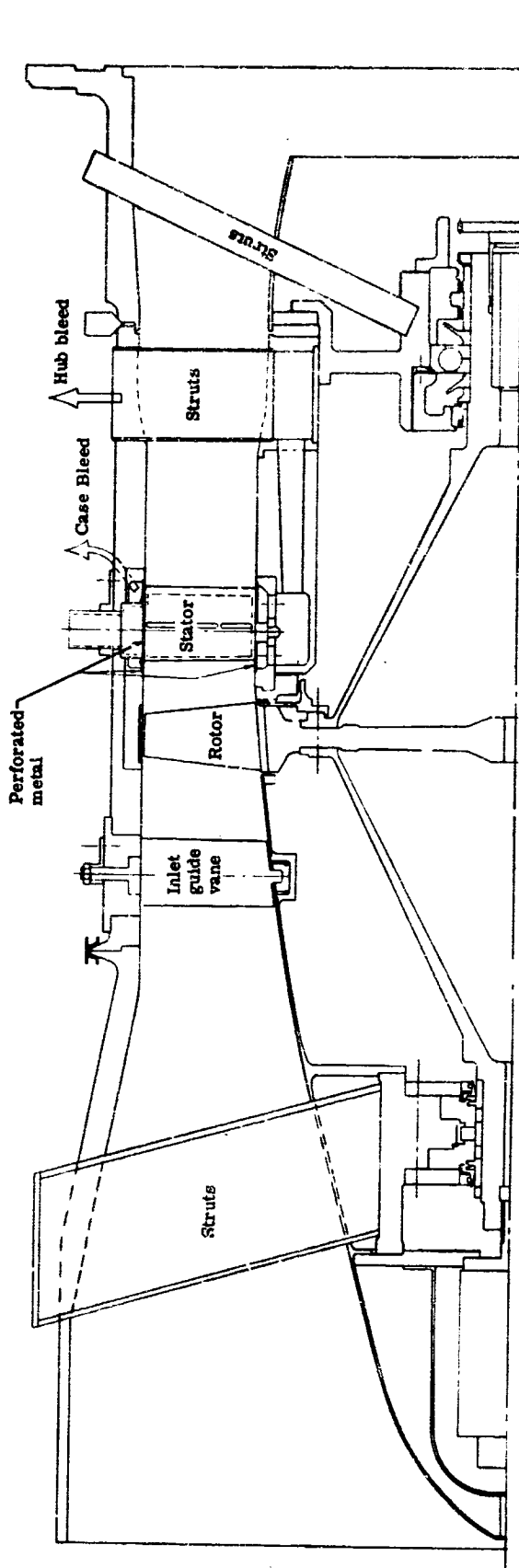
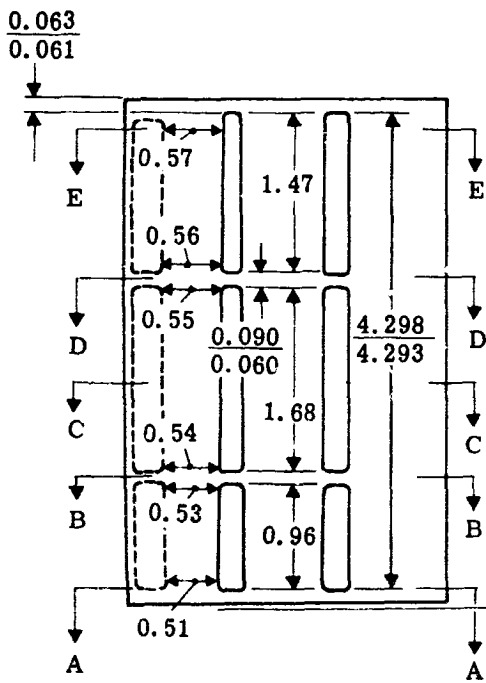
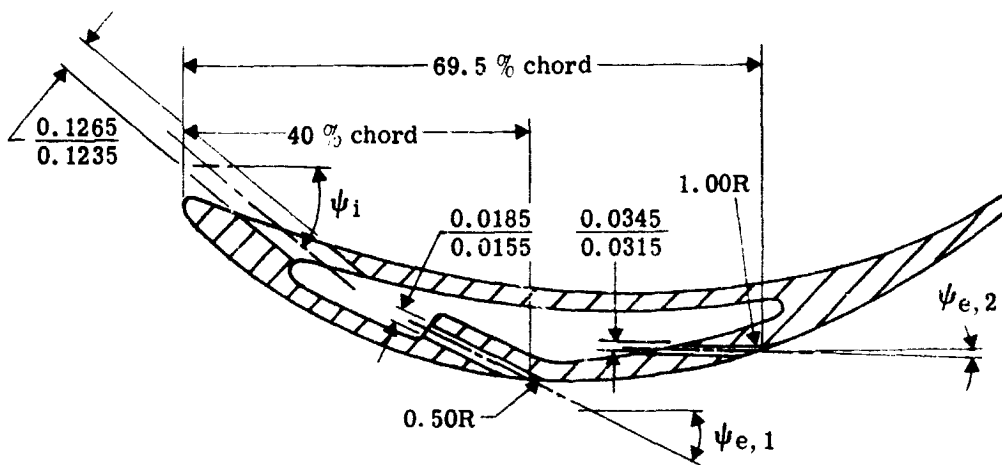


Figure 1. Compressor test facility.



5636-42

Figure 2. Layout of compressor test rig.



Note: Dimensions are in inches

Section	ψ_i	$\psi_{e,1}$	$\psi_{e,2}$
A - A	36° 30'	22° 30'	-1° 30'
B - B	37° 35'	23° 35'	-0° 25'
C - C	38° 19'	24° 19'	0° 19'
D - D	38° 50'	24° 50'	0° 50'
E - E	39° 42'	25° 42'	1° 42'

5861-3

Figure 3. Double slotted 0.75 hub diffusion factor stator slot configuration.

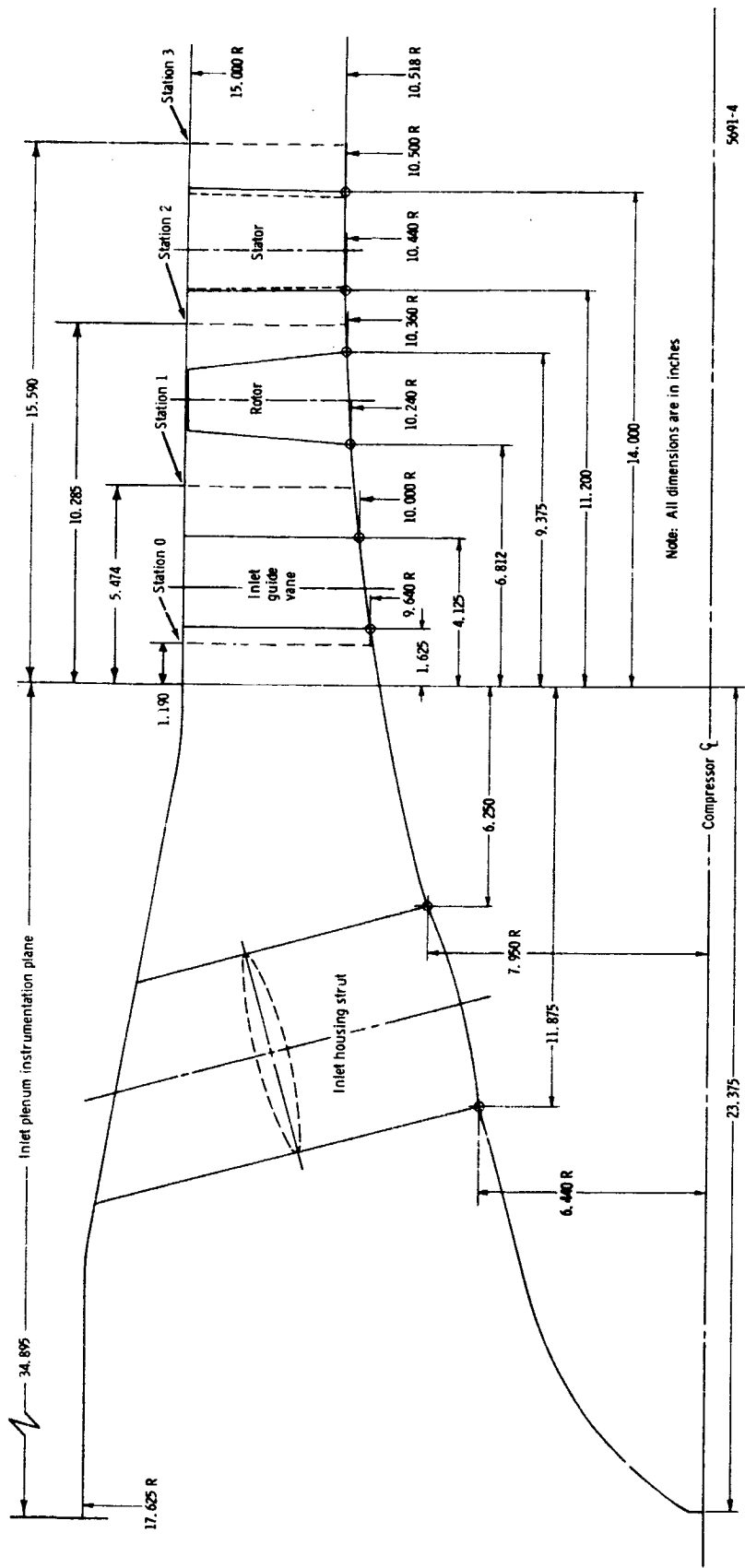
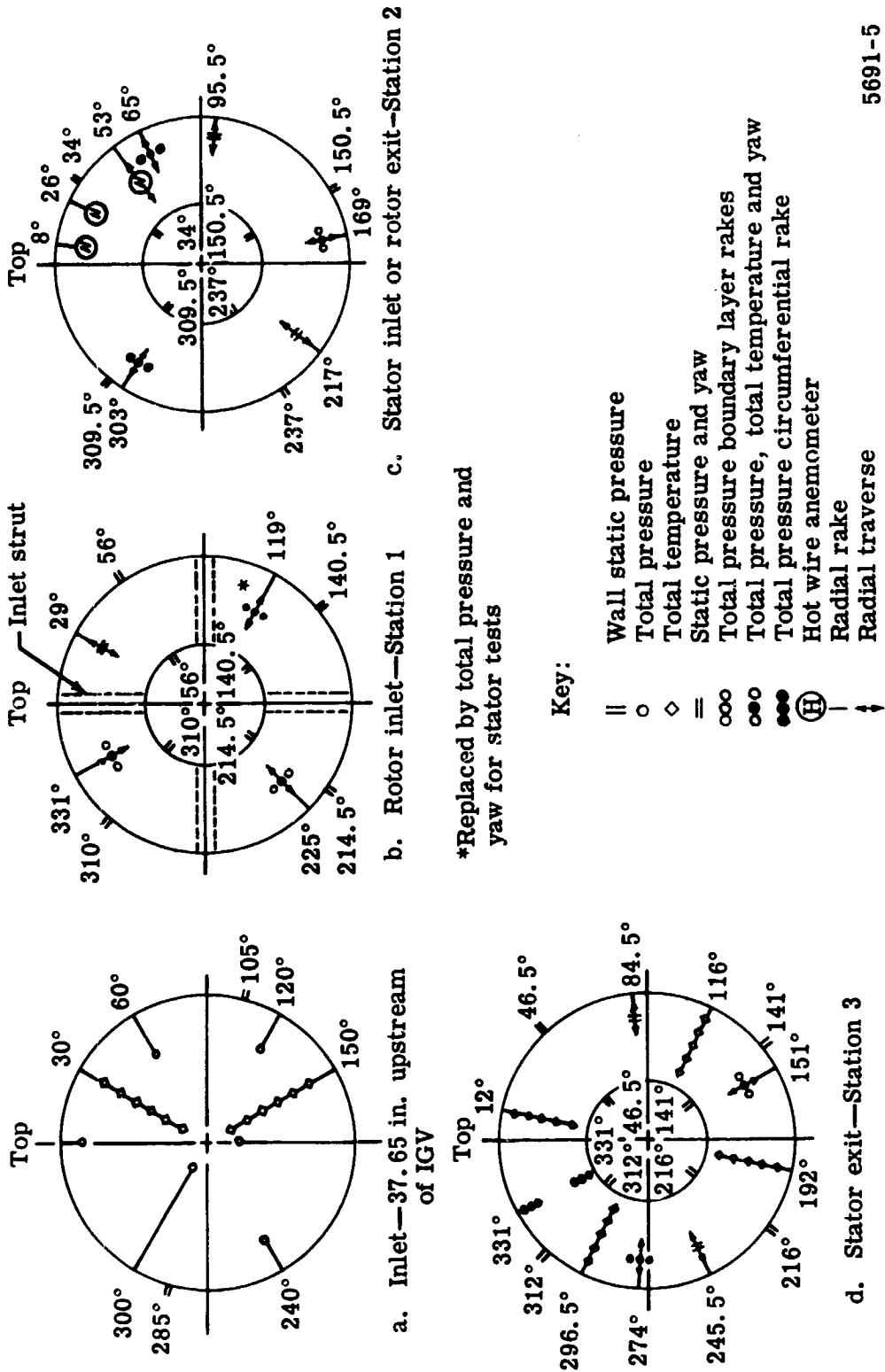
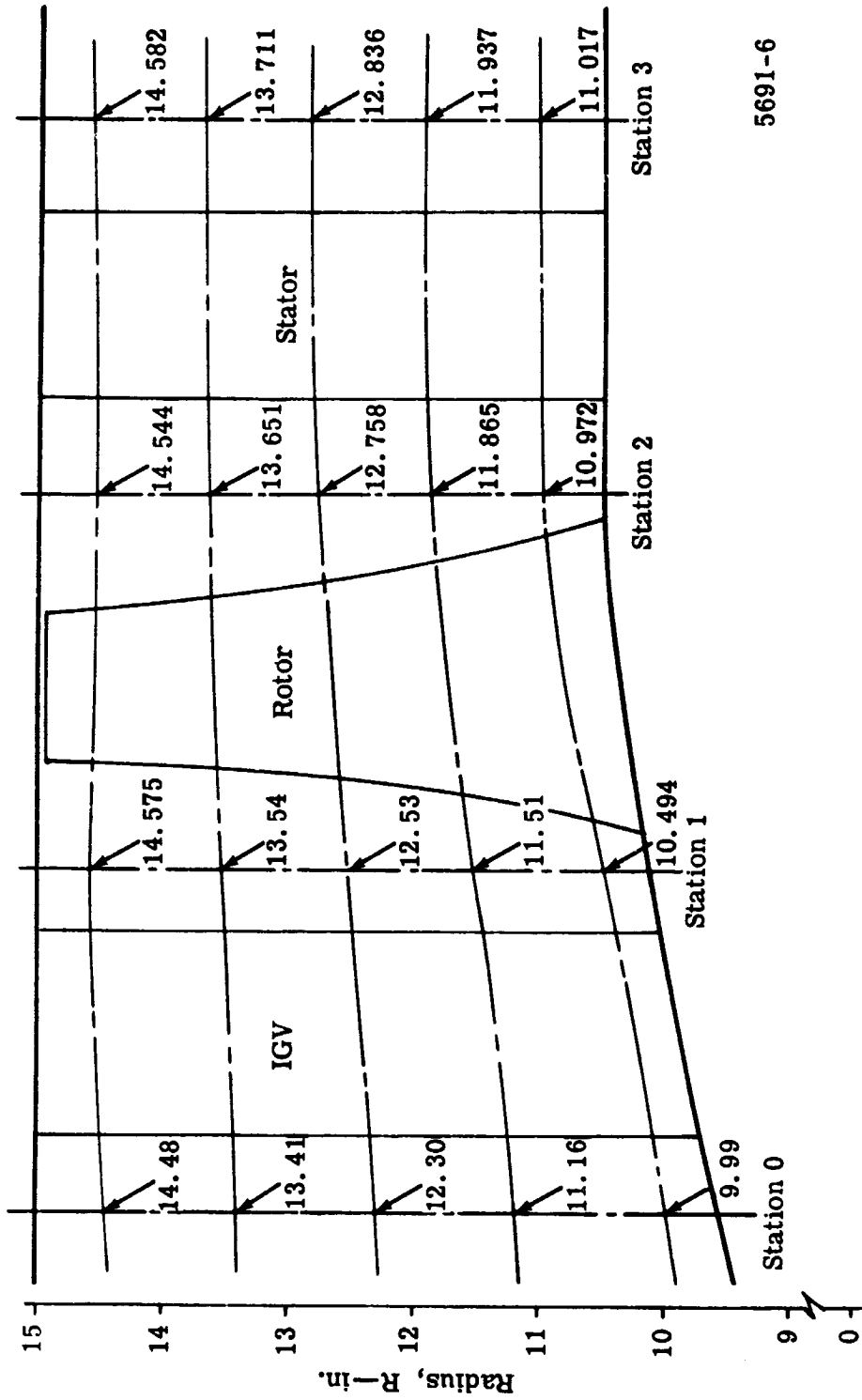


Figure 4. Test rig flow path.



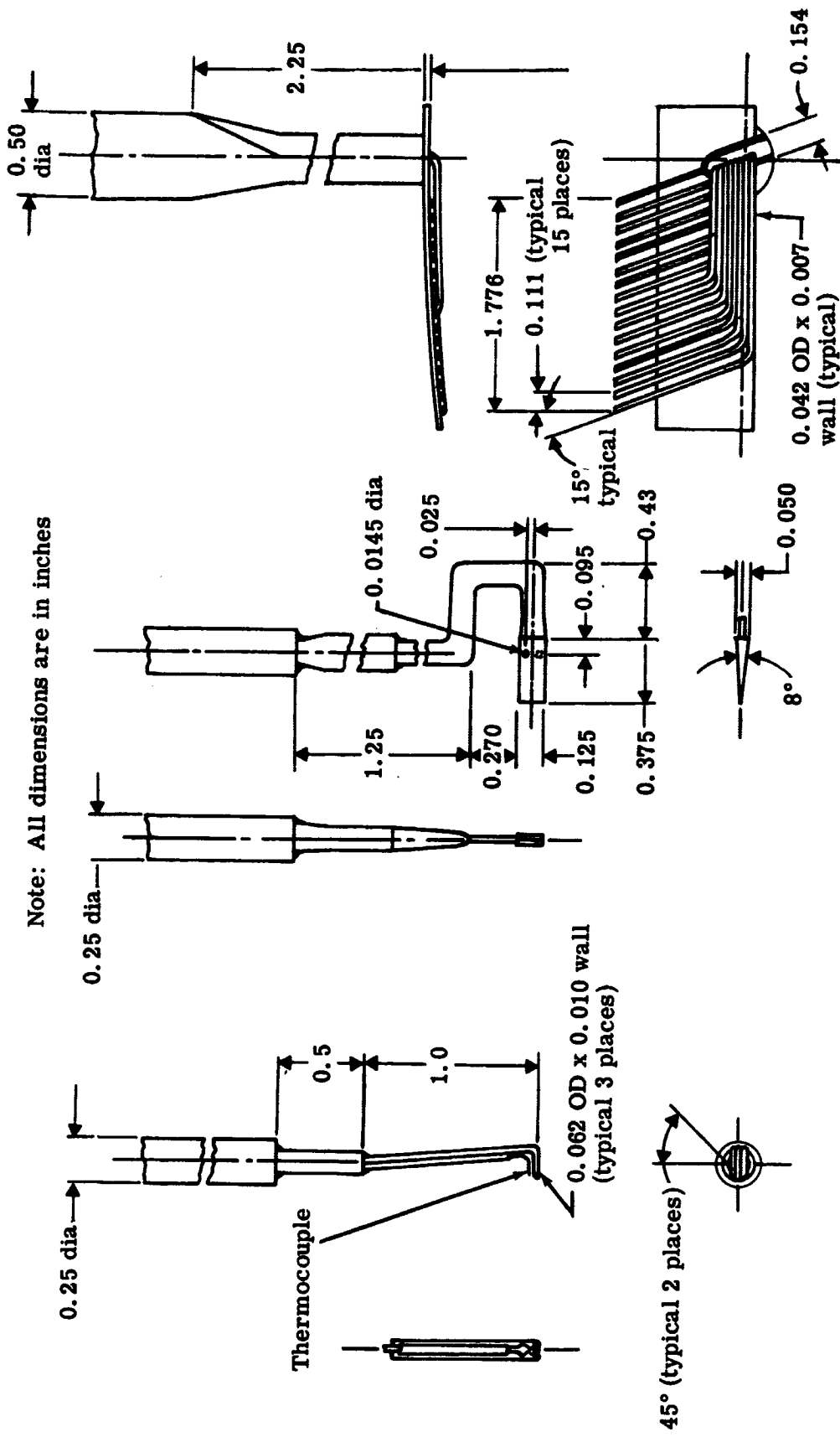
5691-5

Figure 5. Circumferential location of instrumentation viewed downstream.



5691-6

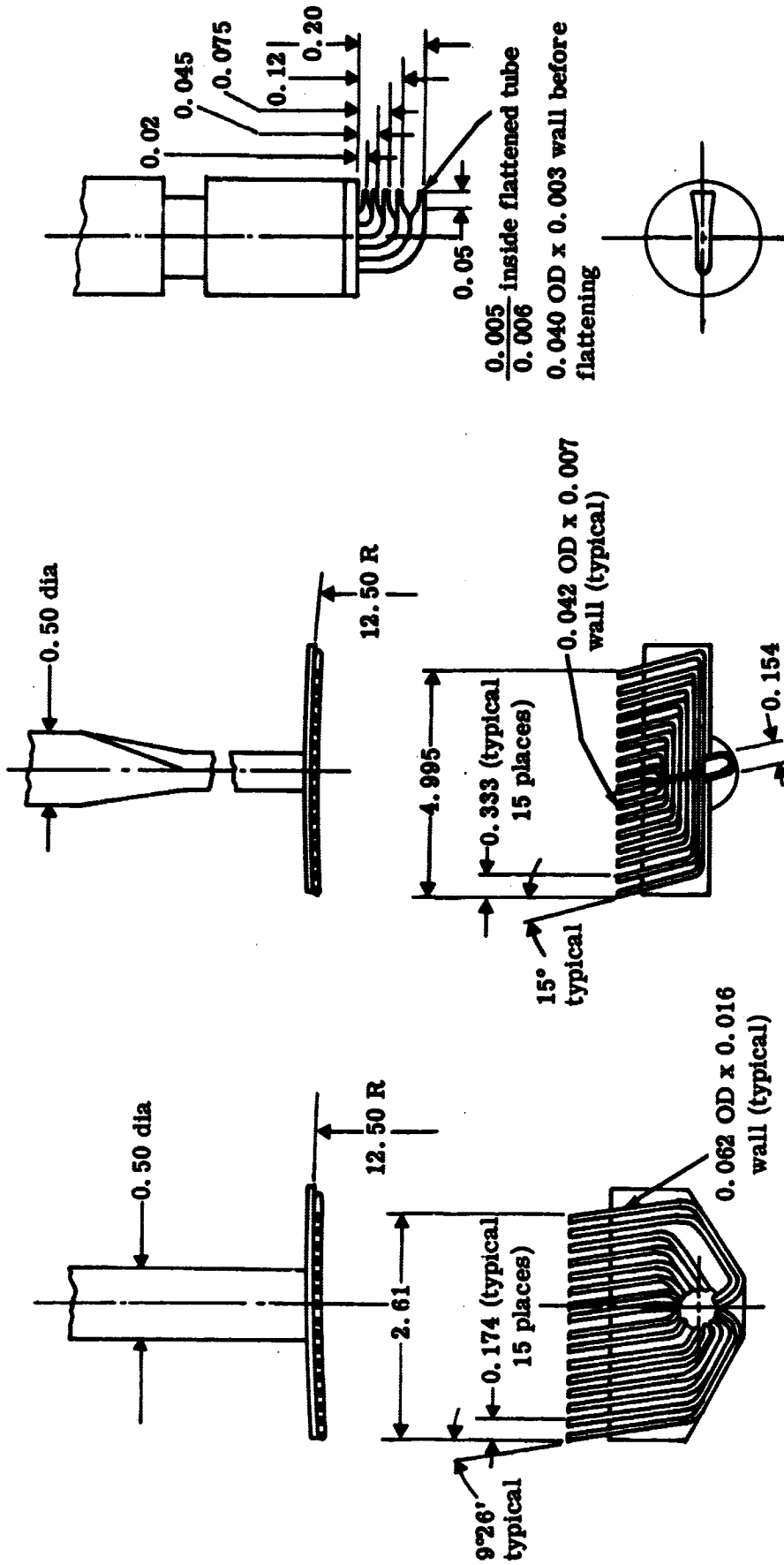
Figure 6. Radial location of streamlines for instrumentation positions.



- a. Total pressure, total temperature, and yaw probe
- b. Static pressure and yaw probe
- c. IGV circumferential rake

Figure 7. Schematics of survey instrumentation.

Note: All dimensions are in inches



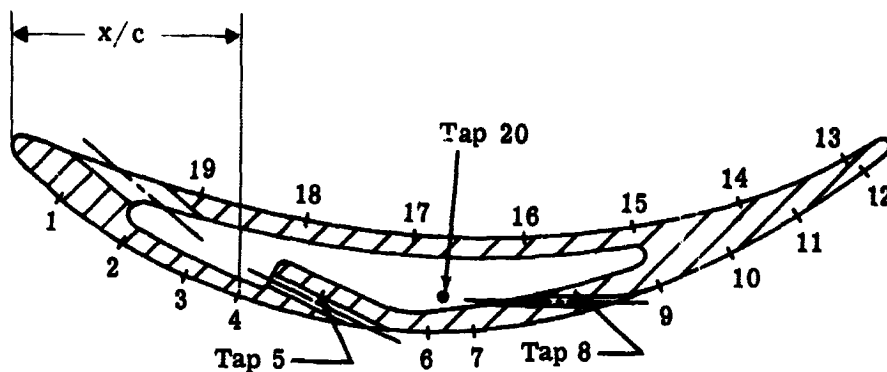
d. Stator circumferential rake

e. IGV wake persistence circumferential rake

f. Boundary layer probe for tip and hub

Figure 7. Schematics of survey instrumentation.

5691-8



Tap	1	2	3	4	5	6	7	8	9
x/c (%)	4.98	11.62	19.59	25.23	—	47.48	52.46	—	73.37
Vane No.	1	2	3	4	1	2	3	4	1

Tap	10	11	12	13	14	15	16	17	18
x/c (%)	81.34	88.98	96.28	94.29	82.67	70.72	58.10	45.82	33.53
Vane No.	2	3	4	1	2	3	4	1	2

Tap	19	20
x/c (%)	21.25	—
Vane No.	3	4

5861-9

Figure 8. Slotted stator vane static pressure tap locations at 10, 50, and 90% streamlines.

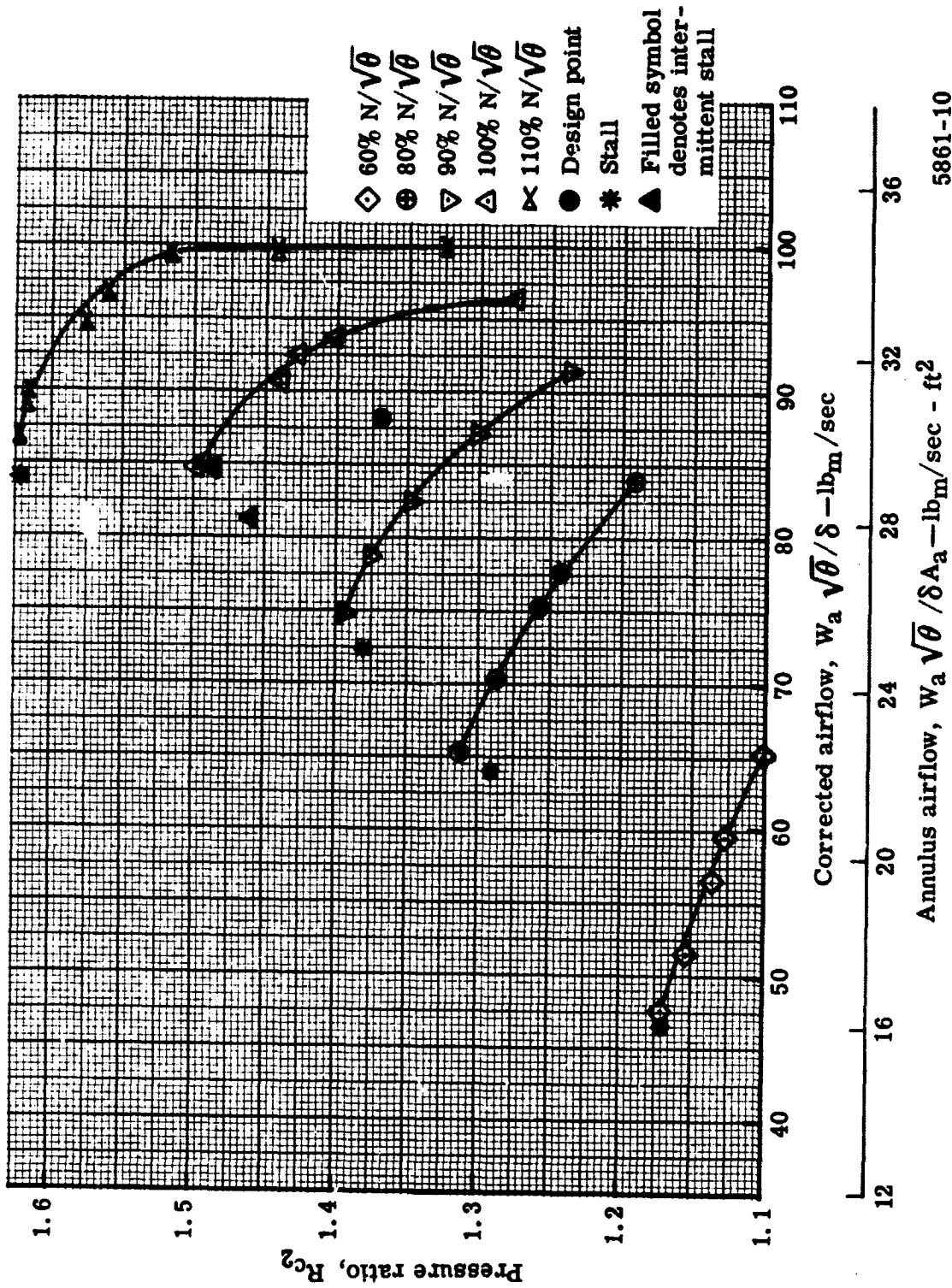
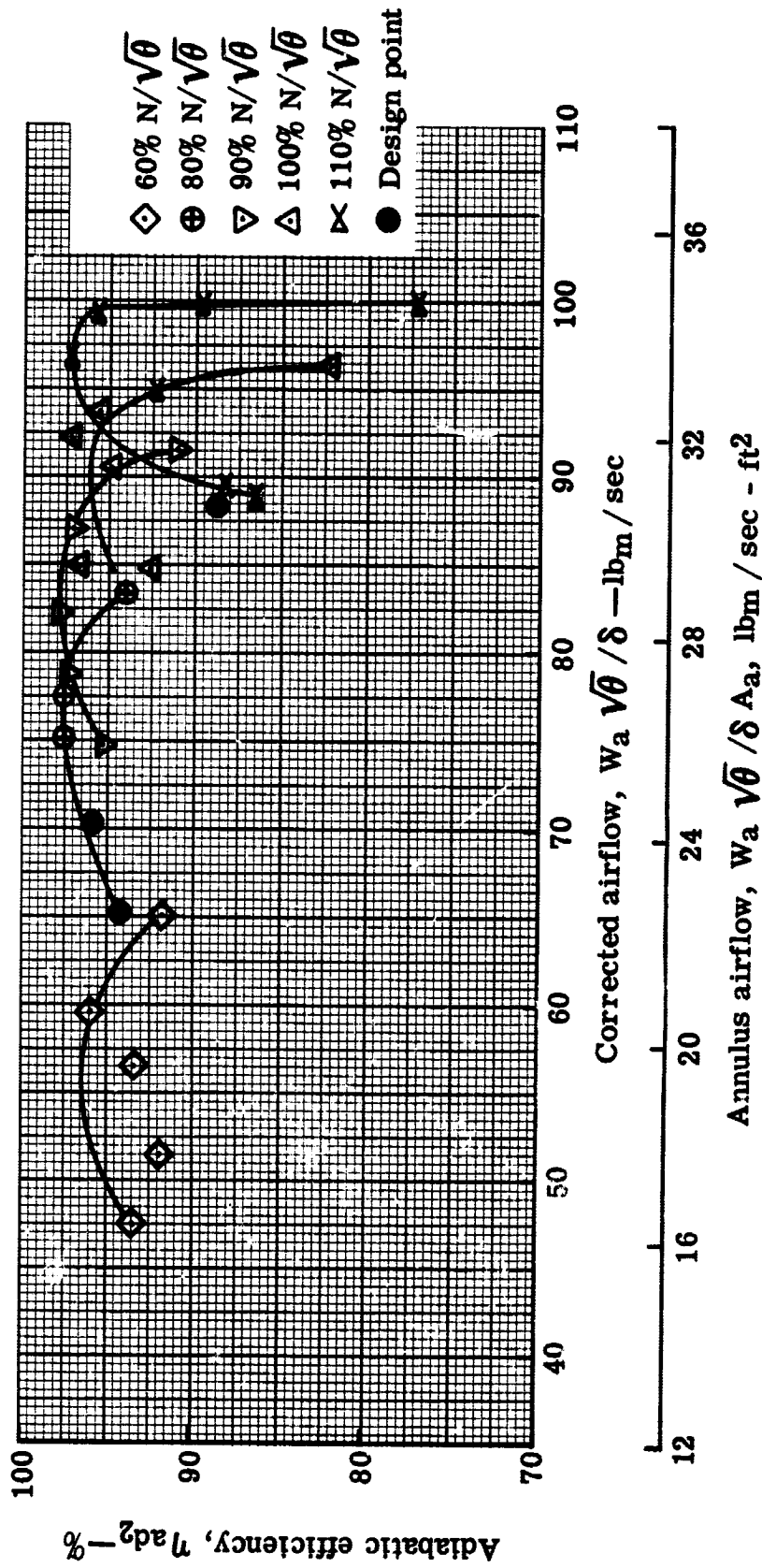
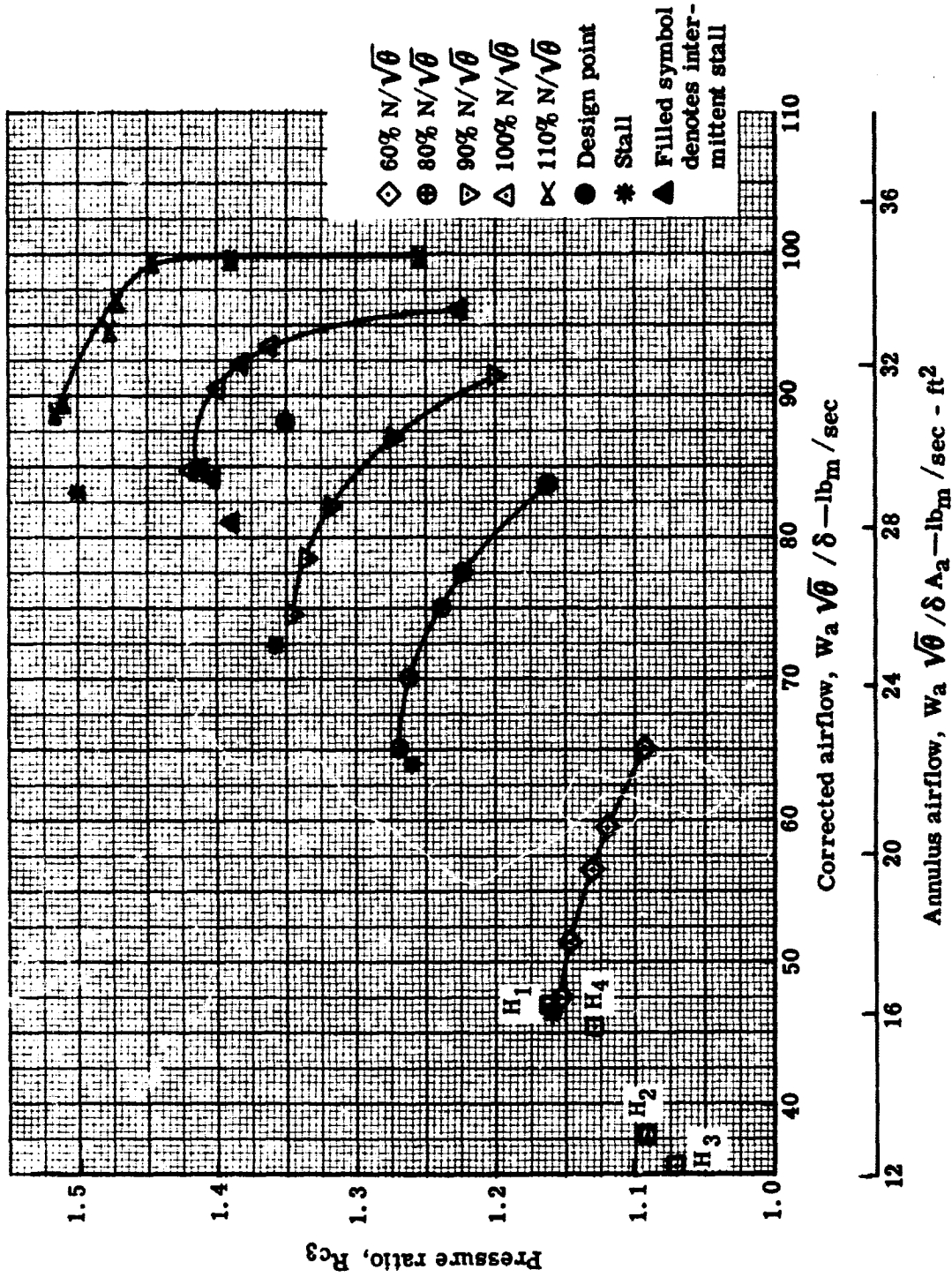


Figure 9. Flow generation rotor overall performance in stage test-pressure ratio.



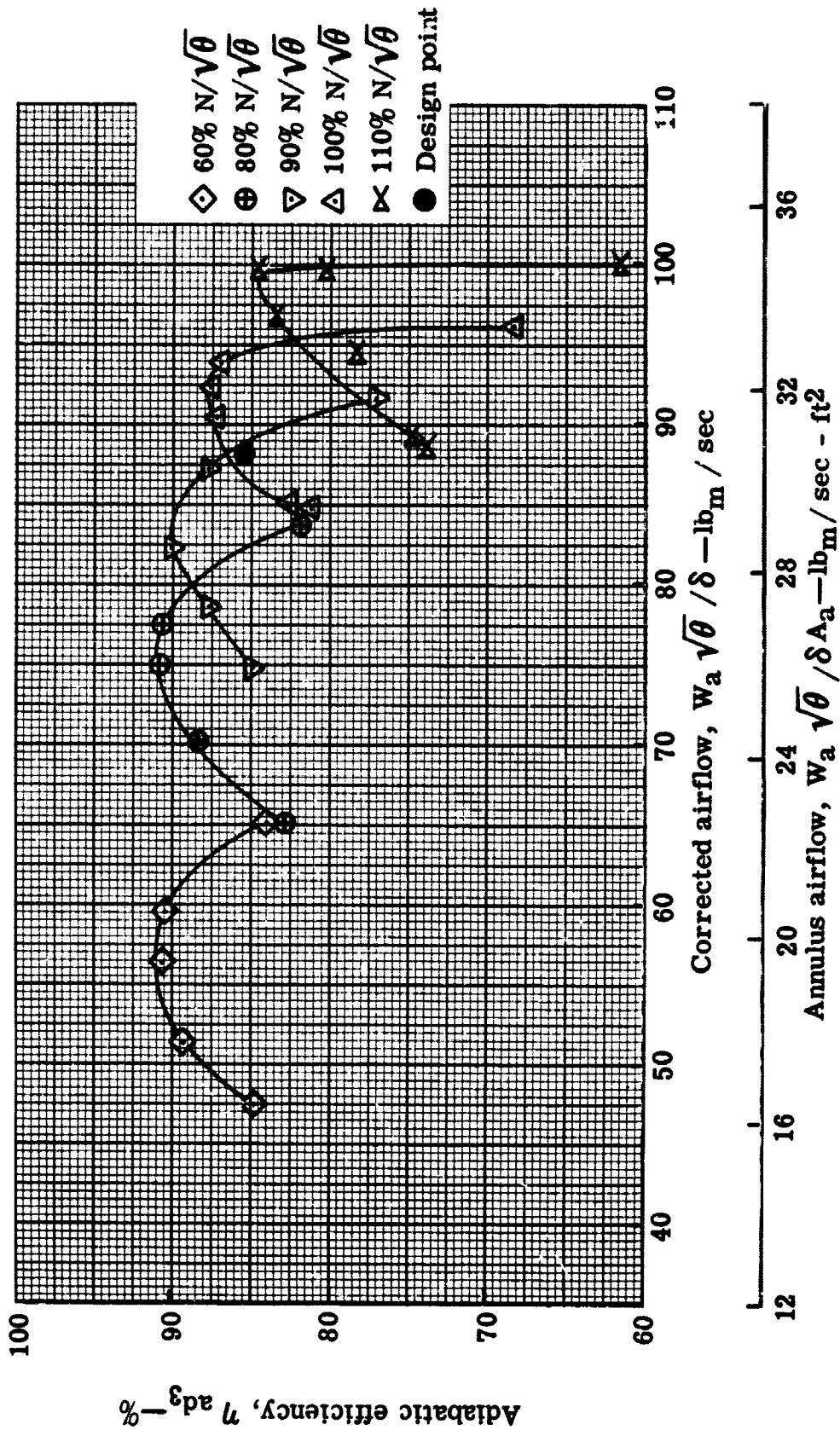
5861-11

Figure 10. Flow generation rotor overall performance in stage test-adiabatic efficiency.



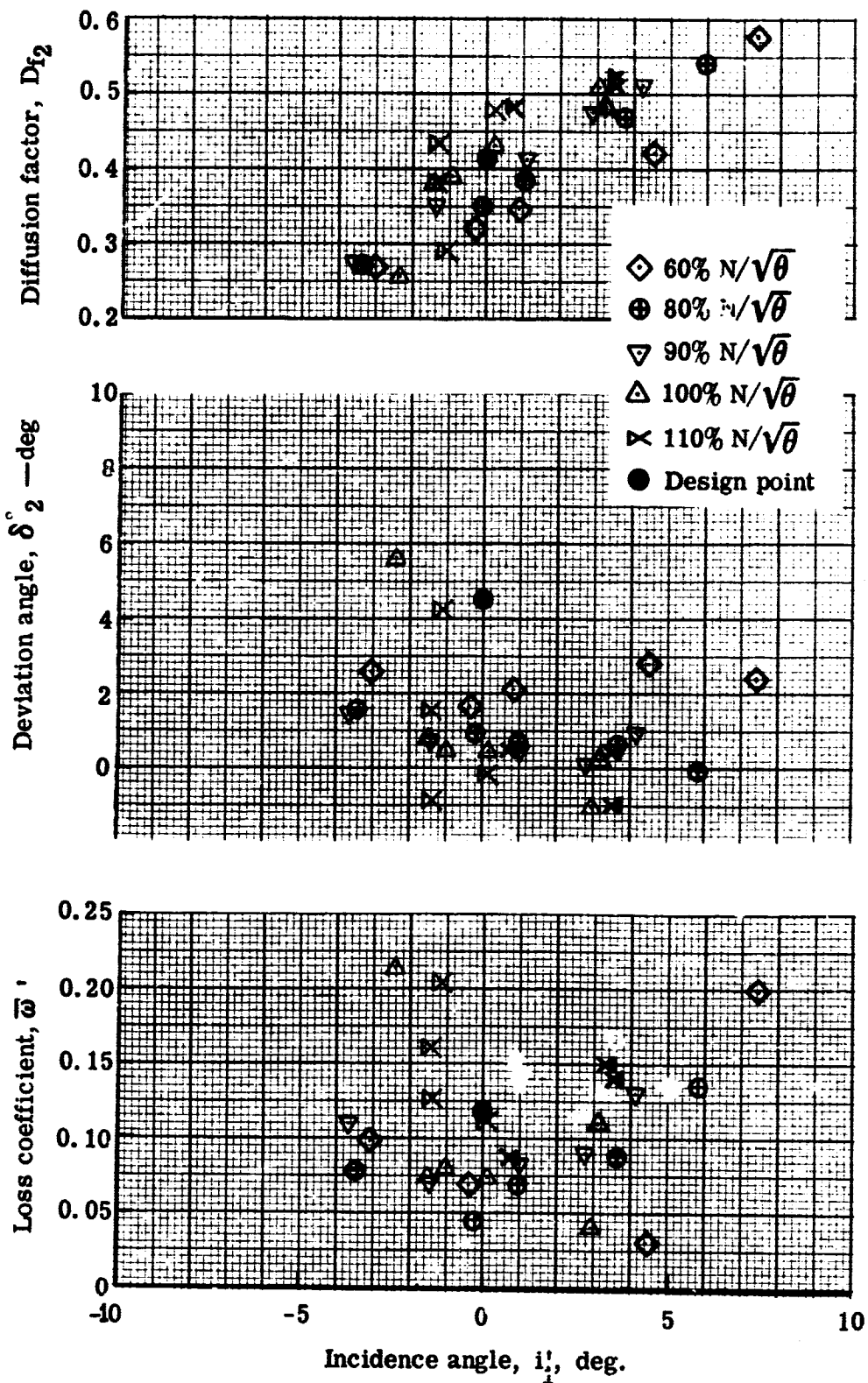
5861-12

Figure 11. Stage overall performance-pressure ratio.



5861-13

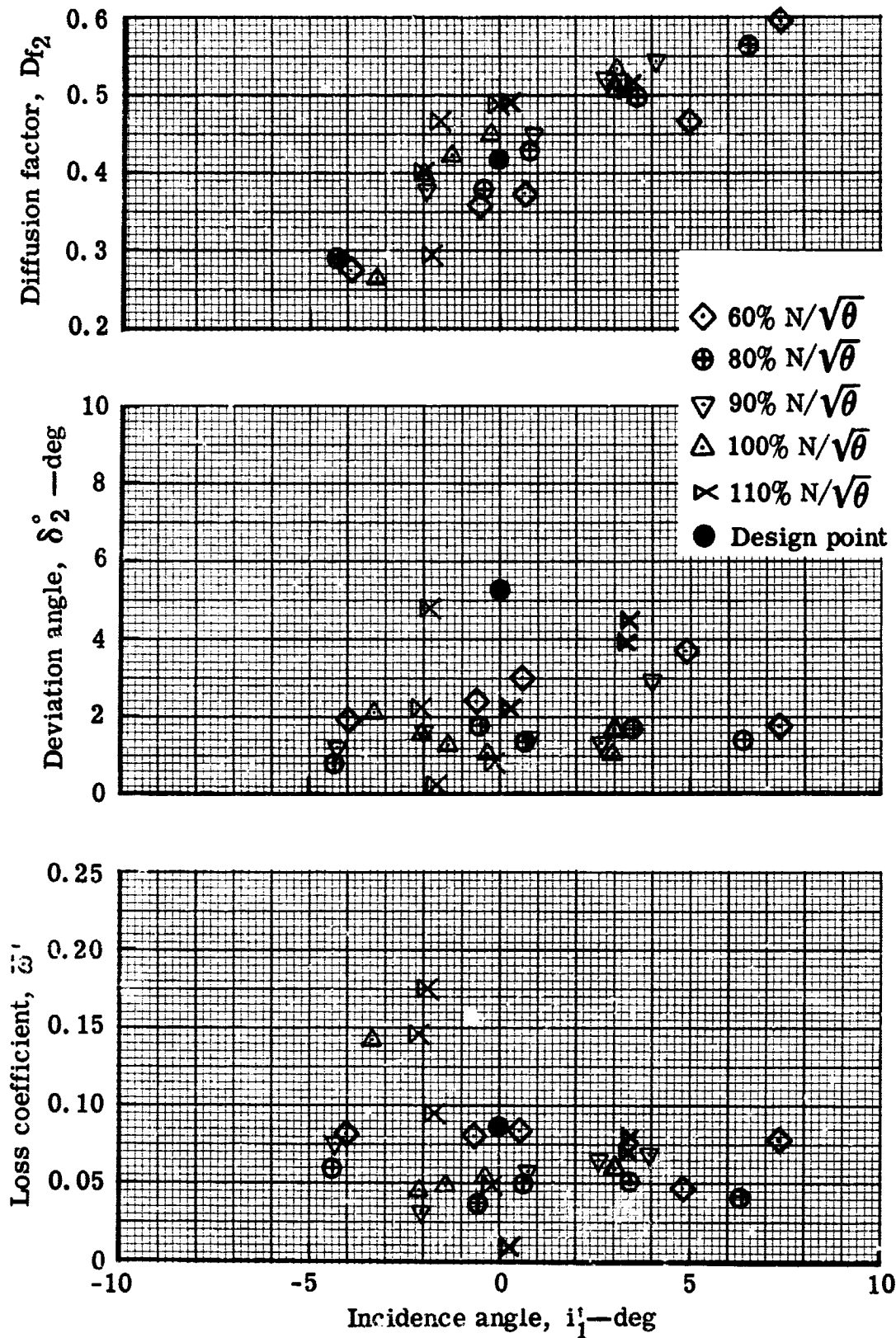
Figure 12. Stage overall performance-adiabatic efficiency.



a. 10% streamline from tip

5861-14

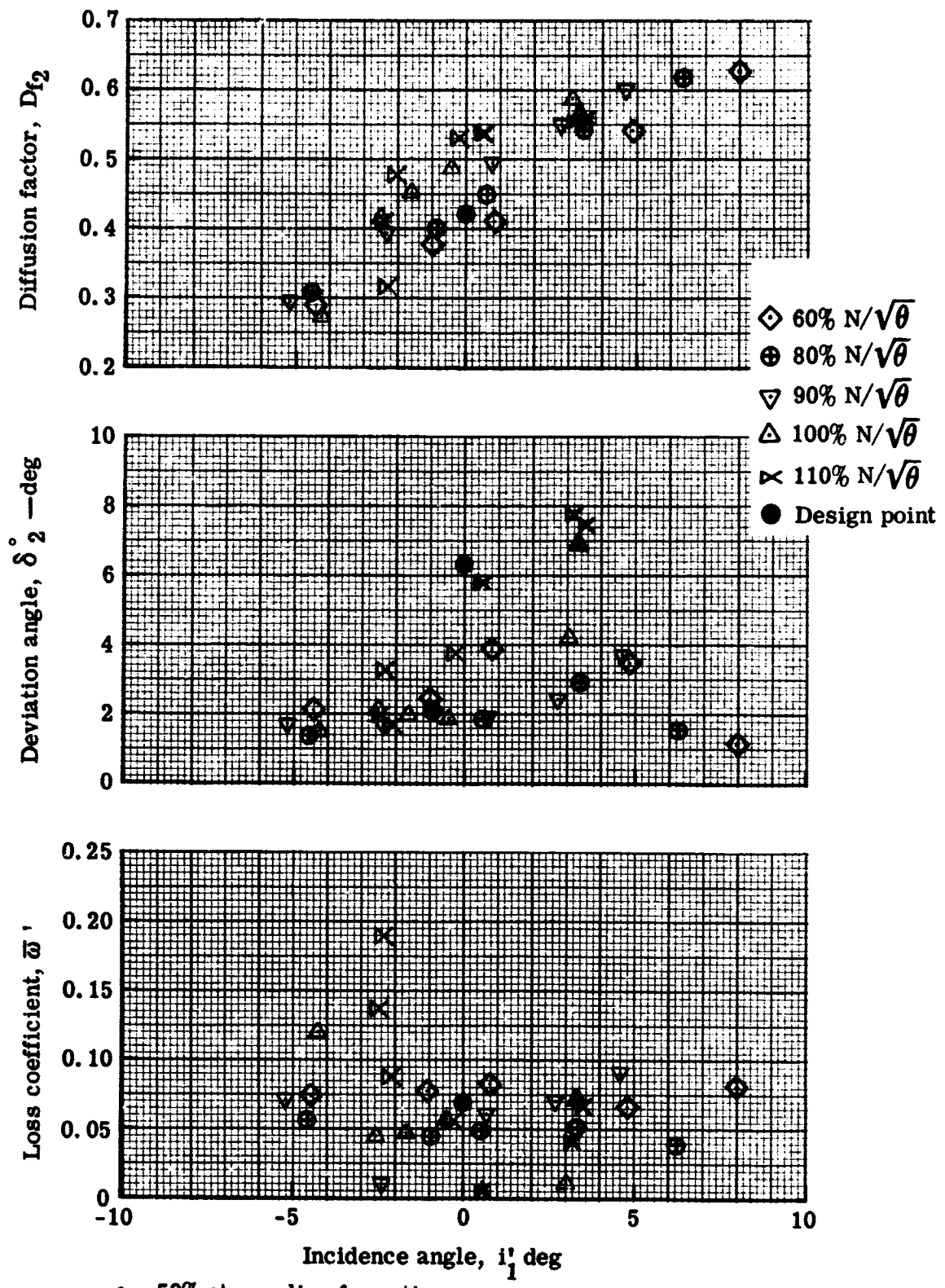
Figure 13. Rotor blade element performance-stage test.



b. 30% streamline from tip

5861-15

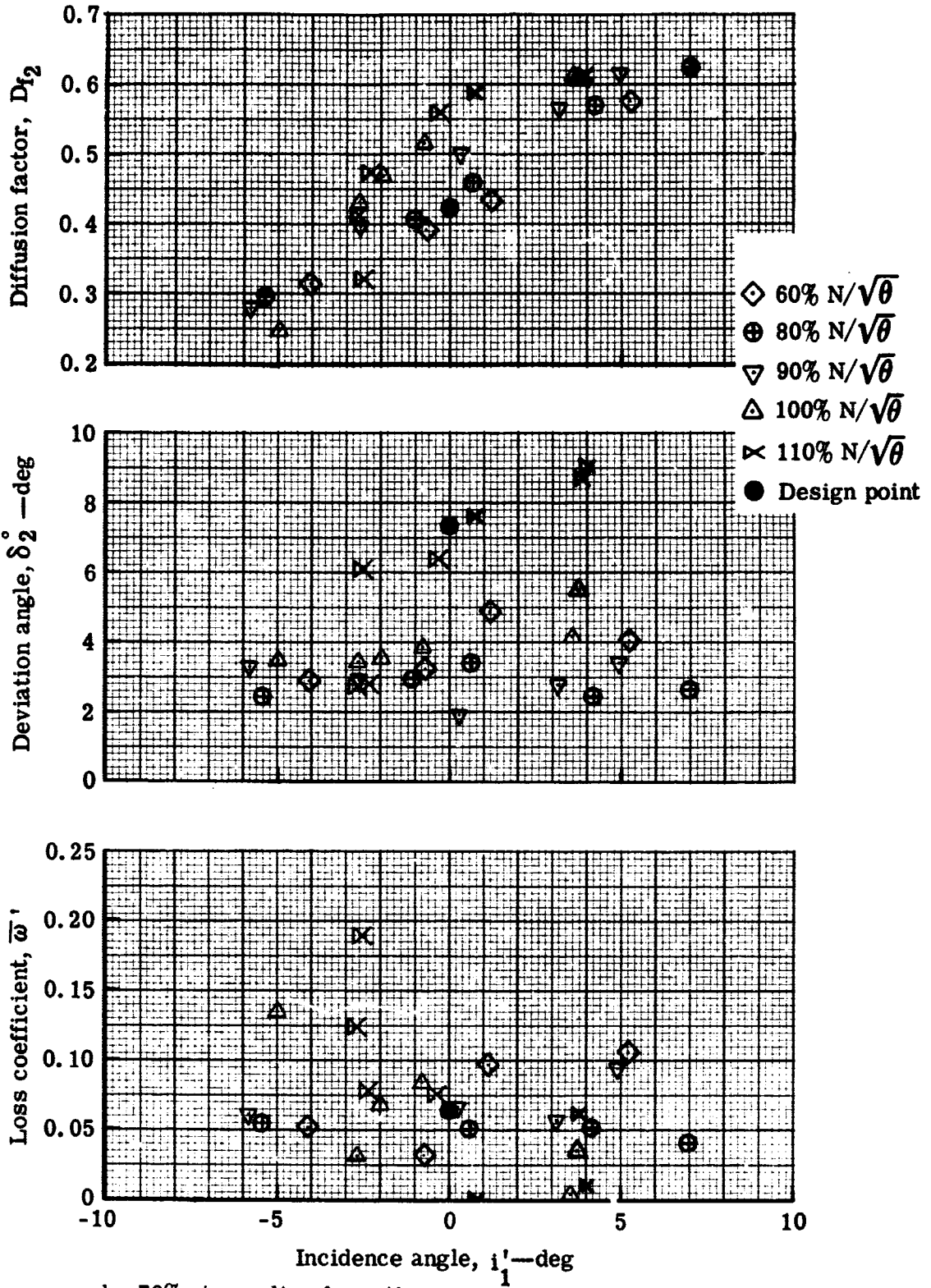
Figure 13. Rotor blade element performance-stage test.



c. 50% streamline from tip

5861-16

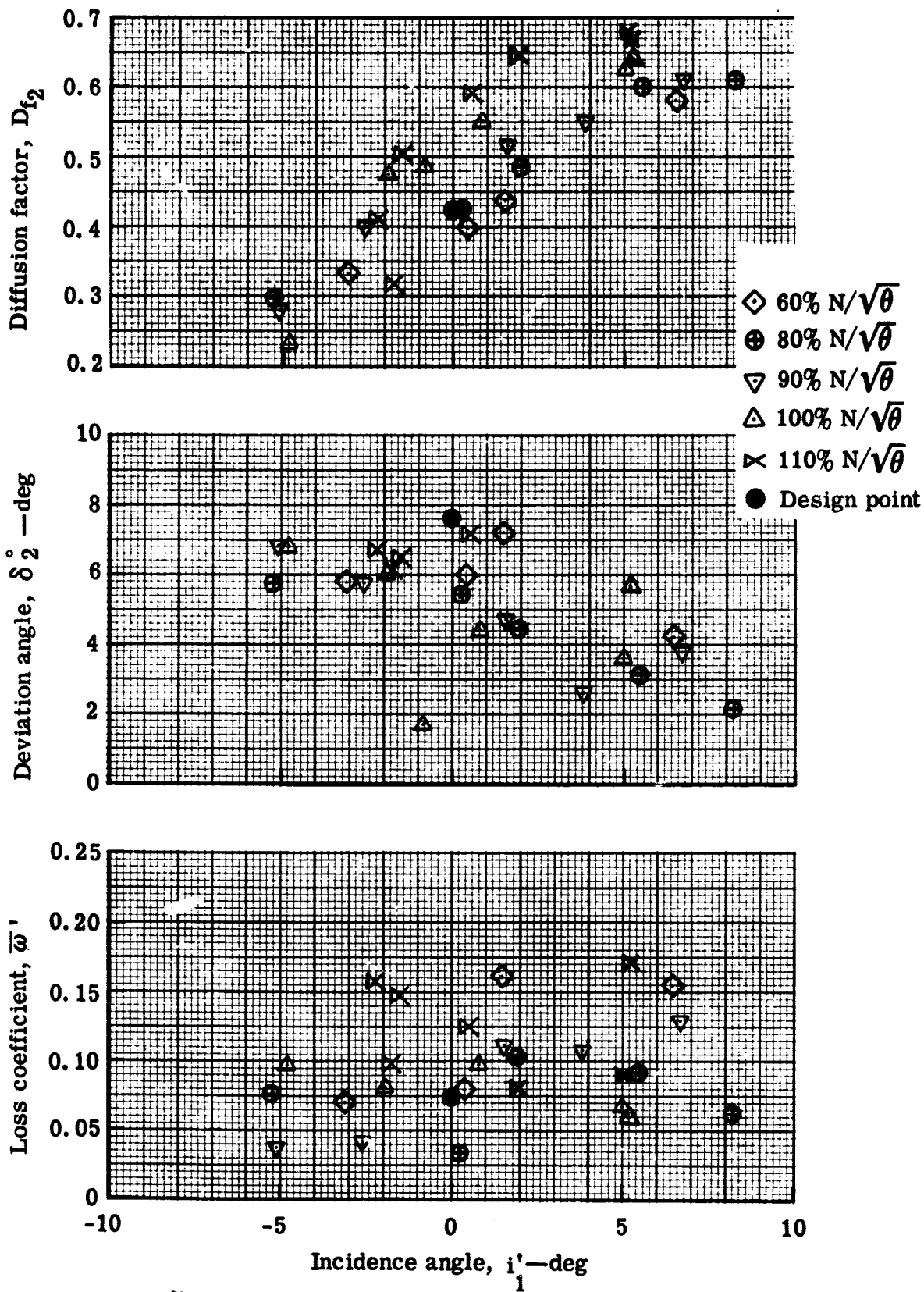
Figure 13. Rotor blade element performance-stage test.



d. 70% streamline from tip

5861-17

Figure 13. Rotor blade element performance-stage test.

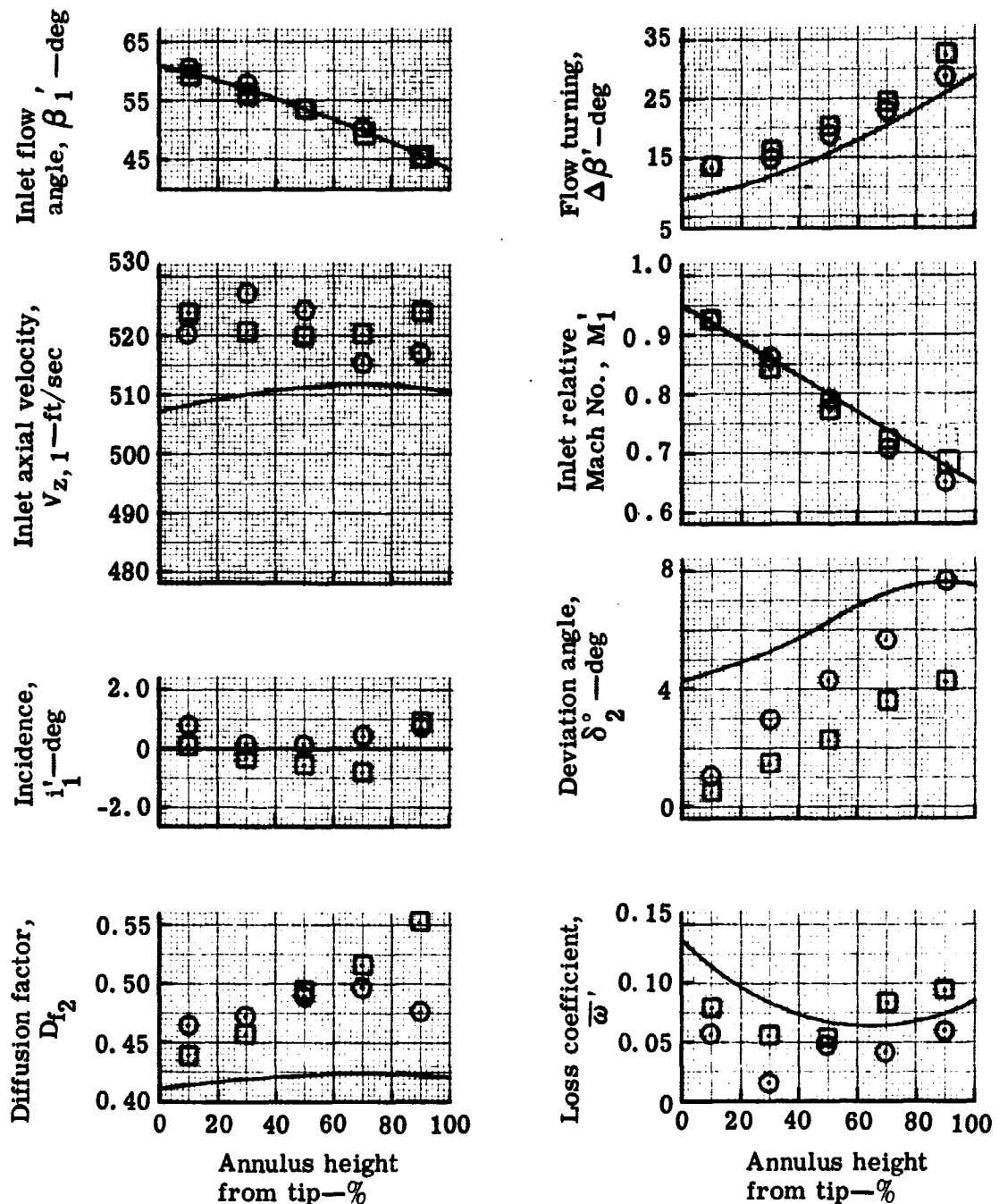


e. 90% streamline from tip

5861-18

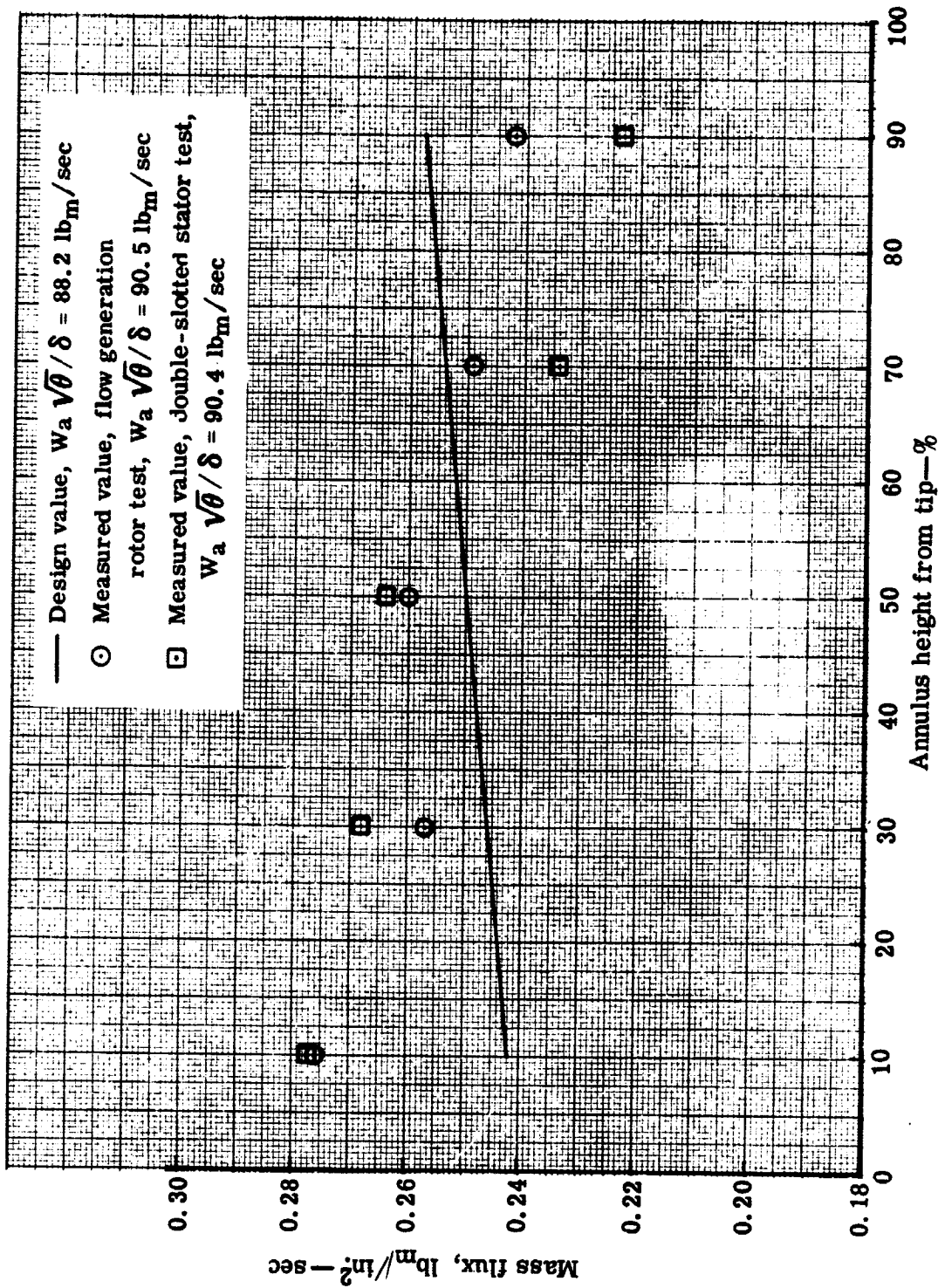
Figure 13. Rotor blade element performance-stage test.

- Design, $W_a \sqrt{\theta}/\delta = 88.2 \text{ lb}_m/\text{sec}$, $N/\sqrt{\theta} = 100\%$
- Flow generation rotor test, $W_a \sqrt{\theta}/\delta = 89.3 \text{ lb}_m/\text{sec}$, $N/\sqrt{\theta} = 99.3\%$
- Slotted stator test, $W_a \sqrt{\theta}/\delta = 90.4 \text{ lb}_m/\text{sec}$, $N/\sqrt{\theta} = 99.9\%$



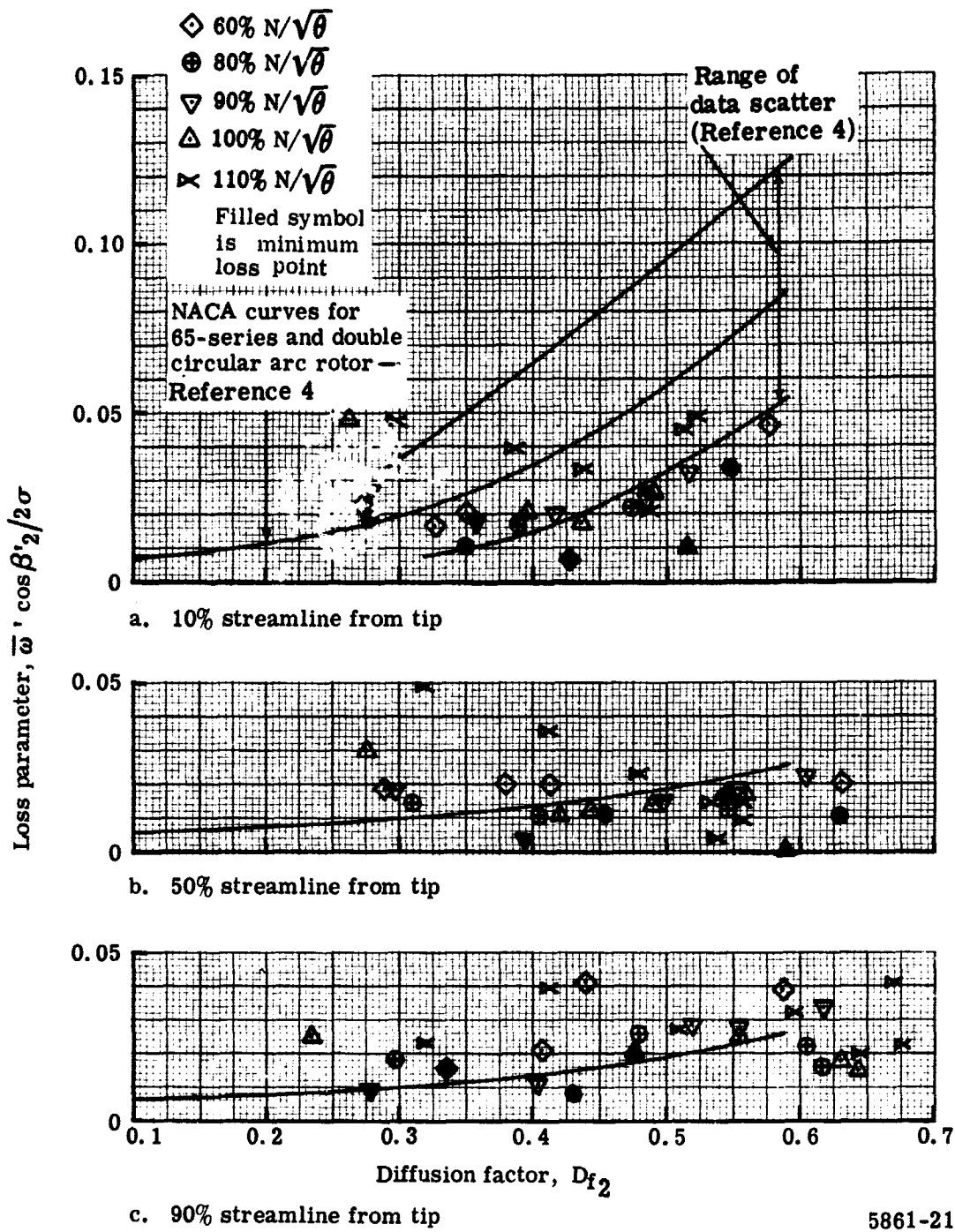
5861-19

Figure 14. Radial variation of rotor blade element performance.



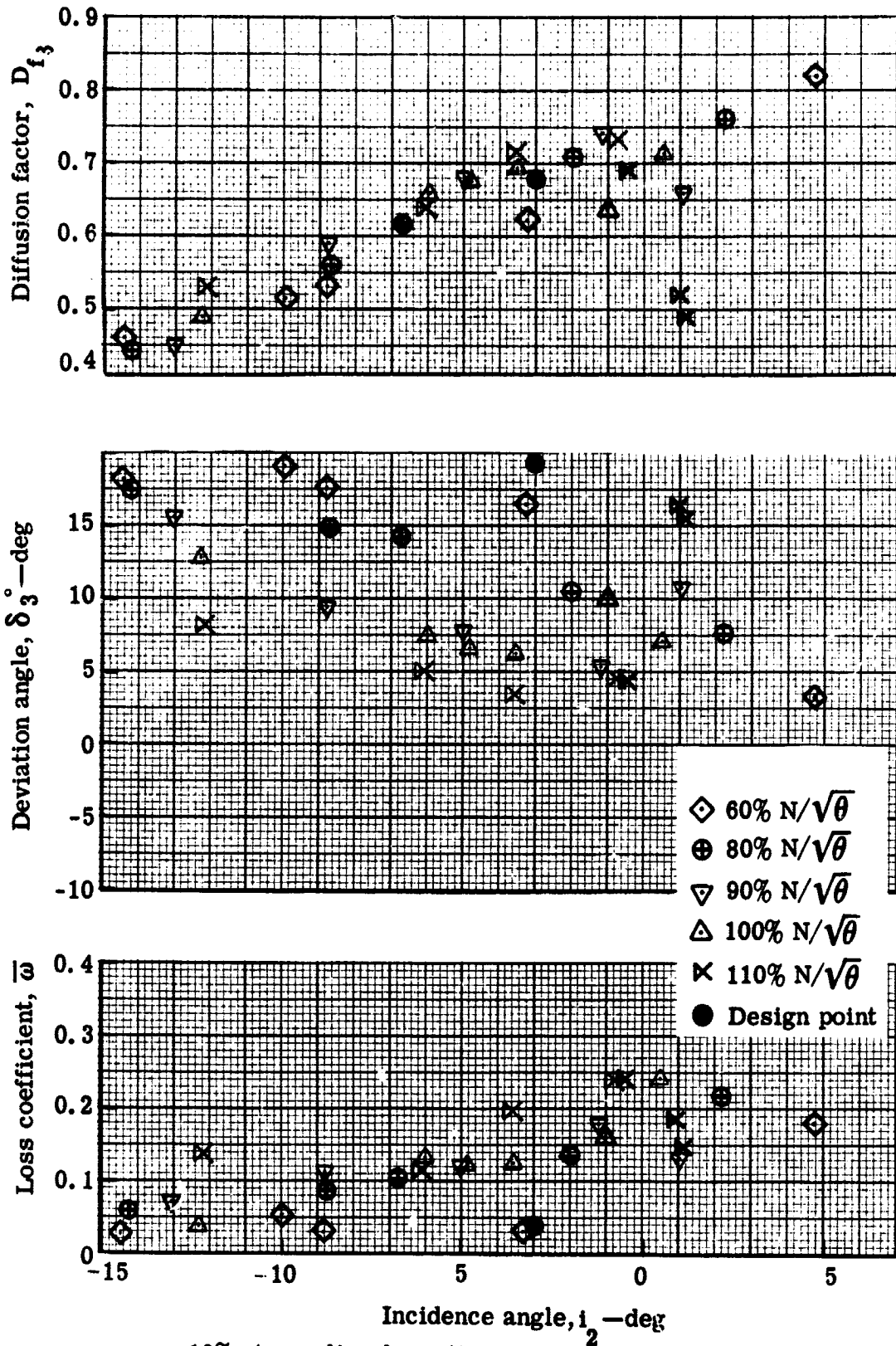
5861-20

Figure 15. Rotor out radial mass flux distribution at design speed.



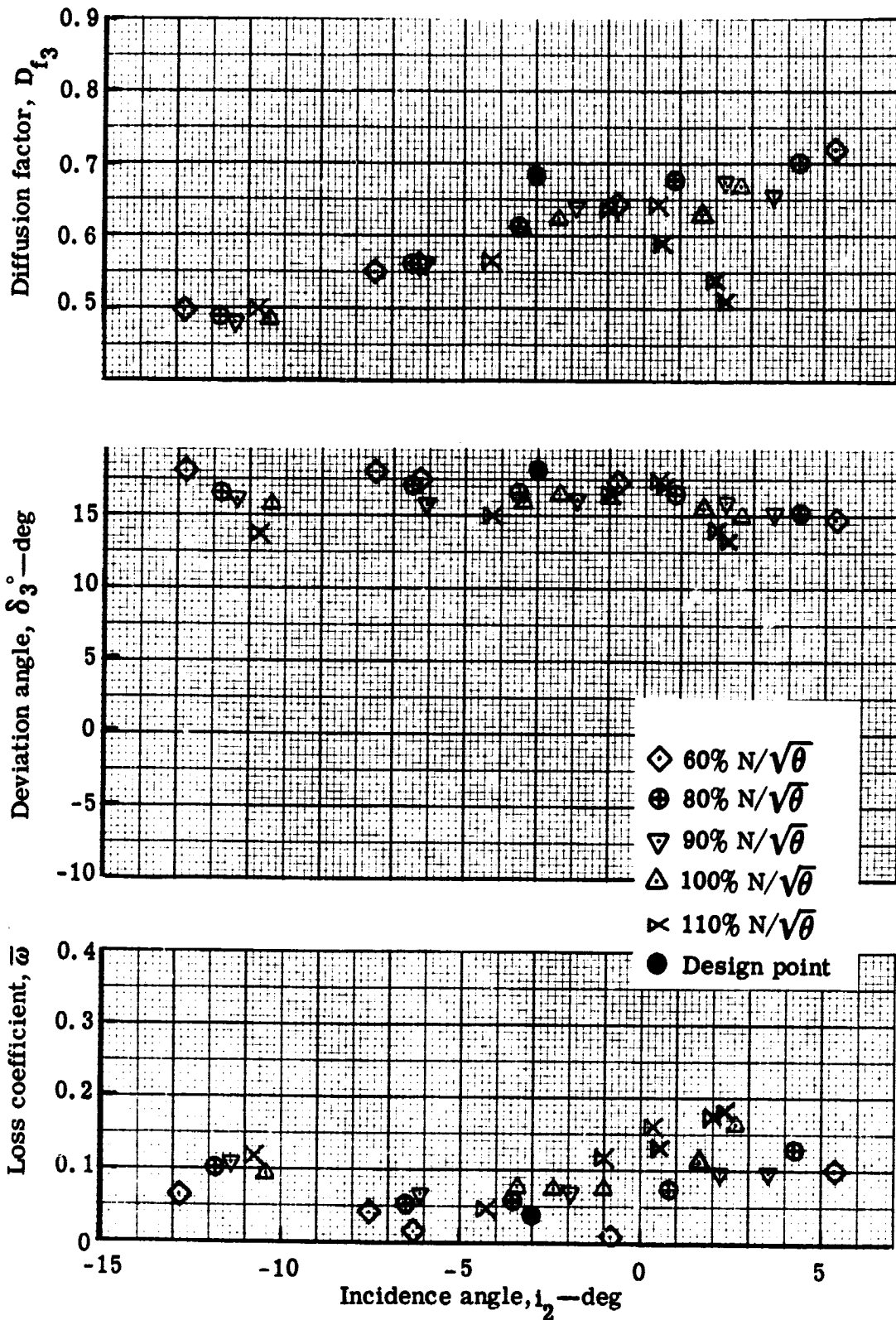
5861-21

Figure 16. Rotor loss parameter versus diffusion factor.



5861-22

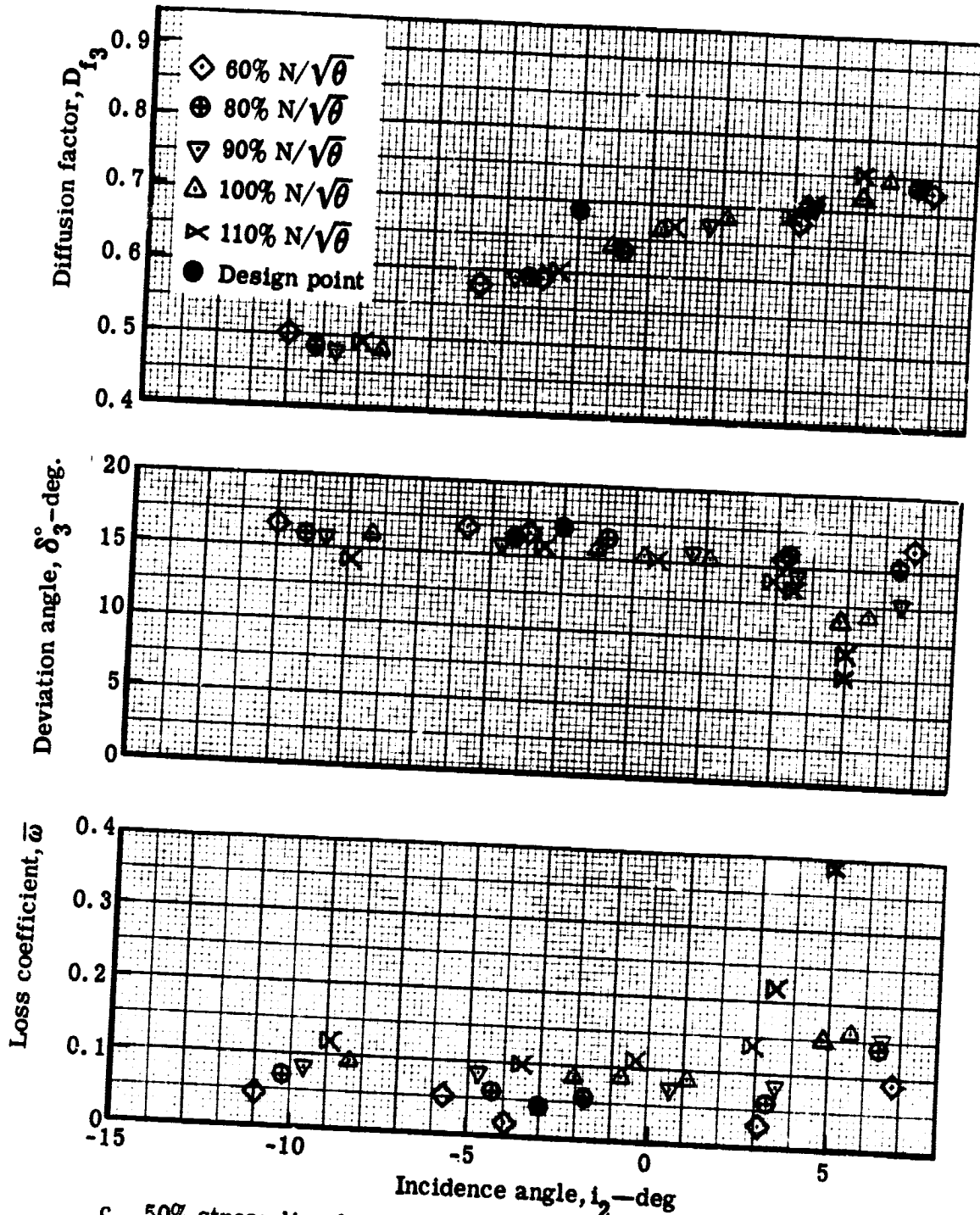
Figure 17. Slotted stator blade element performance.



b. 30% streamline from tip

5861-23

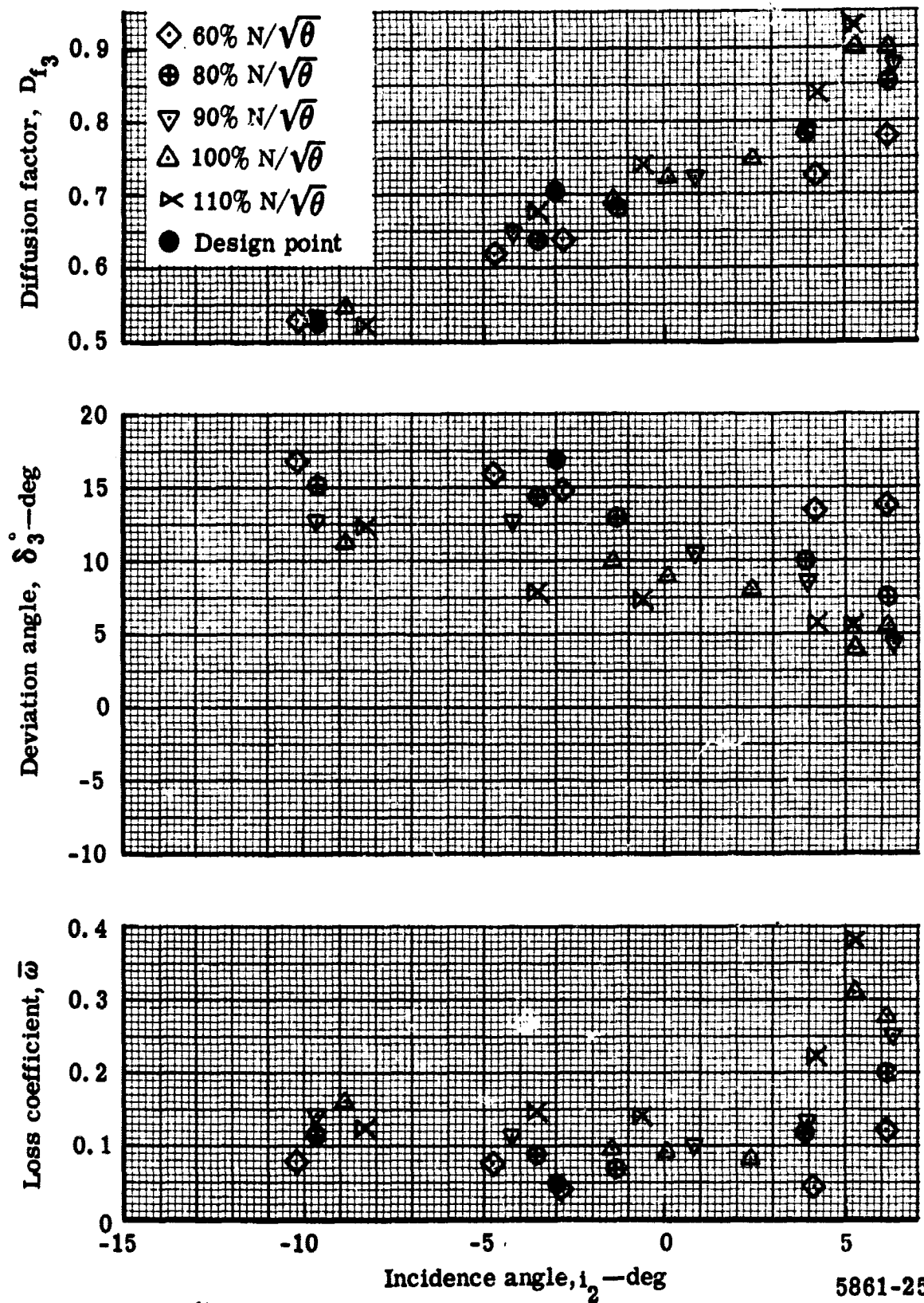
Figure 17. Slotted stator blade element performance.



c. 50% streamline from tip

5861-24

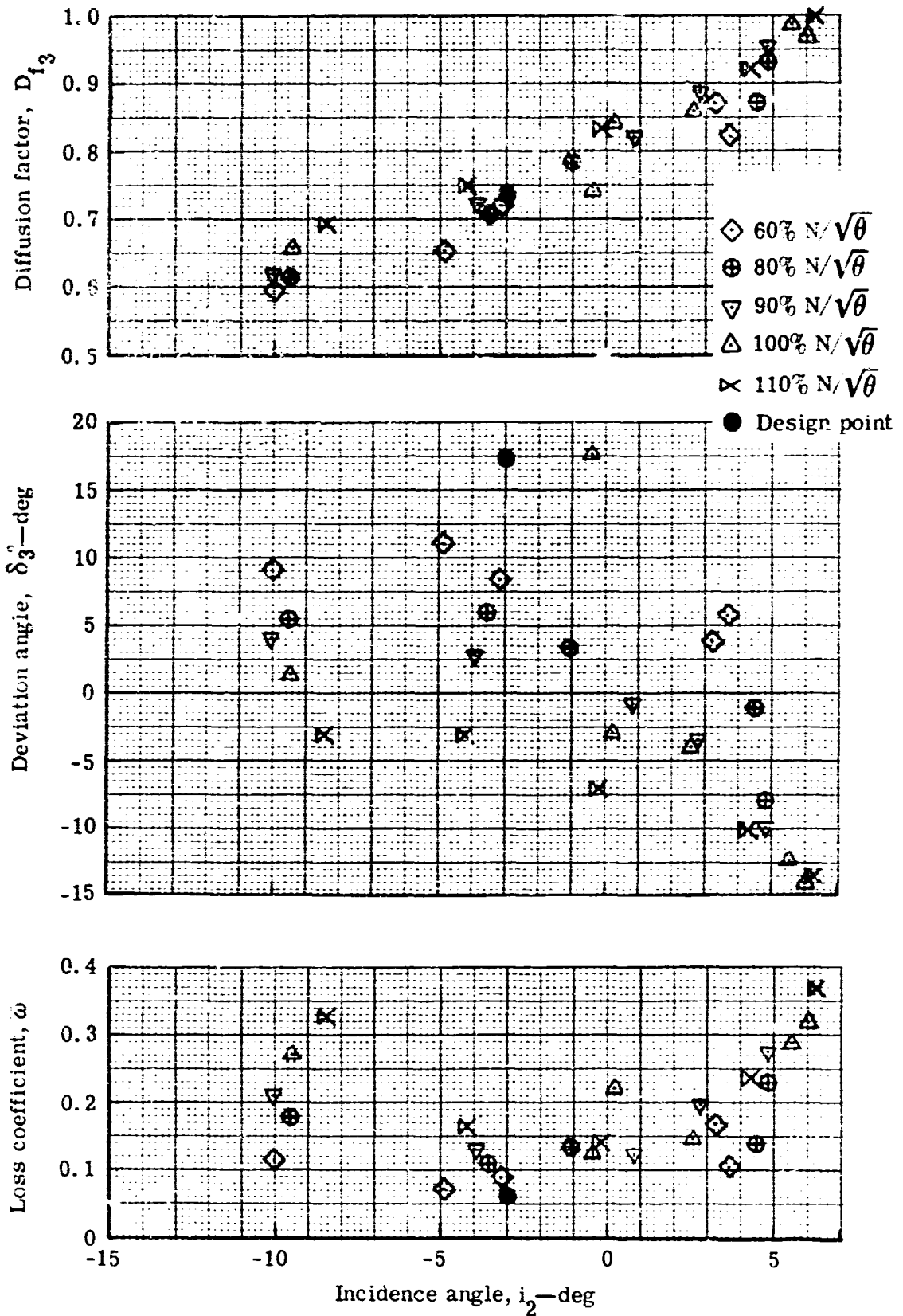
Figure 17. Slotted stator blade element performance.



d. 70% streamline from tip

5861-25

Figure 17. Slotted stator blade element performance.



e. 90% streamline from tip

5861-26

Figure 17. Slotted stator b' de element performance.

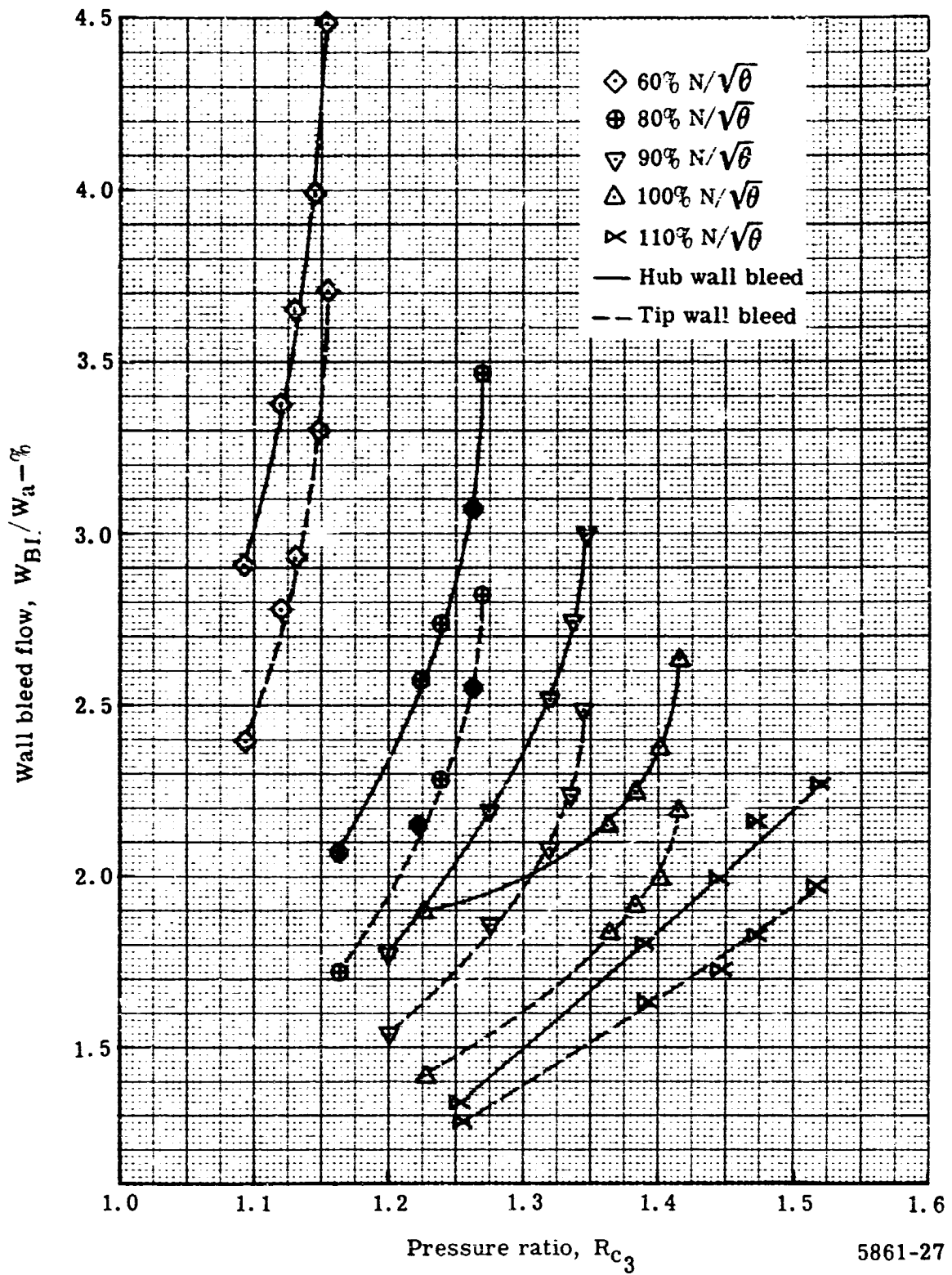
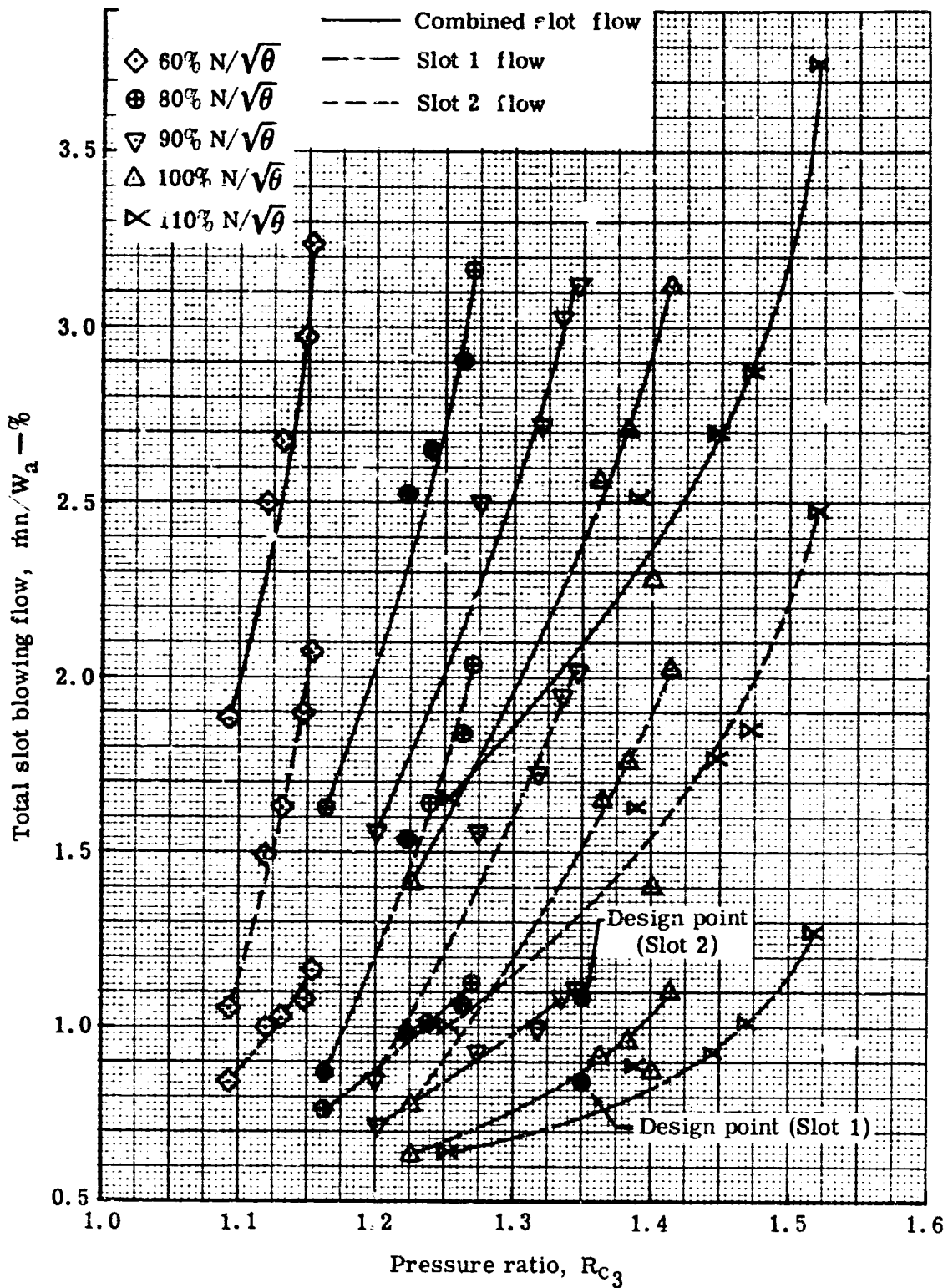
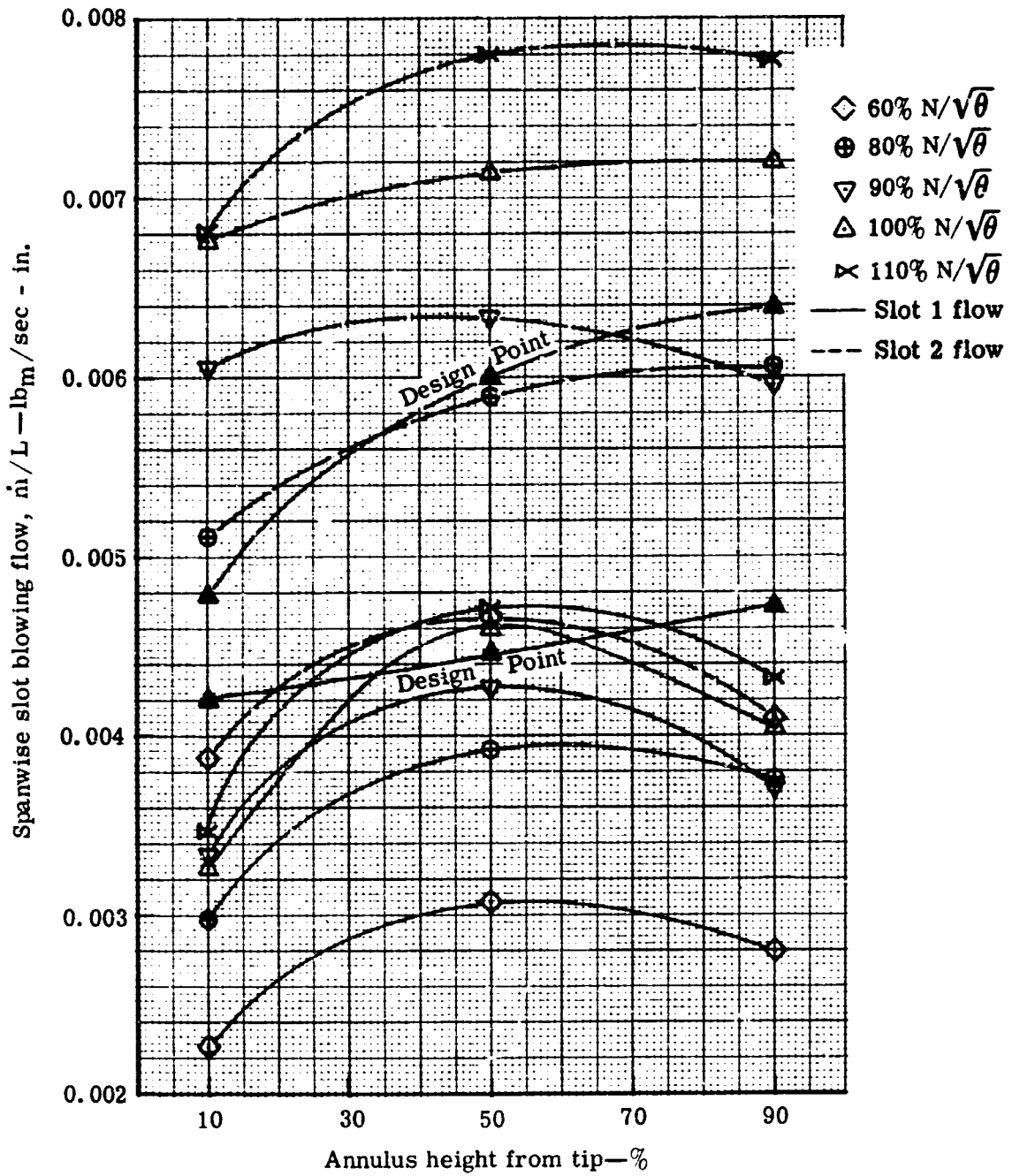


Figure 18. Variation of wall bleed flows with stage pressure ratio.



5861-28

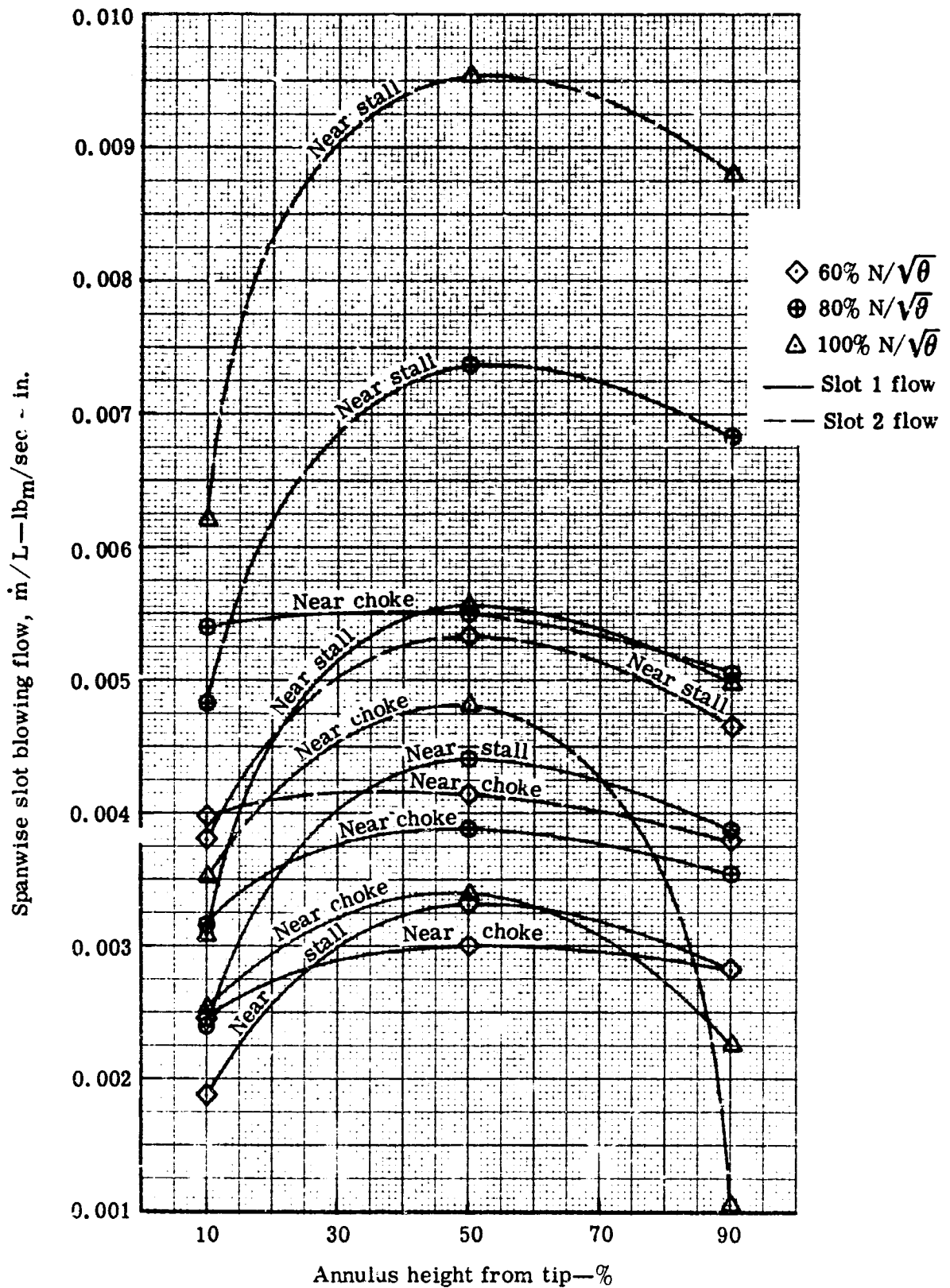
Figure 19. Stator slot blowing flow versus stage pressure ratio.



a. At stator design incidence

5861-29

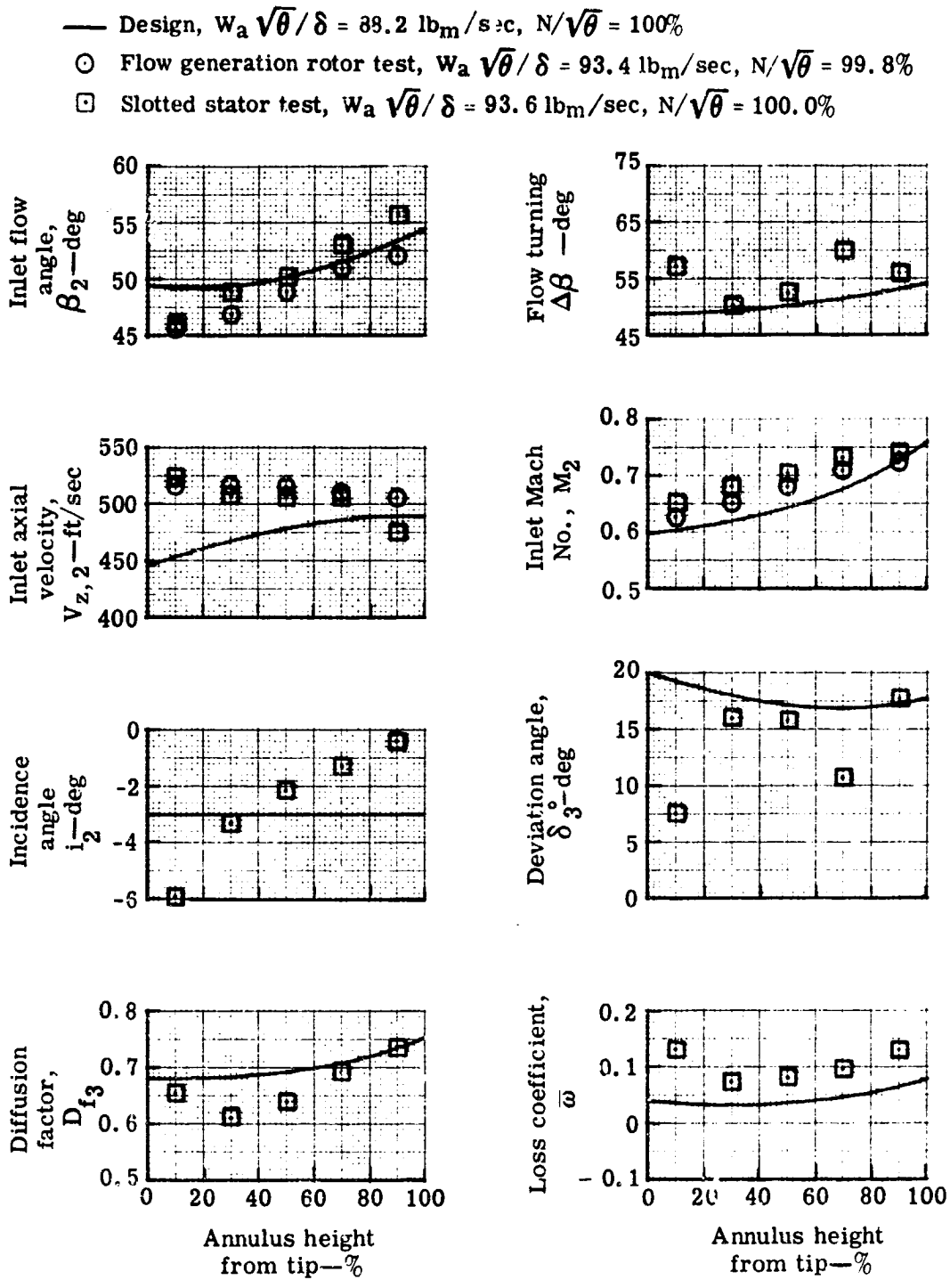
Figure 20. Stator slot blowing flow spanwise distribution.



b. Variation over speed characteristic

5861-30

Figure 20. Stator slot blowing flow spanwise distribution.



5861-31

Figure 21. Radial variation of 0.75 D_f slotted stator blade element performance.

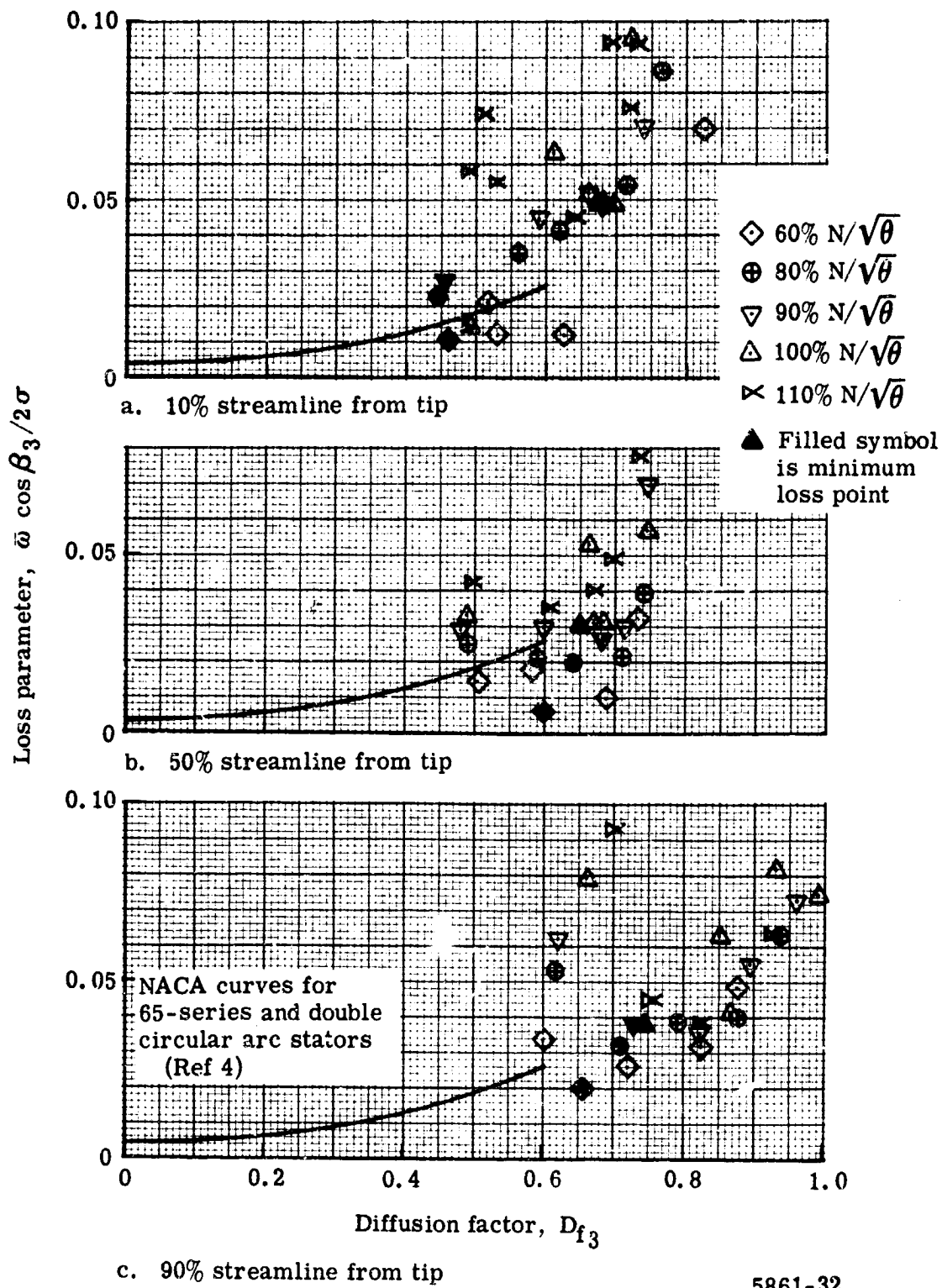
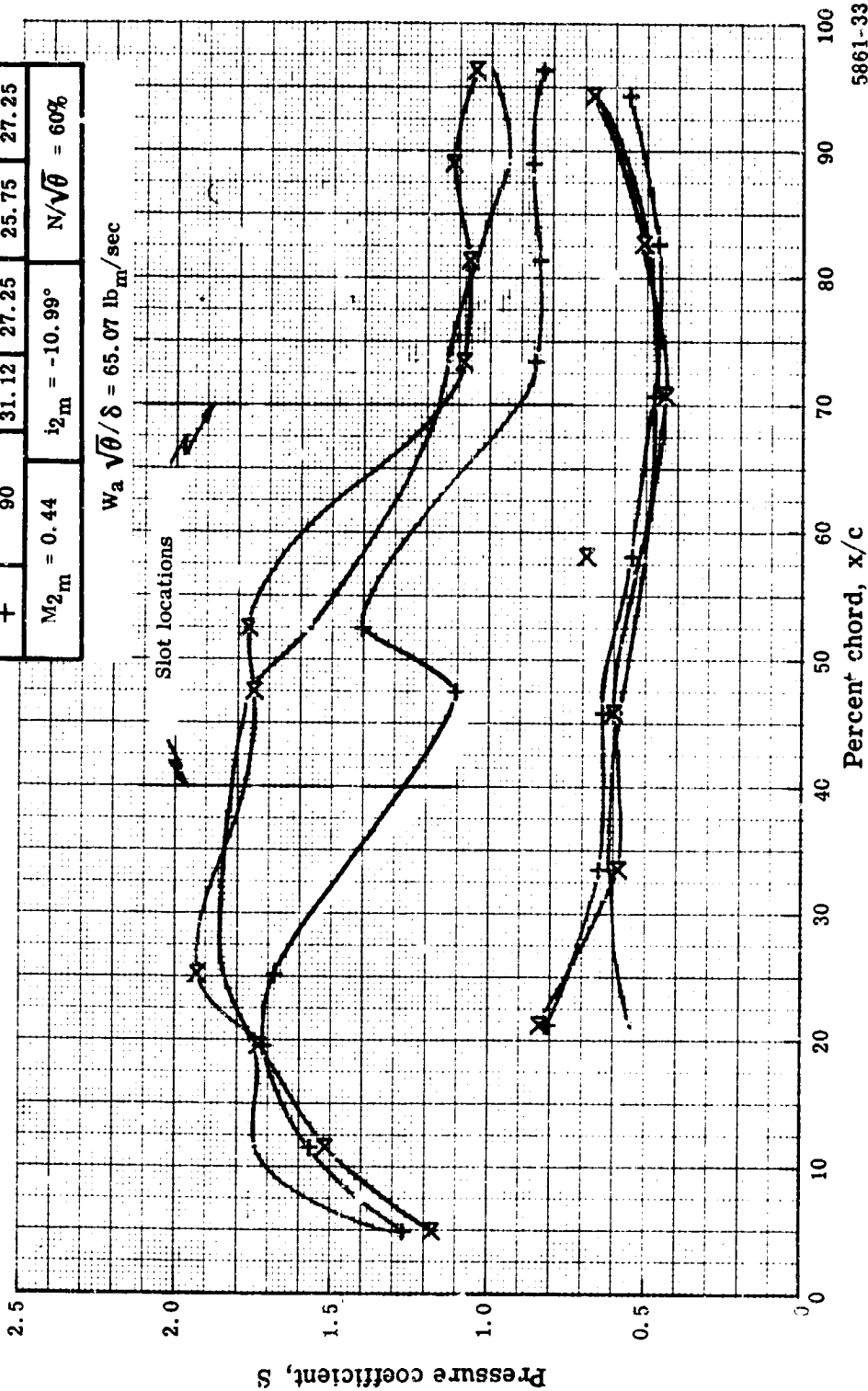


Figure 22. Stator loss parameter versus diffusion factor.

Symbol	Streamline from tip (%)	In. Hg abs			
		P_{t2}	$P_{t \text{ core}}$	$P_{\text{ slot 1}}$ $P_{\text{ slot 2}}$	
X	10	30.47	28.15	26.45	26.95
.	50	30.82	28.25	25.49	26.99
+	90	31.12	27.25	25.75	27.25

$M_{2m} = 0.44$ $i_{2m} = -10.99^\circ$ $N/\sqrt{\theta} = 60\%$

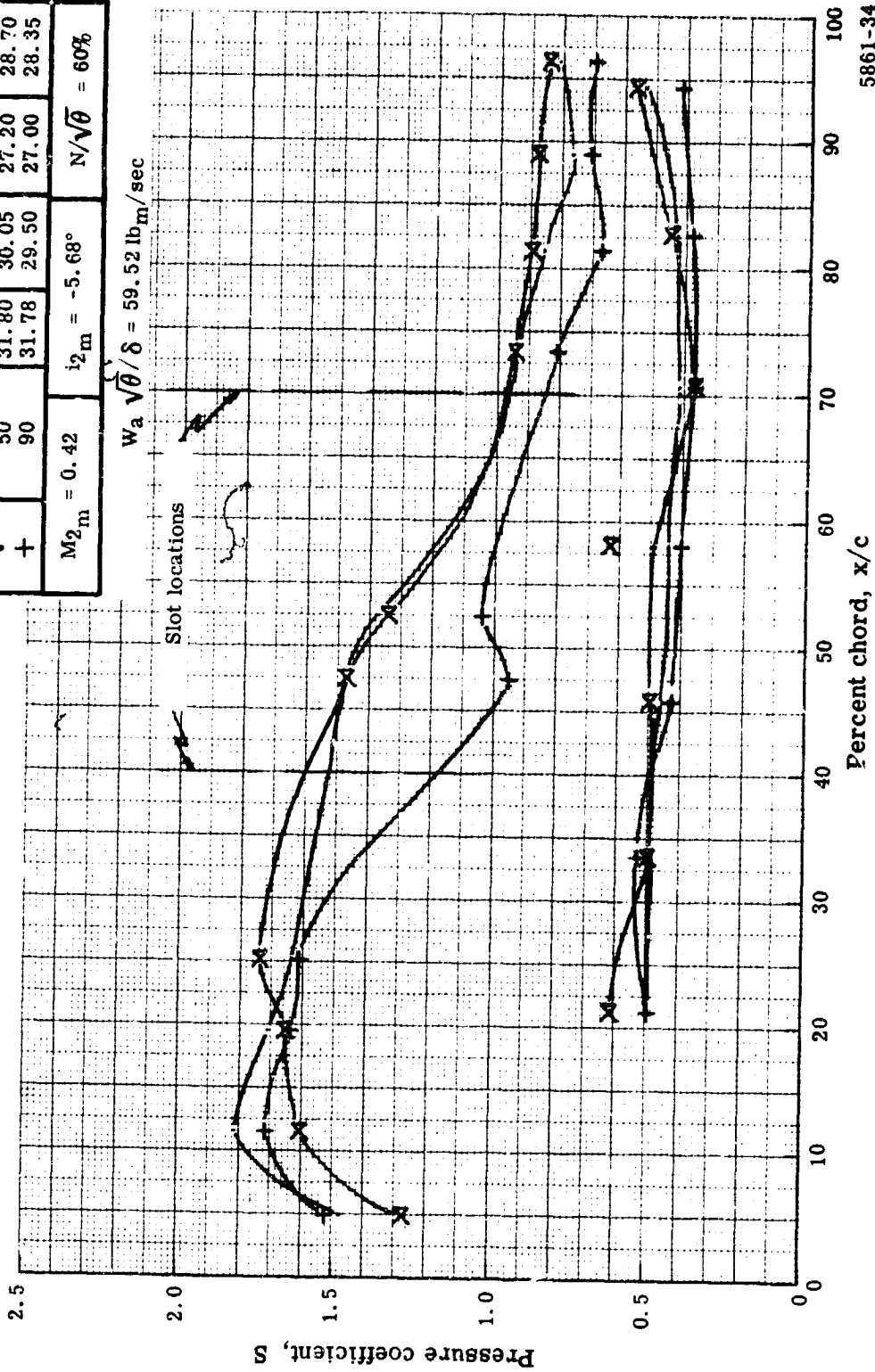
$W_a \sqrt{\theta} / \delta = 65.07 \text{ lb}_m/\text{sec}$



5861-33

Figure 23a. Slotted stator static pressure distribution at 60% speed.

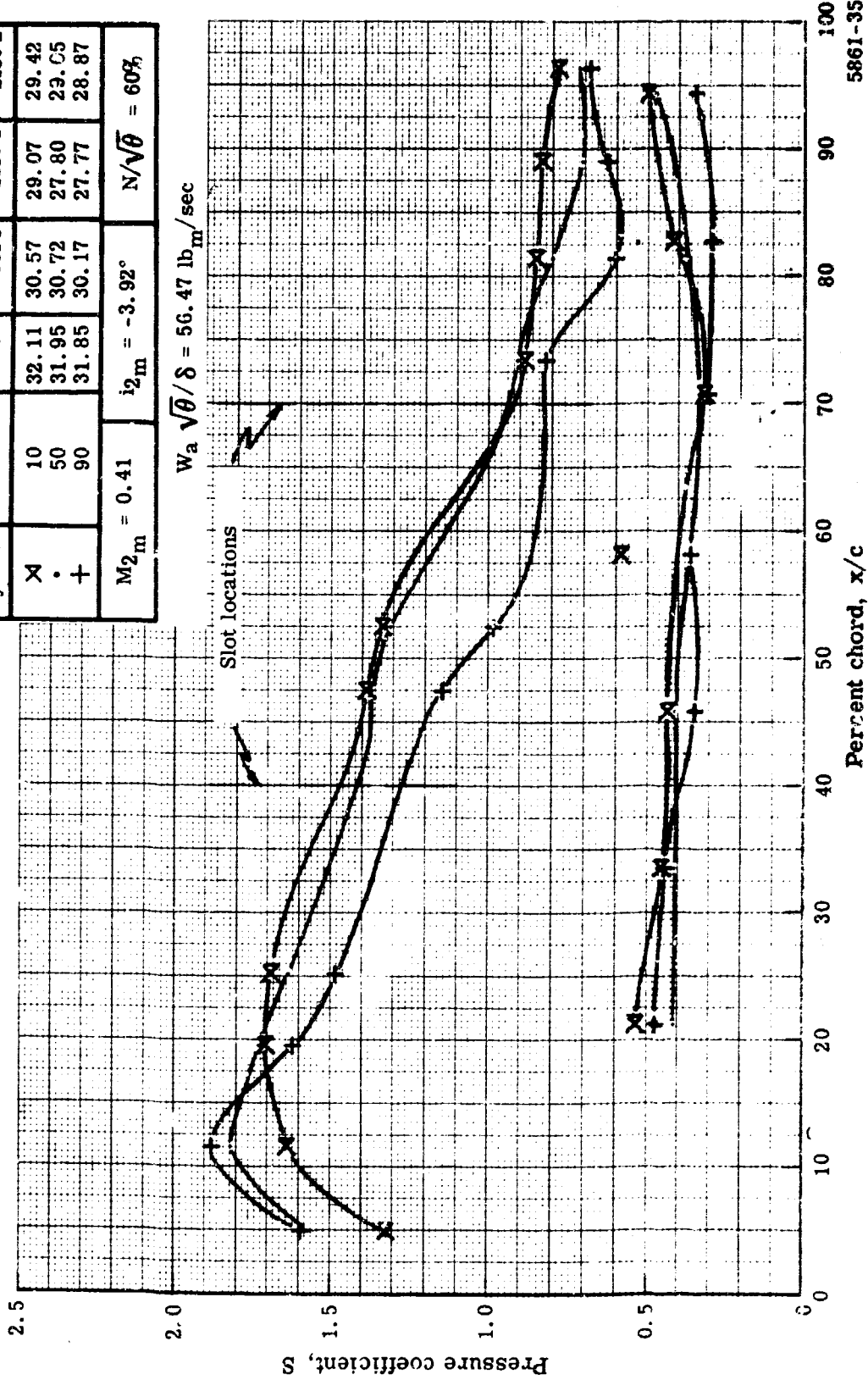
Symbol	Streamline from tip (%)	In. Hg abs			
		P _{t2}	P _t core	P slot 1	P slot 2
X	10	31.80	30.00	28.20	28.75
.	50	31.80	30.05	27.20	28.70
+	90	31.78	29.50	27.00	28.35
M _{2m} = 0.42		i _{2m} = -5.68°		N/√θ = 60%	



5861-34

Figure 23b. Slotted stator static pressure distribution at 60% speed.

Symbol	Streamline from tip (%)	In. Hg abs			
		P _{t2}	P _t core	P slot 1	P slot 2
X	10	32.11	30.57	29.07	29.42
.	50	31.95	30.72	27.80	29.05
+	90	31.85	30.17	27.77	28.87
M _{2m} = 0.41		i _{2m} = -3.92°		N/√θ = 60%	

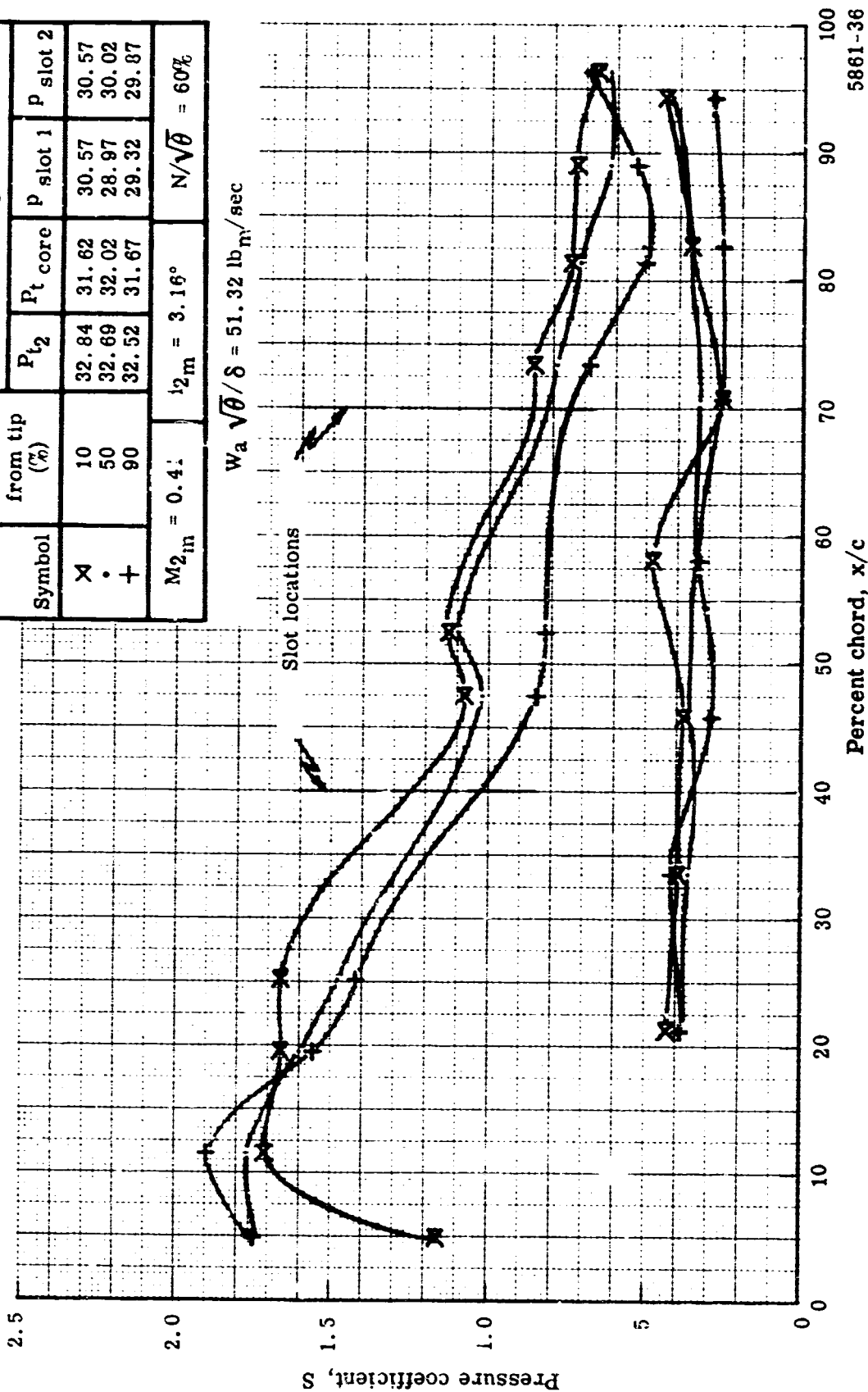


5861-35

Figure 23c. Slotted stator static pressure distribution at 60% speed.

Symbol	Streamline from tip (%)	In. Hg abs			
		P _{t2}	P _t core	P slot 1	P slot 2
X	10	32.84	31.62	30.57	30.57
•	50	32.69	32.02	28.97	30.02
+	90	32.52	31.67	29.32	29.87

M _{2in} = 0.4:	l _{2m} = 3.16°	N/√θ = 60%
-------------------------	-------------------------	------------



5861-36

Figure 23d. Slotted stator static pressure distribution at 60% speed.

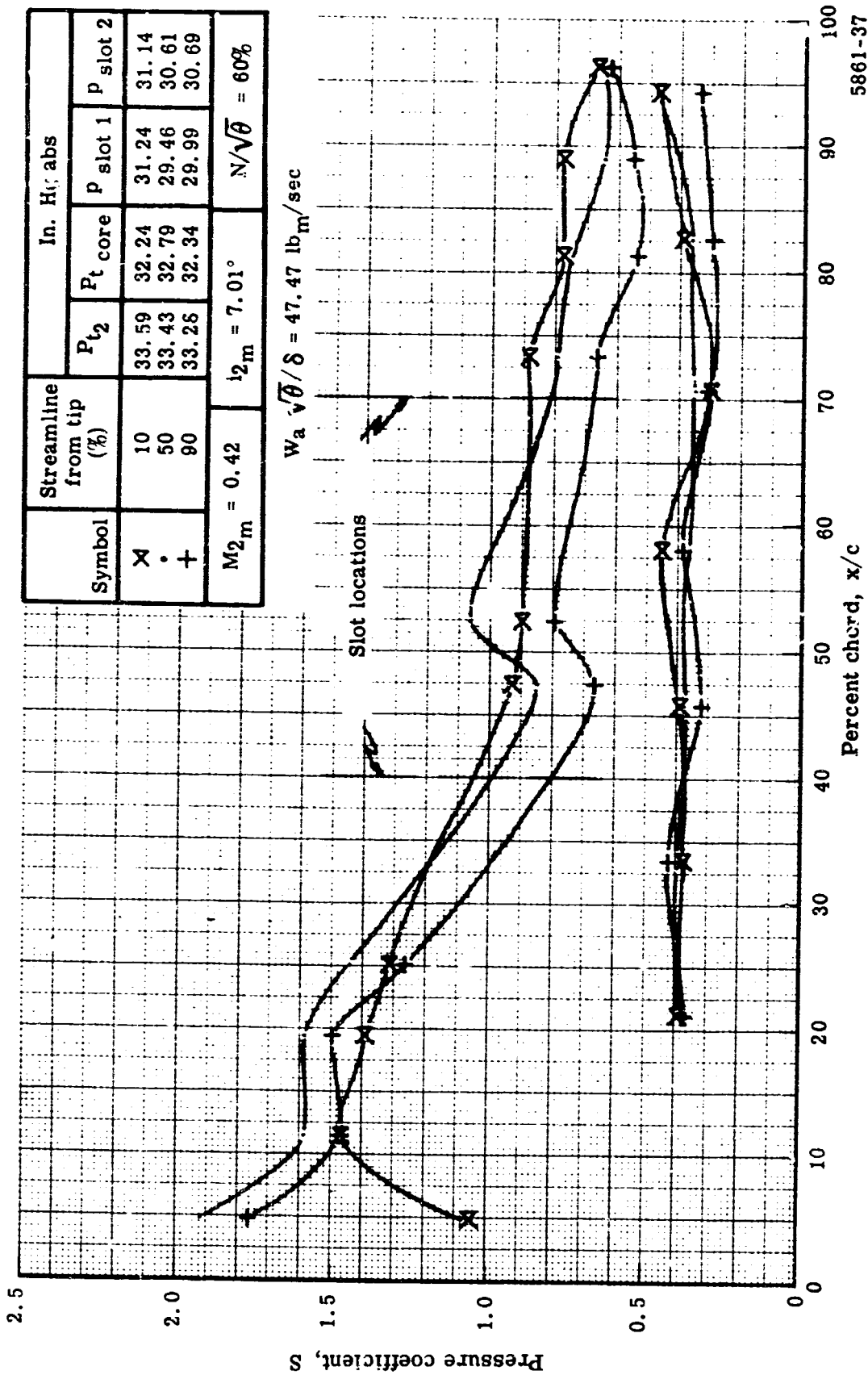


Figure 23e. Slotted stator static pressure distribution at 60% speed.

Symbol	Streamline from tip (%)	In. Hg abs			
		P_{t2}	$P_{t \text{ core}}$	$P \text{ slot 1}$	$P \text{ slot 2}$
x	10	31.74	26.84	24.59	25.54
.	50	32.31	26.84	22.46	25.21
+	90	32.71	25.49	23.19	25.49
$M_{2m} = 0.59$		$\iota_{2m} = -10.21^\circ$		$N/\sqrt{\theta} = 80\%$	

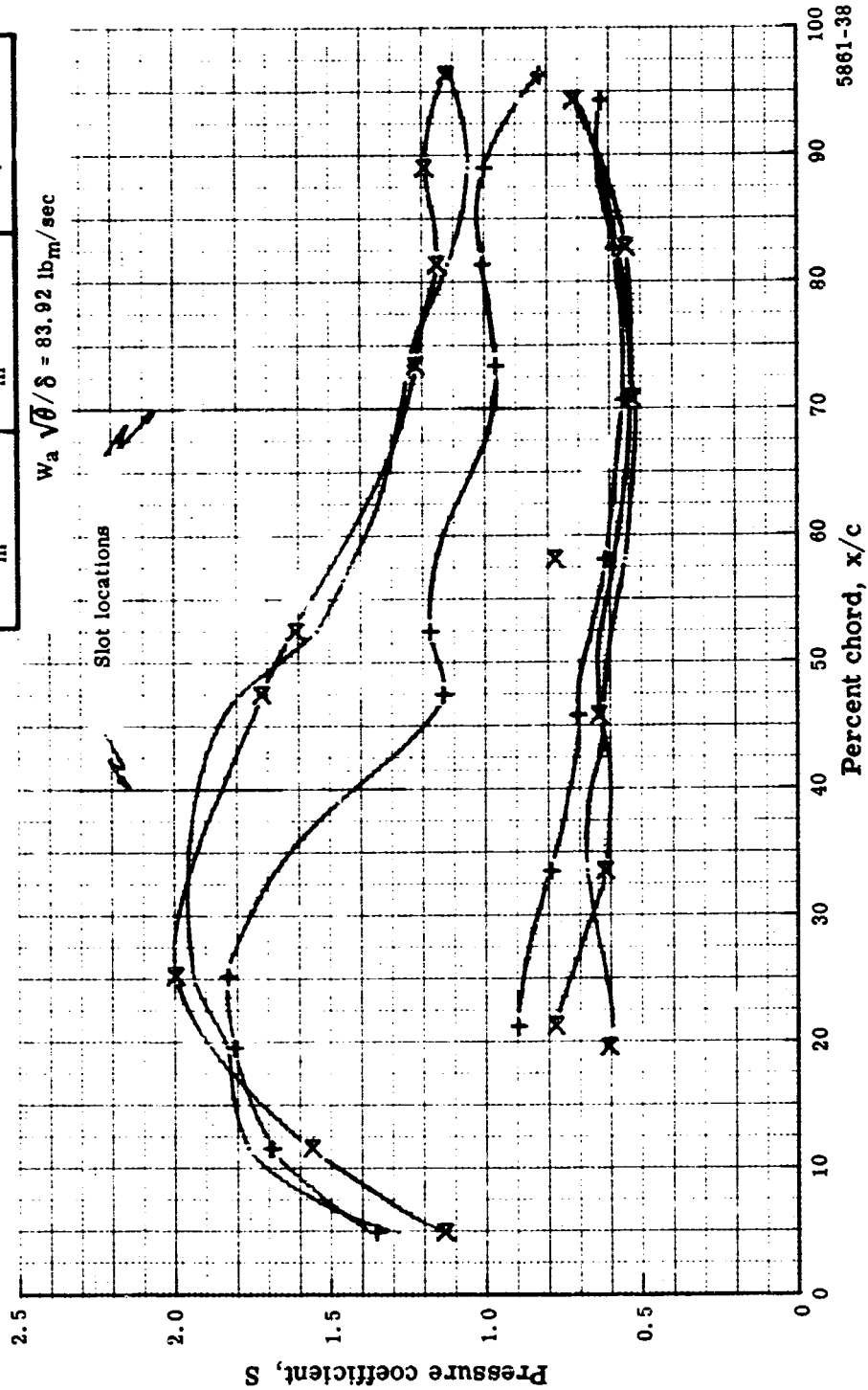
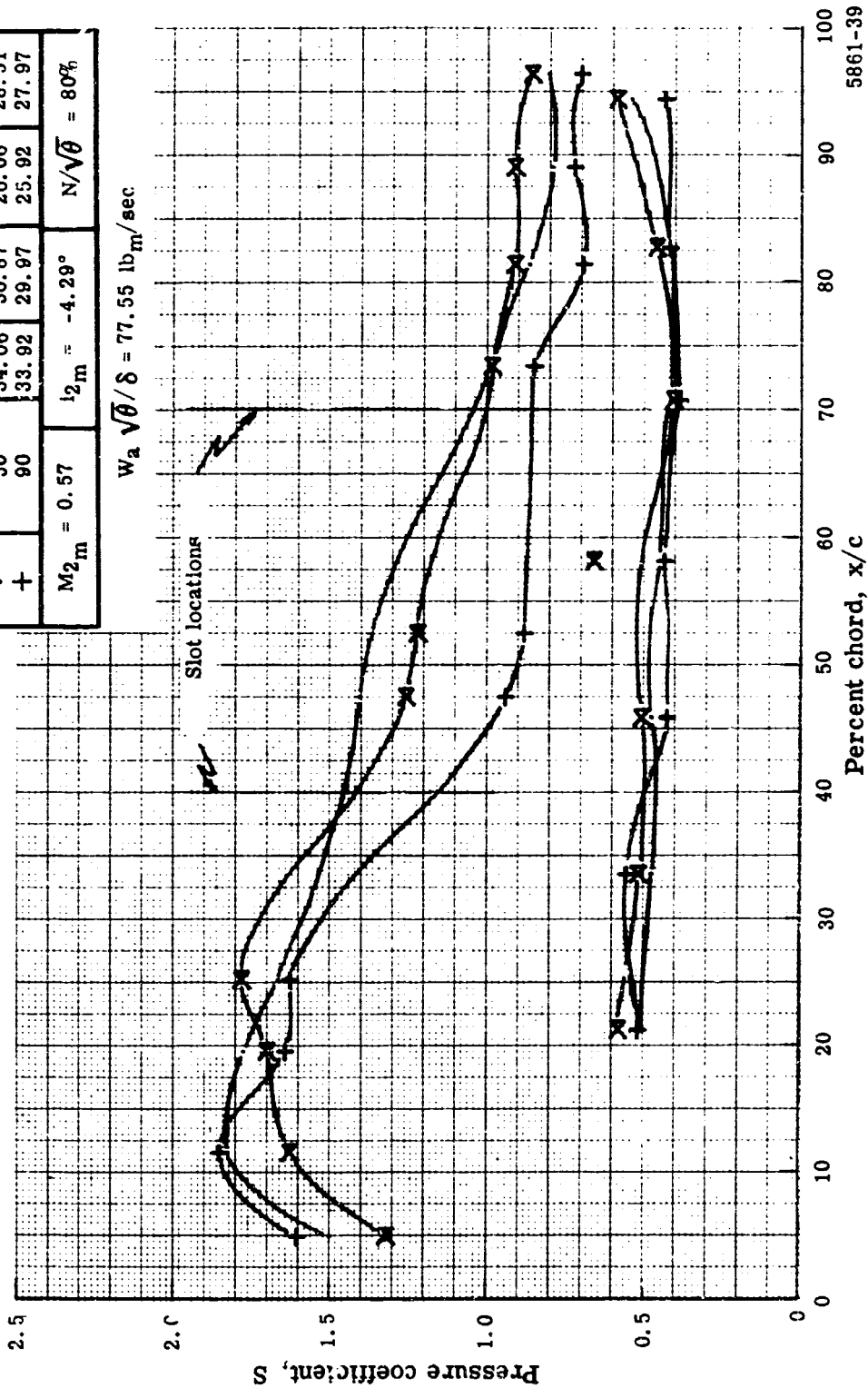


Figure 24a. Slotted stator static pressure distribution at 80% speed.

Symbol	Streamline from tip (%)	In. Hg abs			
		P _{t2}	P _t core	p slot 1	p slot 2
X	10	34.25	30.92	27.92	28.67
•	50	34.06	30.87	26.06	28.51
+	90	33.92	29.97	25.92	27.97

M _{2m} = 0.57	l _{2m} = -4.29°	N/√θ = 80%
------------------------	--------------------------	------------

W_a √θ / δ = 77.55 lb_m/sec



5861-39

Figure 24b. Slotted stator static pressure distribution at 80% speed.

Symbol	Streamline from tip (%)	In. Hg abs			
		P _{t2}	P _{t core}	P slot 1	P slot 2
X	10	34.90	31.88	29.33	29.93
.	50	34.62	31.93	27.14	29.29
+	90	34.37	31.58	27.18	28.73
M _{2m} = 0.56		i _{2m} = -1.72°		N/√θ = 80%	

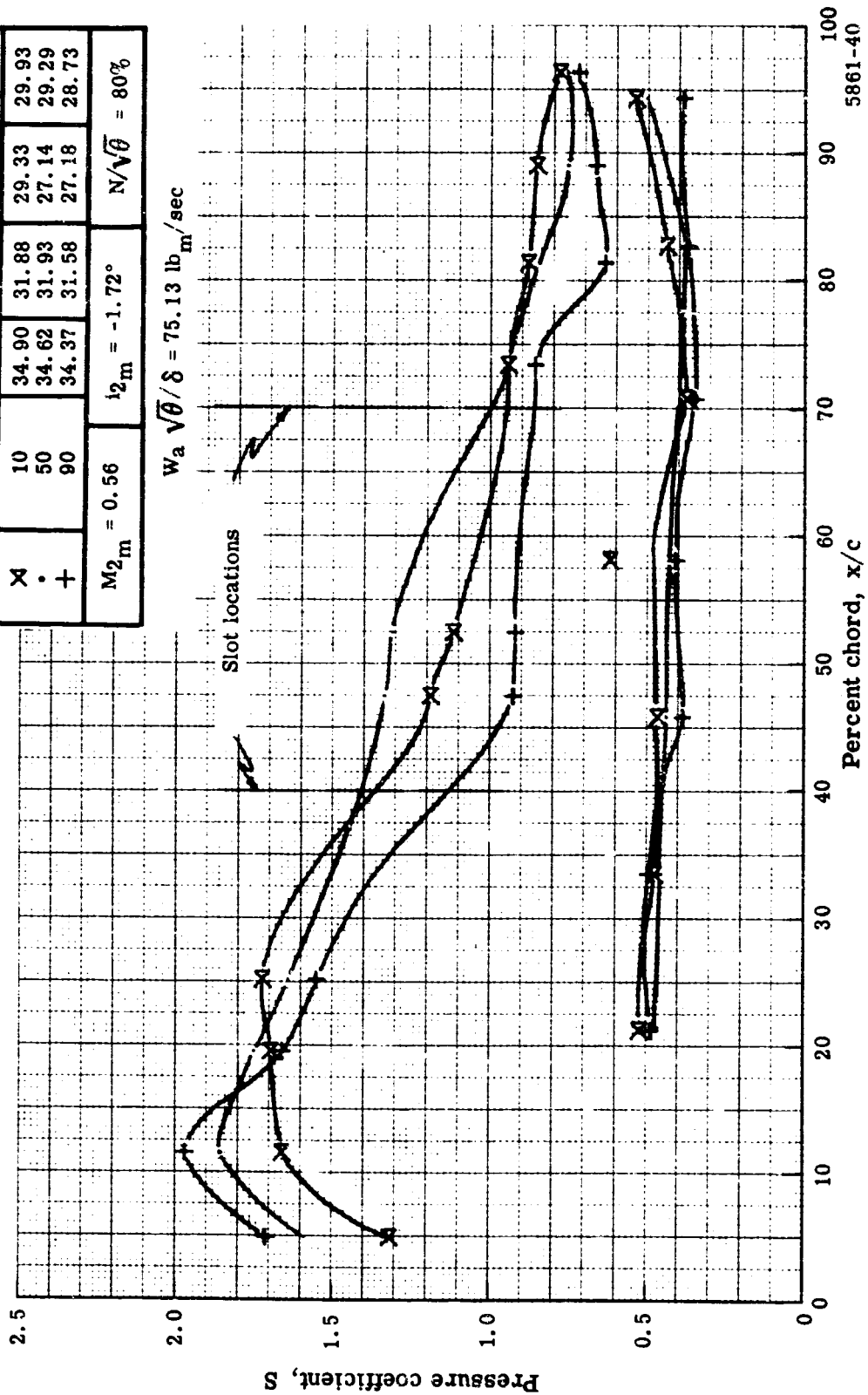


Figure 24c. Slotted stator static pressure distribution at 80% speed.

Symbol	Streamline from tip (%)	In. Hg abs			
		P_{t2}	$P_{t \text{ core}}$	$P \text{ slot 1}$	$P \text{ slot 2}$
X	10	36.22	33.28	31.43	31.48
•	50	35.59	34.03	28.74	30.64
+	90	35.24	33.63	29.03	30.25
$M_{2m} = 0.55$		$i_{2m} = 3.38^\circ$		$N/\sqrt{\theta} = 80\%$	

$W_a \sqrt{\theta} / \delta = 70.16 \text{ lb}_m/\text{sec}$

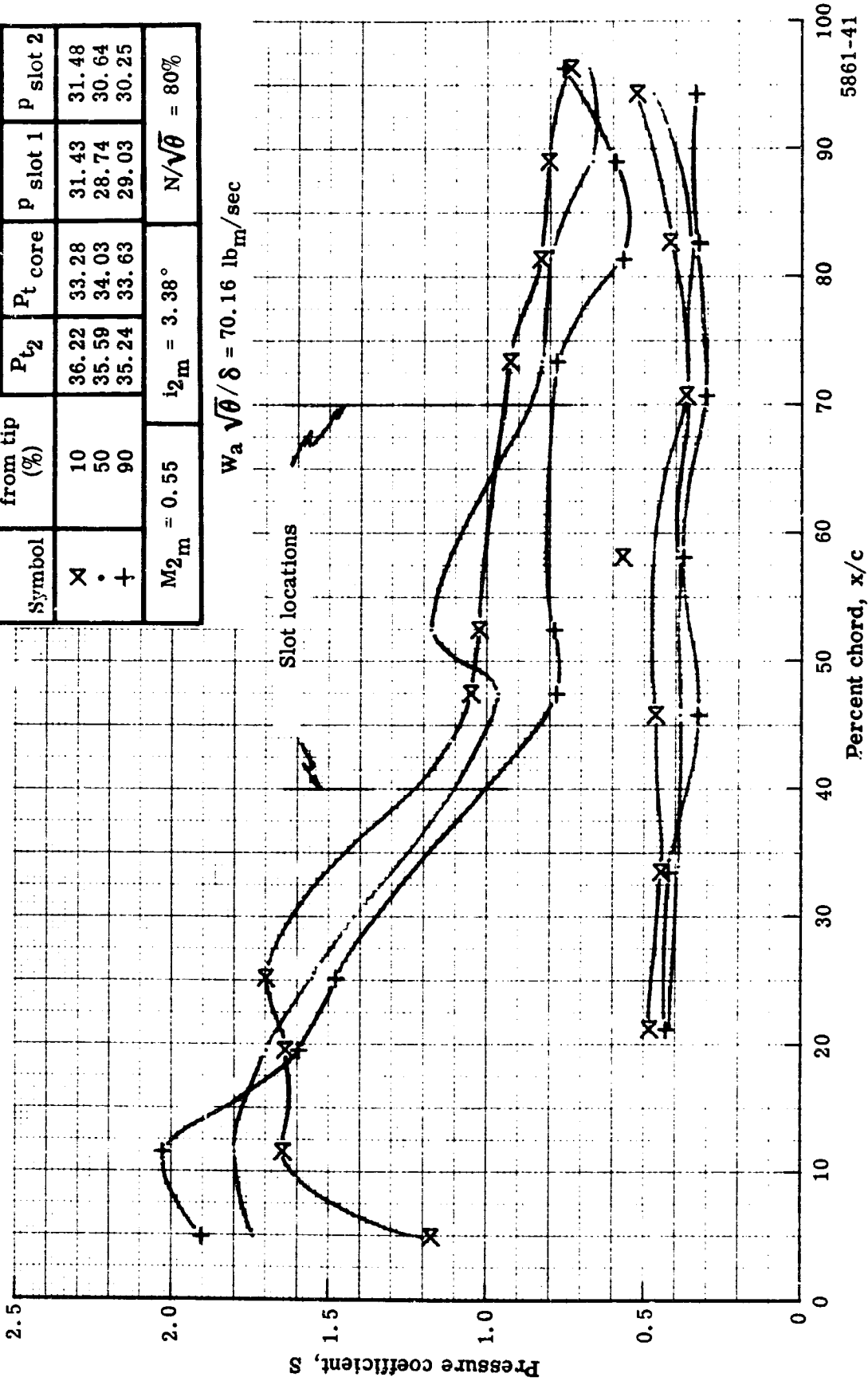
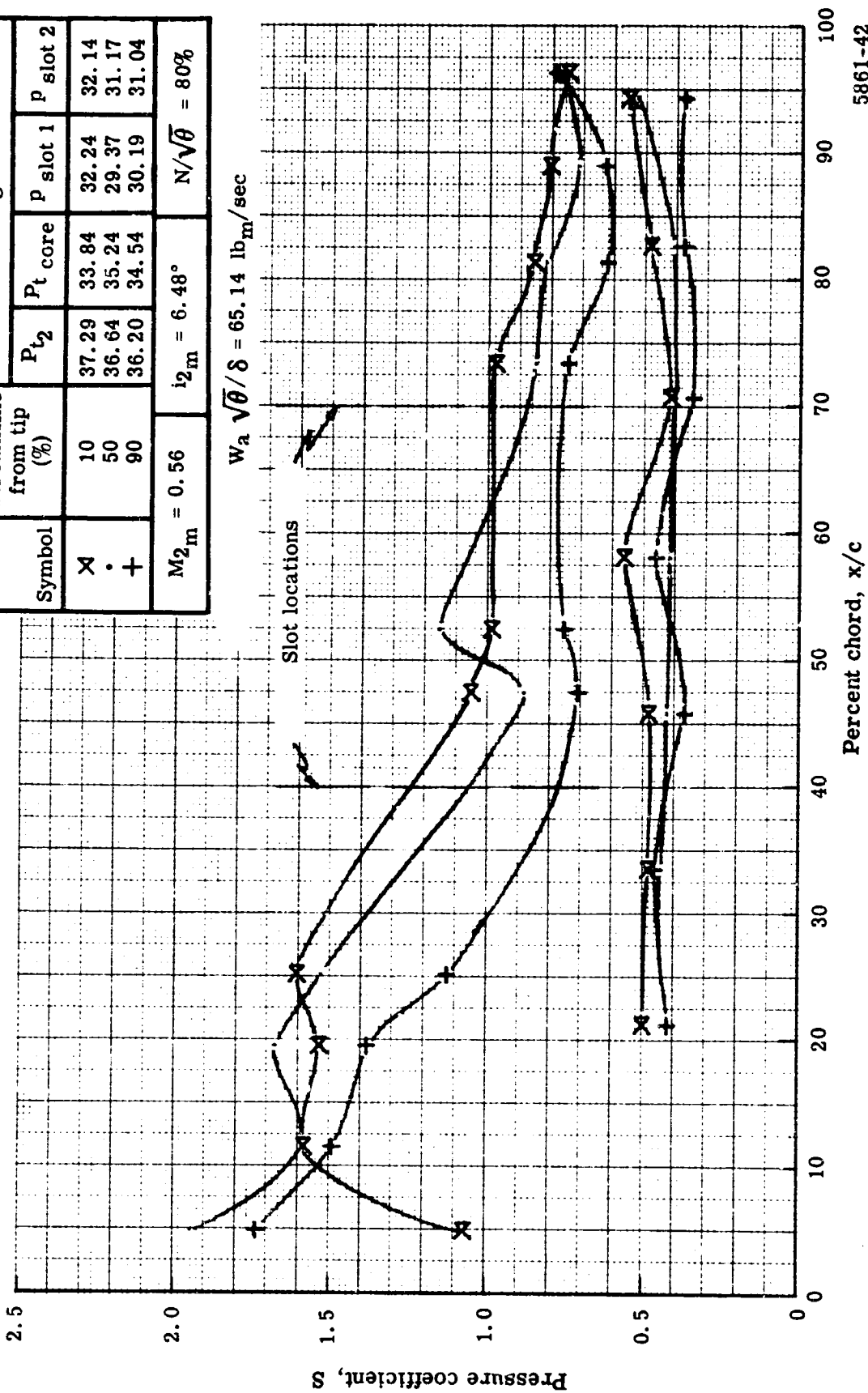


Figure 24d. Slotted stator static pressure distribution at 80% speed.

Symbol	Streamline from tip (%)	In. Hg abs			
		P _{t2}	P _t core	P slot 1	P slot 2
X	10	37.29	33.84	32.24	32.14
•	50	36.64	35.24	29.37	31.17
+	90	36.20	34.54	30.19	31.04
M _{2m} = 0.56		i _{2m} = 6.48°		N/√θ = 80%	

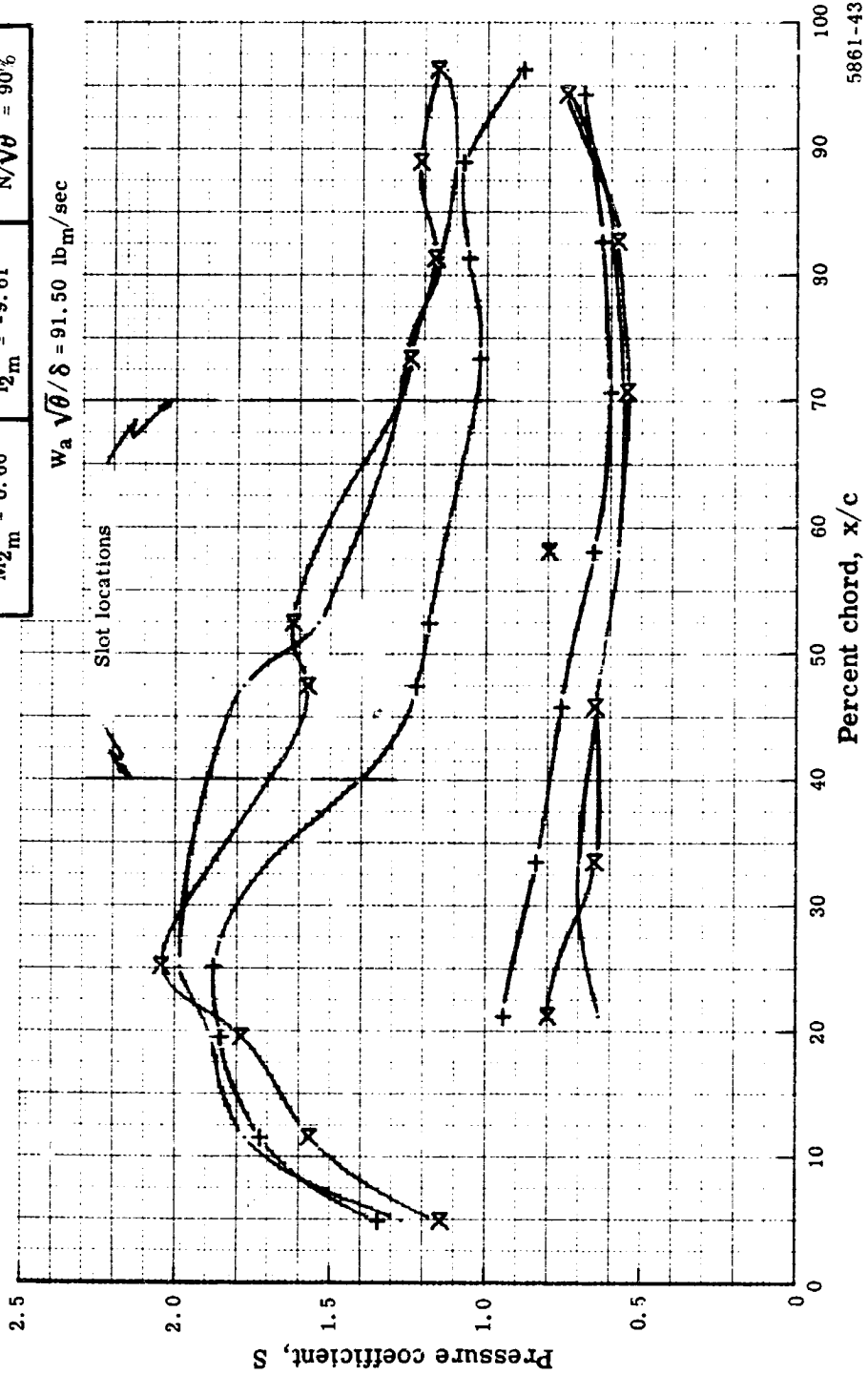


5861-42

Figure 24e. Slotted stator static pressure distribution at 80% speed.

Symbol	Streamline from tip (%)	In. Hg abs			
		P _{t2}	P _{t core}	p slot 1	P slot 2
X	10	32.60	26.13	23.78	24.58
.	50	33.23	26.13	21.11	24.21
+	90	33.68	24.63	22.33	24.63

M _{2m} = 0.66	ι _{2m} = -9.61°	N/√θ = 90%
------------------------	--------------------------	------------



5861-43

Figure 25a. Slotted stator static pressure distribution at 90% speed.

Symbol	Streamline from tip (%)	In. Hg abs			
		P_{t2}	$P_{t \text{ core}}$	P slot 1	P slot 2
X	10	35.33	30.67	27.37	27.82
.	50	35.17	30.87	24.94	27.74
+	90	34.76	29.82	25.42	27.02

$M_{2m} = 0.64$	$i_{2m} = -4.68^\circ$	$N/\sqrt{\theta} = 90\%$
-----------------	------------------------	--------------------------

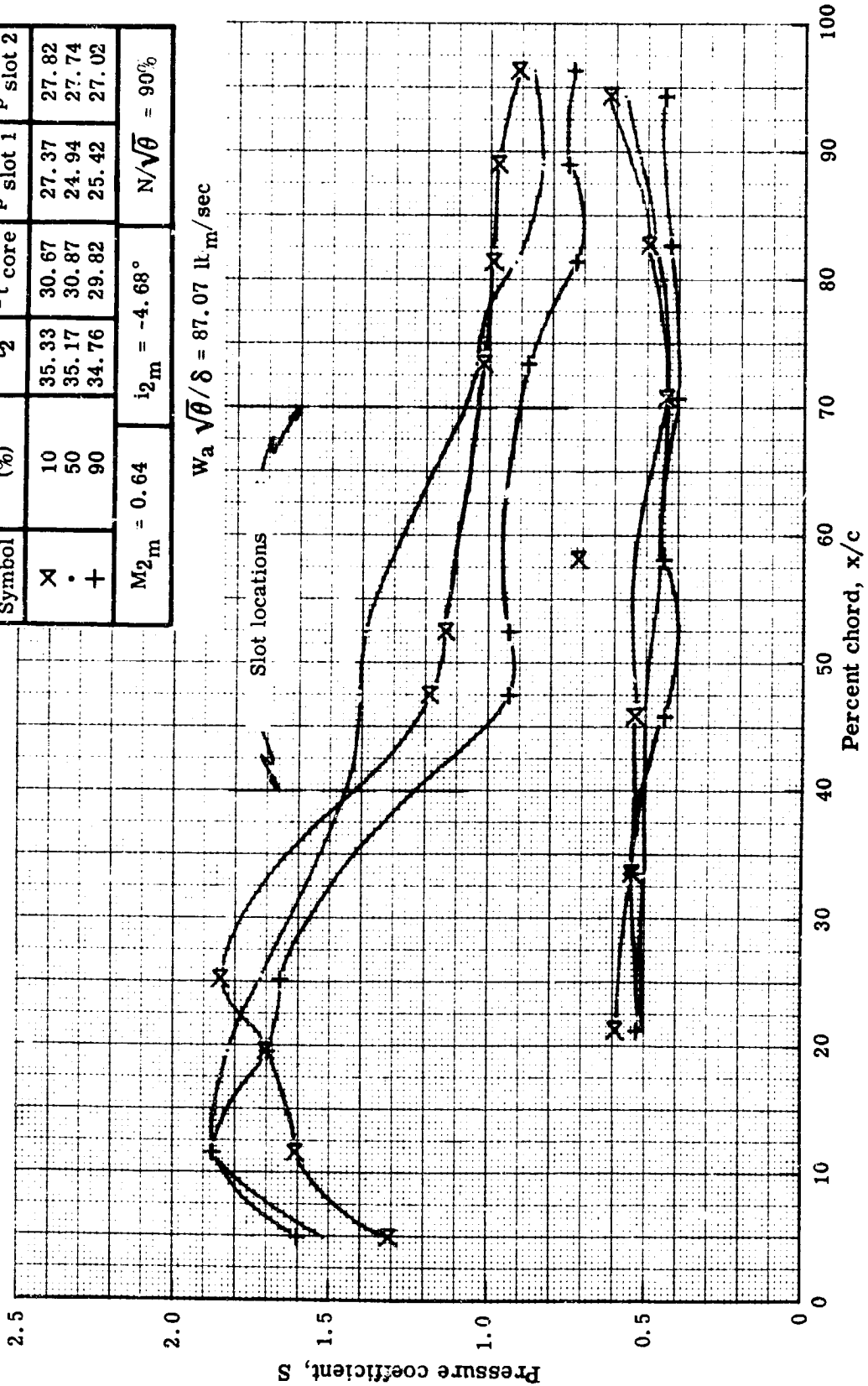
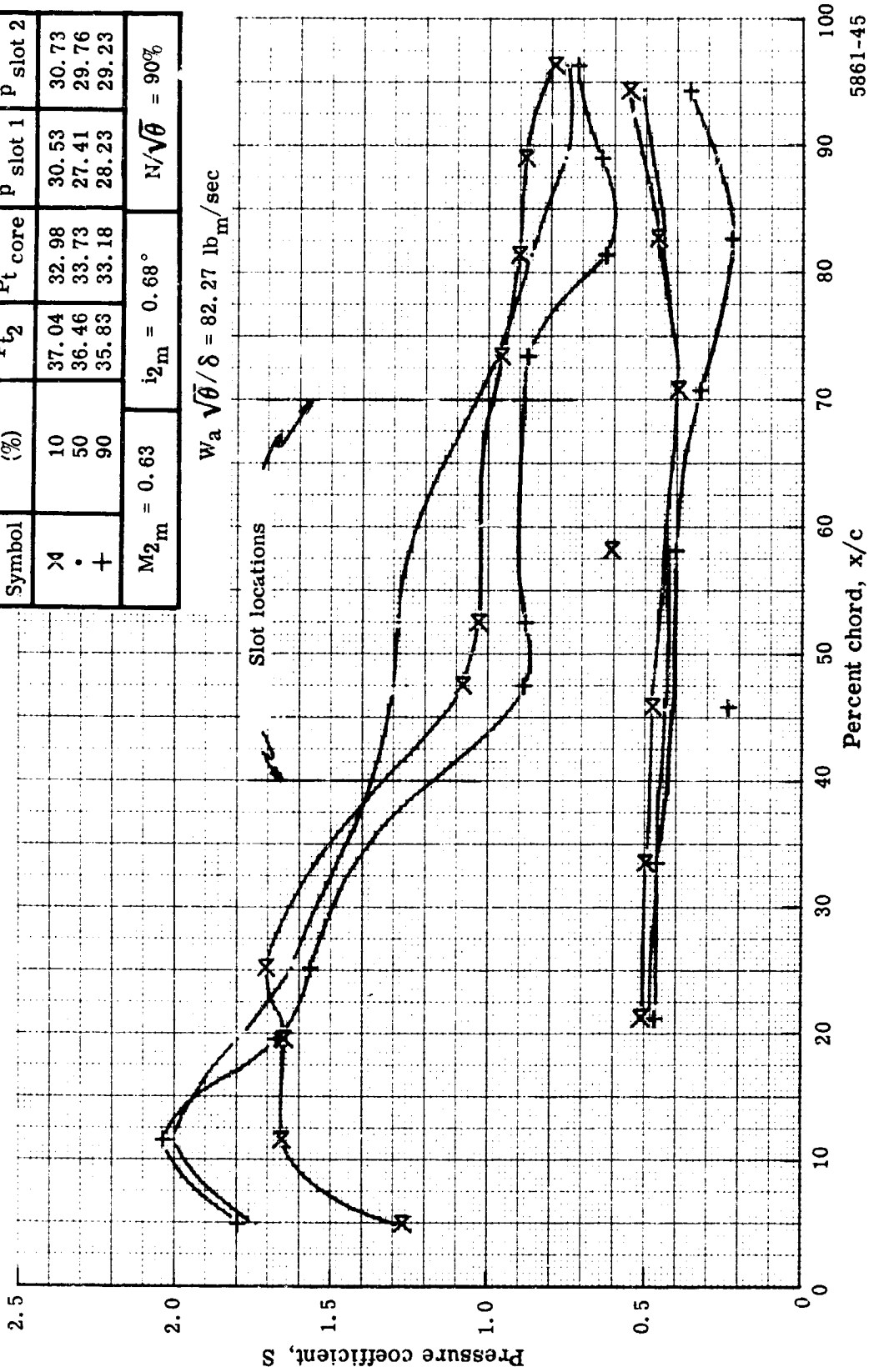


Figure 25b. Slotted stator static pressure distribution at 90% speed.

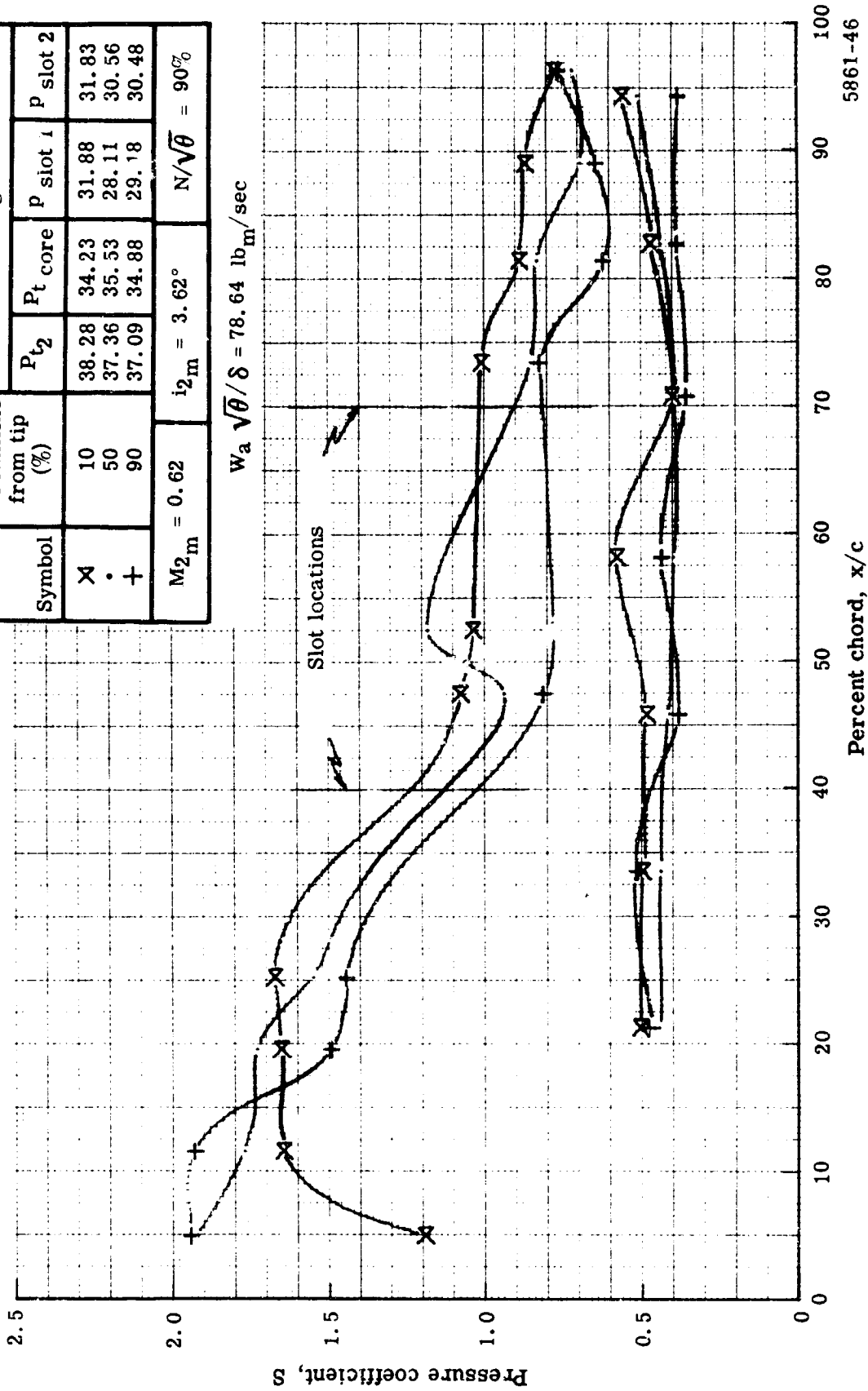
Symbol	Streamline from tip (%)	In. Hg abs			
		P _{t2}	P _{t core}	P slot 1	P slot 2
>	10	37.04	32.98	30.53	30.73
•	50	36.46	33.73	27.41	29.76
+	90	35.83	33.18	28.23	29.23
M _{2m} = 0.63		i _{2m} = 0.68°		N/√θ = 90%	



5861-45

Figure 25c. Slotted stator static pressure distribution at 90% speed.

Symbol	Streamline from tip (%)	In. Hg abs			
		P_{t2}	$P_{t \text{ core}}$	$P_{\text{ slot 1}}$	$P_{\text{ slot 2}}$
X	10	38.28	34.23	31.88	31.83
.	50	37.36	35.53	28.11	30.56
+	90	37.09	34.88	29.18	30.48
$M_{2m} = 0.62$		$i_{2m} = 3.62^\circ$		$N/\sqrt{\theta} = 90\%$	



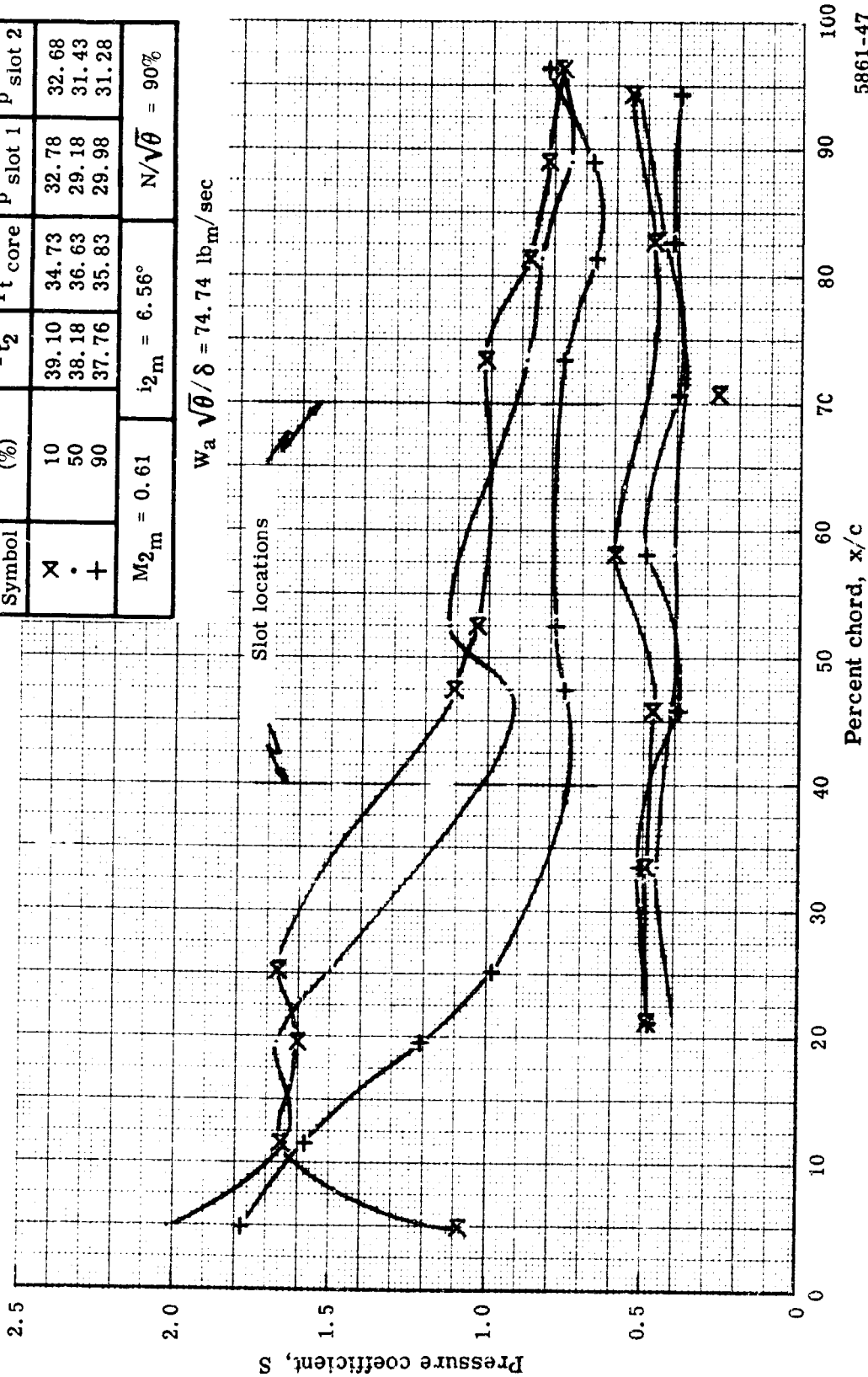
5861-46

Figure 25d. Slotted stator static pressure distribution at 90% speed.

Symbol	Streamline from tip (%)	In. Hg abs			
		P _{t2}	P _t core	P slot 1	P slot 2
X	10	39.10	34.73	32.78	32.68
•	50	38.18	36.63	29.18	31.43
+	90	37.76	35.83	29.98	31.28

M _{2m} = 0.61	i _{2m} = 6.56°	N/√θ = 90%
------------------------	-------------------------	------------

W_a √θ / δ = 74.74 lb_m/sec

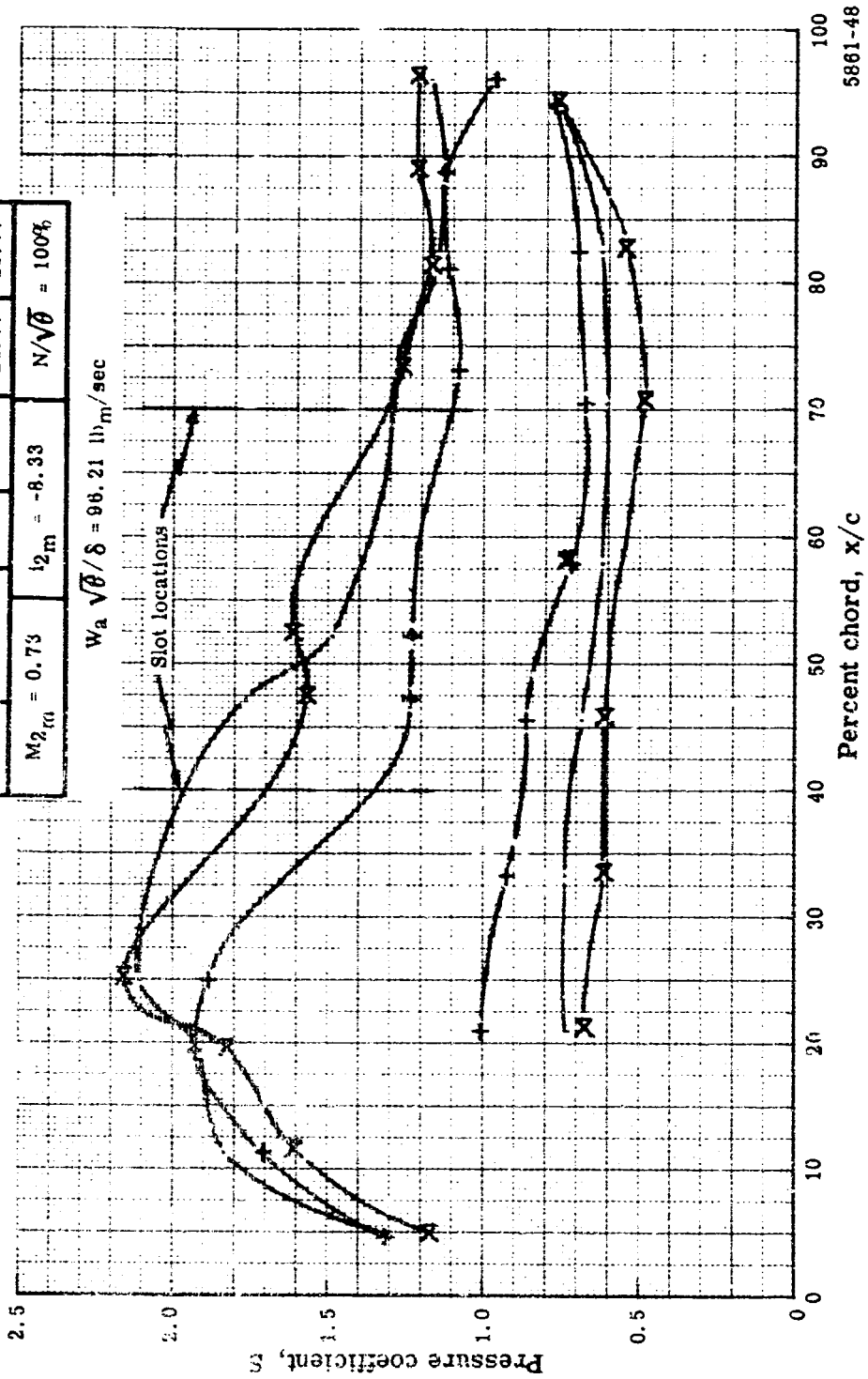


5861-47

Figure 25e. Slotted stator static pressure distribution at 90% speed.

Symbol	Streamline from tip (%)	In. Hg abs			
		P_{t2}	$P_{t \text{ core}}$	$P \text{ slot 1}$	$P \text{ slot 2}$
x	10	32.08	24.77	22.47	23.67
.	50	34.51	25.67	21.33	23.58
+	90	35.22	23.67	21.77	23.77

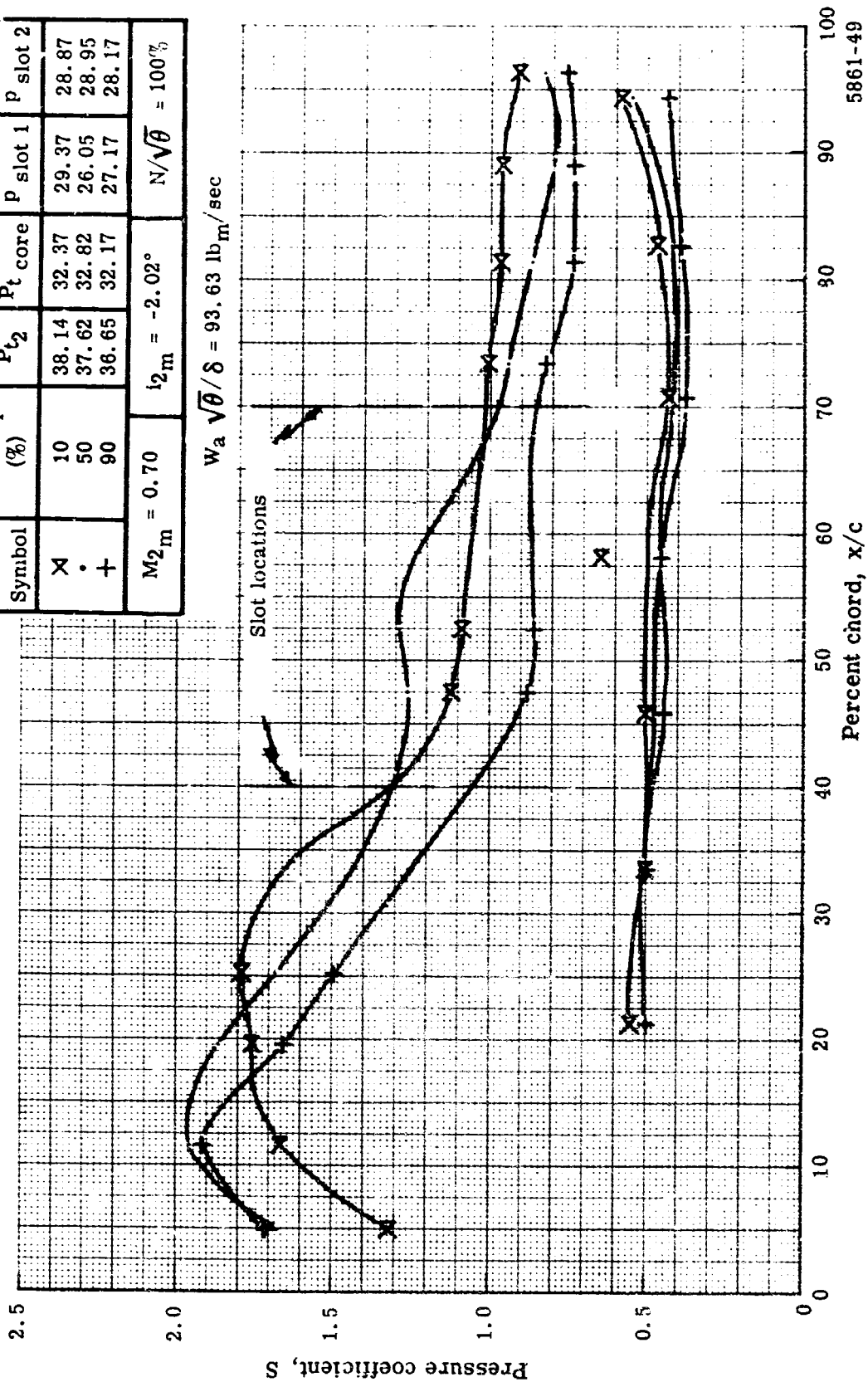
$M_{2m} = 0.73$	$l_{2m} = -8.33$	$N/\sqrt{\theta} = 100\%$
-----------------	------------------	---------------------------



5861-48

Figure 26a. Slotted stator static pressure distribution at 100% speed.

Streamline from tip (%)		In. Hg abs			
Symbol	P _{t2}	P _{t core}	P slot 1	P slot 2	
X	38.14	32.37	29.37	28.87	
.	37.62	32.82	26.05	28.95	
+	36.65	32.17	27.17	28.17	
M _{2m} = 0.70		l _{2m} = -2.02°		N/√θ = 100%	



5861-49

Figure 26b. Slotted stator static pressure distribution at 100% speed.

Symbol	Streamline from tip (%)	In. Hg abs			
		P_{t2}	$P_{t \text{ core}}$	$P \text{ slot 1}$	$P \text{ slot 2}$
X	10	38.76	33.34	30.24	29.79
.	50	38.06	33.94	26.86	29.56
+	90	38.30	33.54	27.99	29.14
$M_{2m} = 0.70$		$i_{2m} = -0.68^\circ$		$N/\sqrt{\theta} = 100\%$	

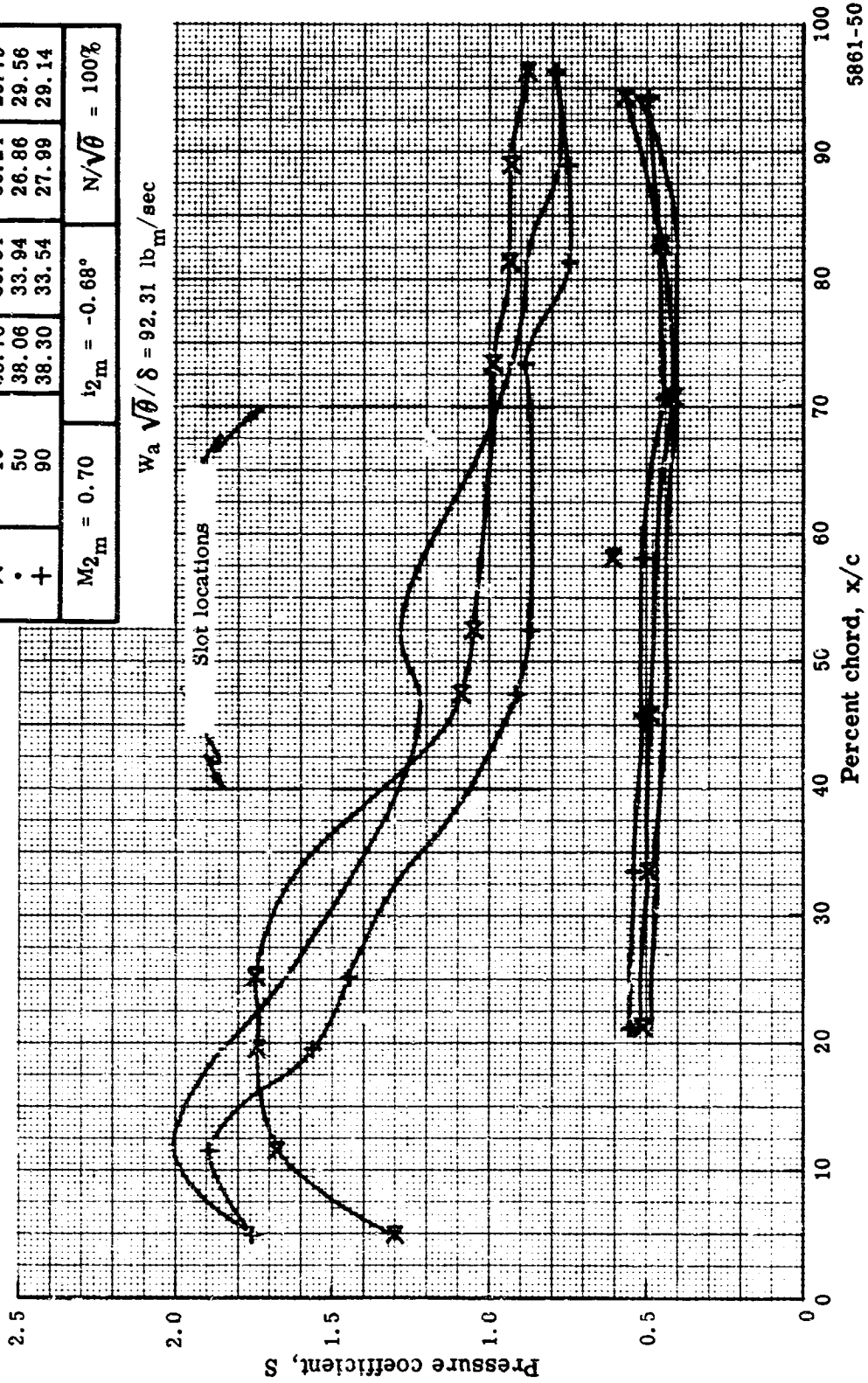
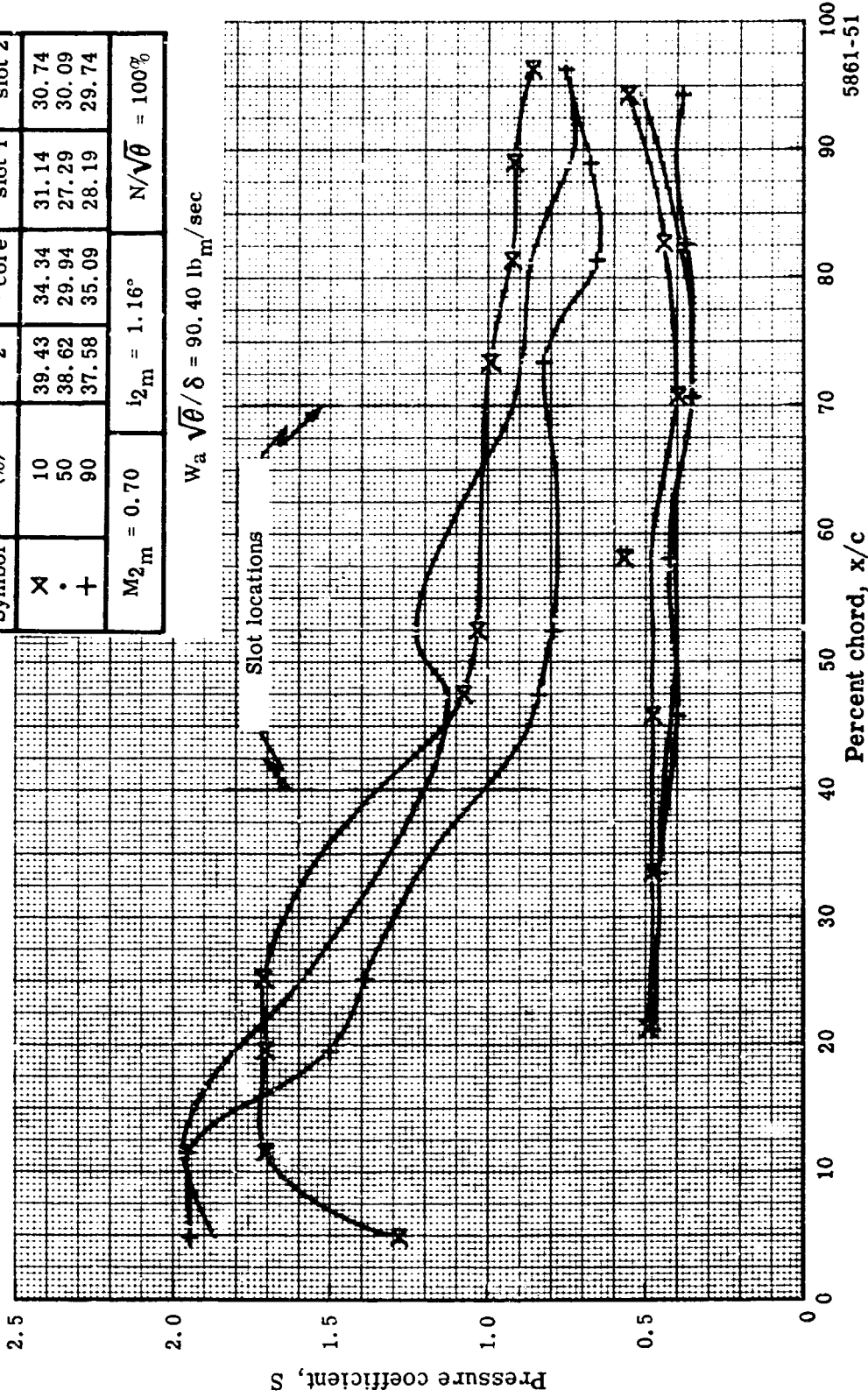


Figure 26c. Slotted stator static pressure distribution at 100% speed.

Symbol	Streamline from tip (%)	In. Hg abs			
		P_{t2}	$P_{t \text{ core}}$	$p \text{ slot 1}$	$p \text{ slot 2}$
X	10	39.43	34.34	31.14	30.74
•	50	38.62	29.94	27.29	30.09
+	90	37.58	28.19	29.74	
$M_{2m} = 0.70$		$i_{2m} = 1.16^\circ$		$N/\sqrt{\theta} = 100\%$	

$W_a \sqrt{\theta} / \delta = 90.40 \text{ lb}_m/\text{sec}$

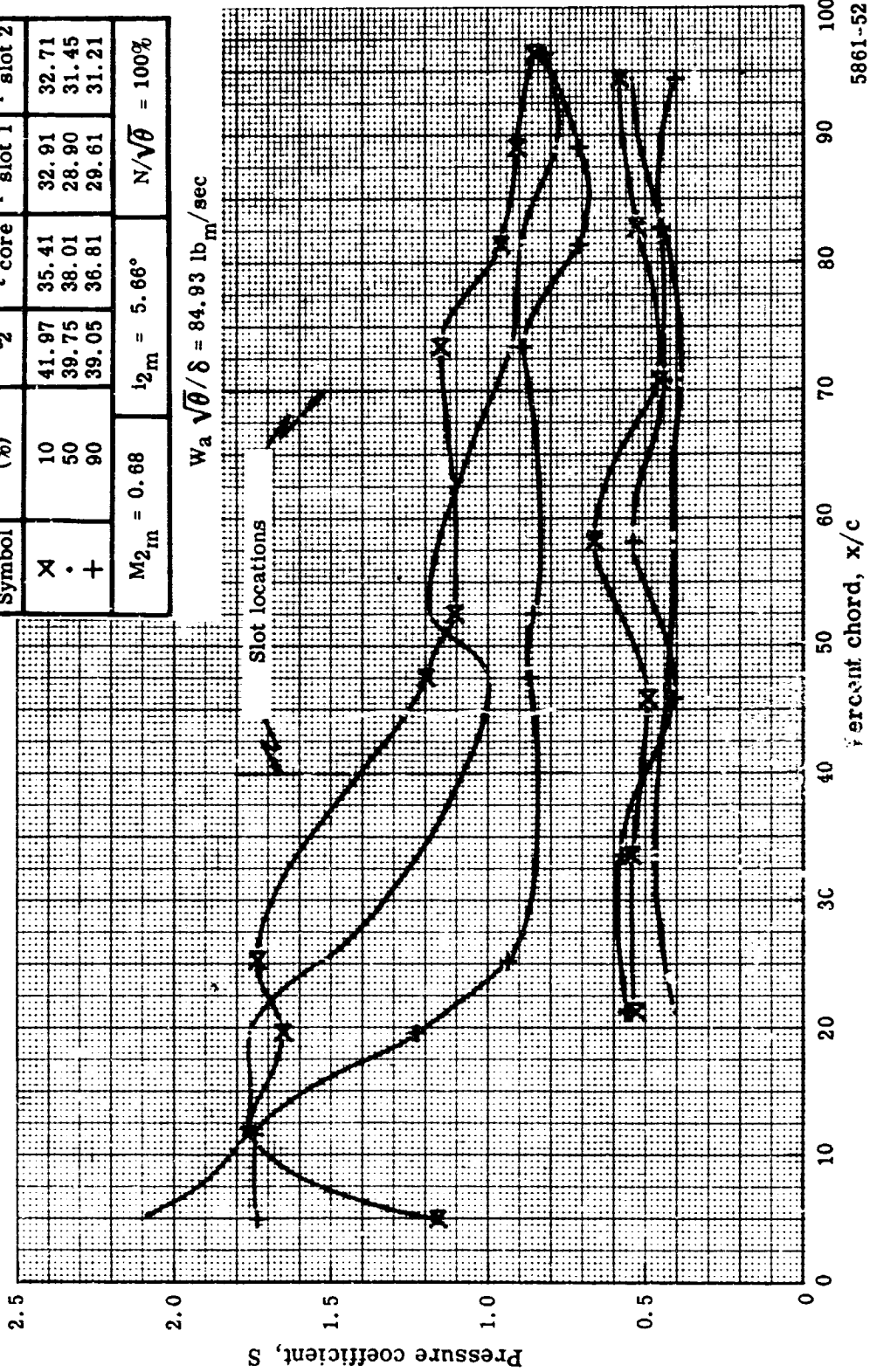


5861-51

Figure 26d. Slotted stator static pressure distribution at 100% speed.

Symbol	Streamline from tip (%)	In. Hg abs			
		P_{t2}	$P_{t \text{ core}}$	$P \text{ slot 1}$	$P \text{ slot 2}$
X	10	41.97	35.41	32.91	32.71
.	50	39.75	38.01	28.90	31.45
+	90	39.05	36.81	29.61	31.21
$M_{2m} = 0.68$		$l_{2m} = 5.66^\circ$		$N/\sqrt{\theta} = 100\%$	

$$W_a \sqrt{\theta} / \delta = 84.93 \text{ lb}_m/\text{sec}$$

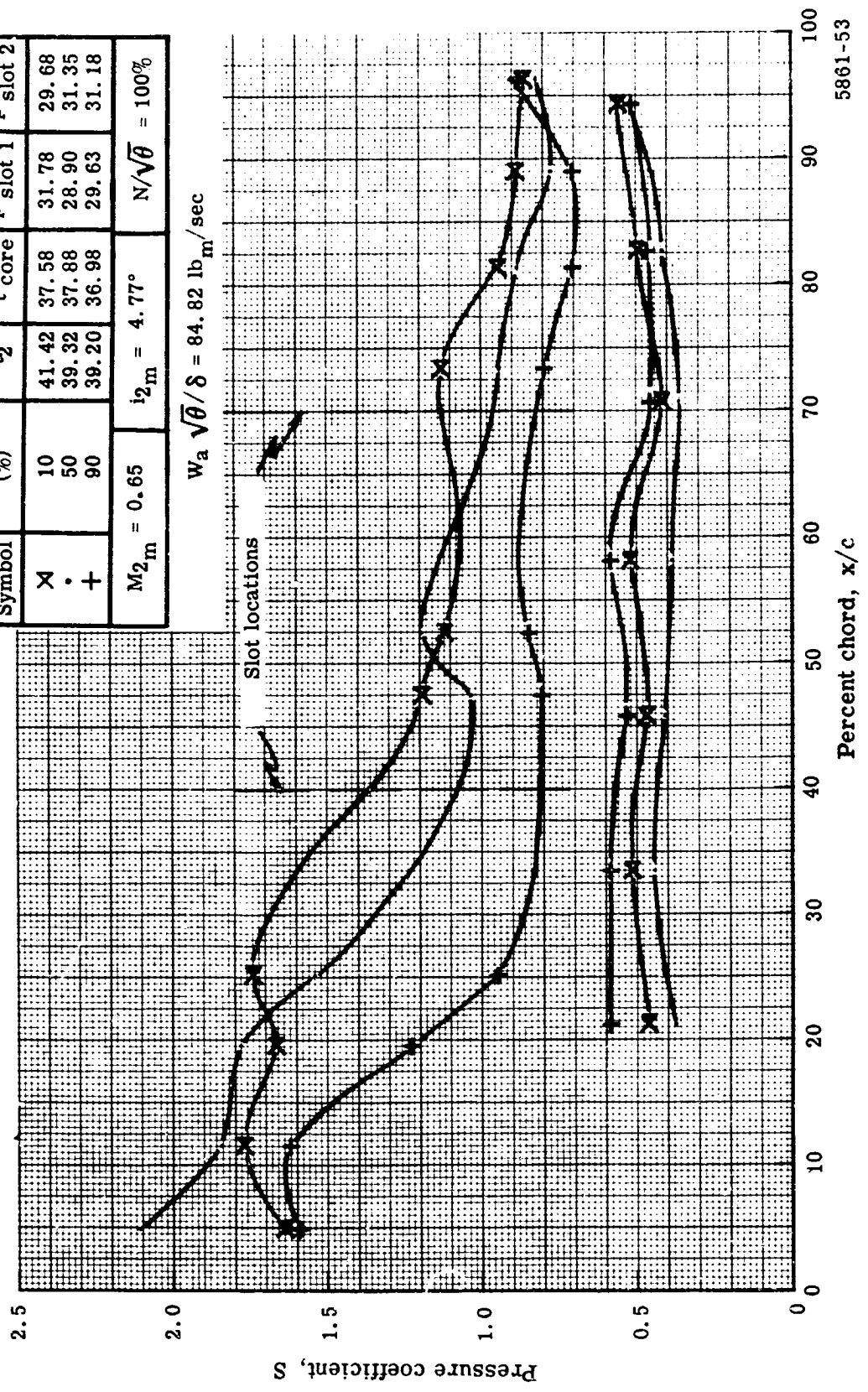


5861-52

Figure 26e. Slotted stator static pressure distribution at 100% speed.

Symbol	Streamline from tip (%)	In. Hg abs			
		P _{t2}	P _t core	P slot 1	P slot 2
X	10	41.42	37.58	31.78	29.68
.	50	39.32	37.88	28.90	31.35
+	90	39.20	36.98	29.63	31.18
$M_{2,m} = 0.65$		$i_{2,m} = 4.77^\circ$		$N/\sqrt{\theta} = 100\%$	

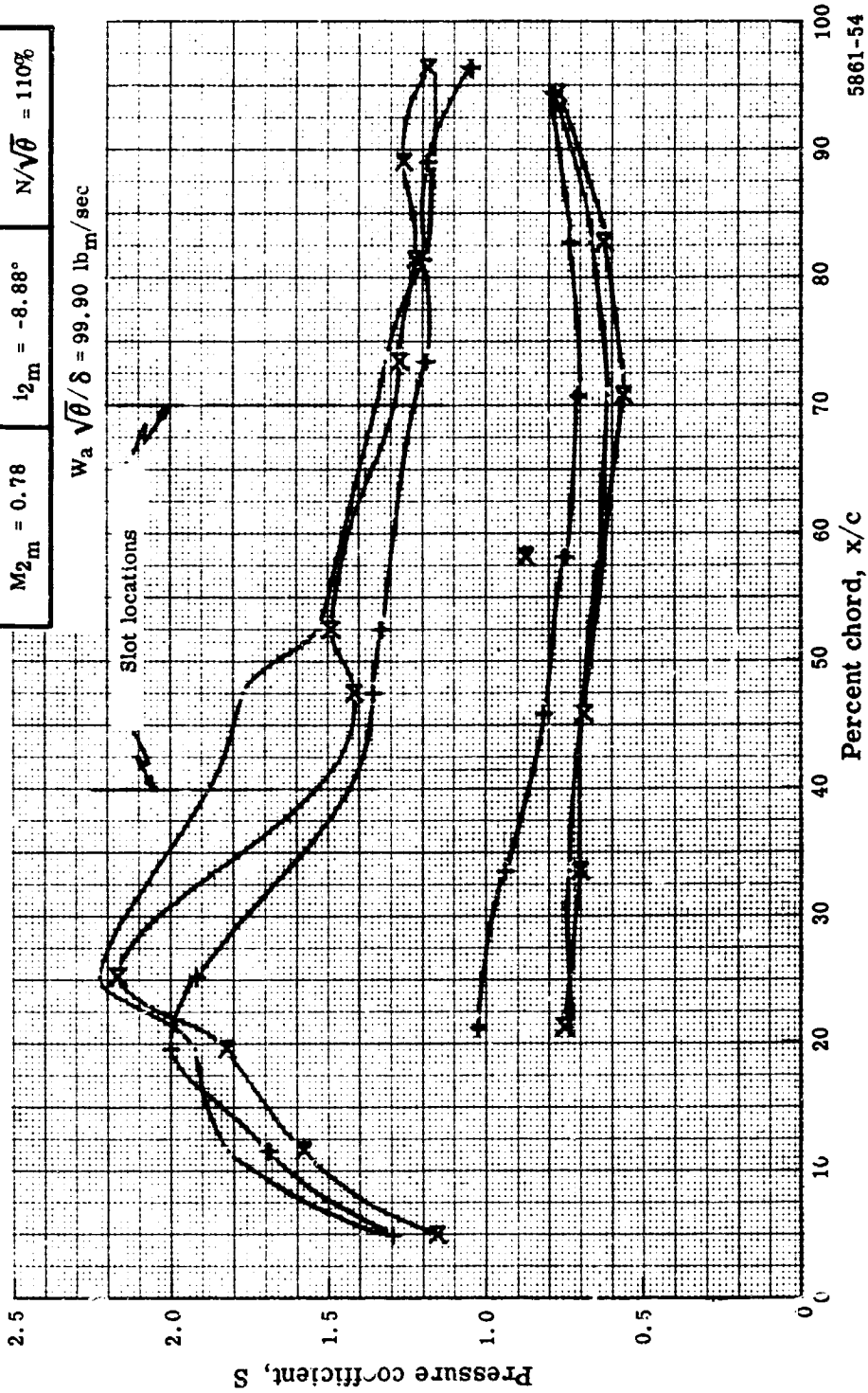
$W_a \sqrt{\theta} / \delta = 84.82 \text{ lb}_m / \text{sec}$



5861-53

Figure 26f. Slotted stator static pressure distribution at 100% speed.

Symbol	Streamline from tip (%)	In. Hg abs			
		P_{t2}	Pt core	P slot 1	P slot 2
X	10	33.55	25.18	22.73	23.23
.	50	35.16	25.33	20.54	22.89
+	90	36.78	23.53	20.98	22.48
$M_{2m} = 0.78$		$i_{2m} = -8.88^\circ$		$N/\sqrt{\theta} = 110\%$	



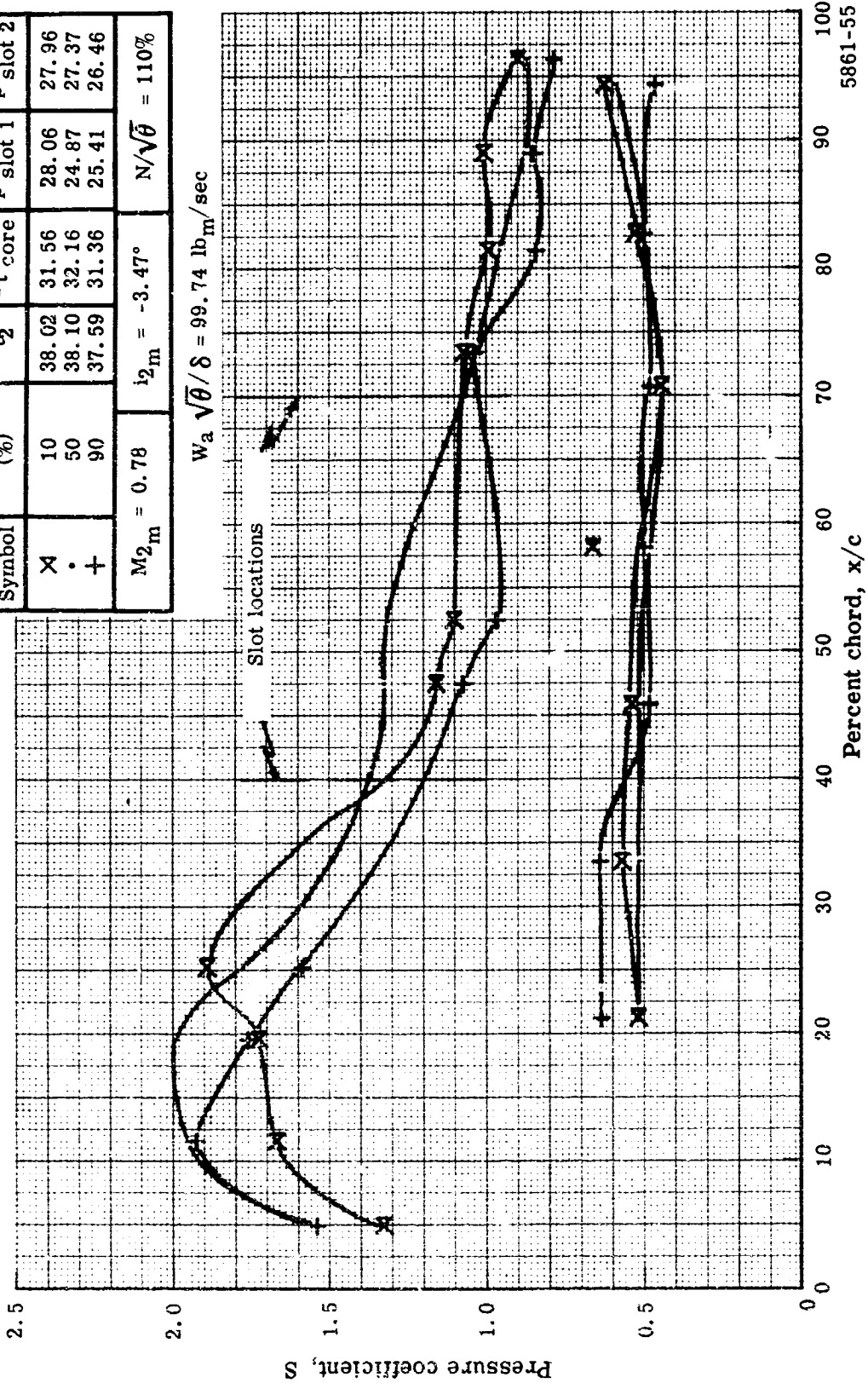
5861-54

Figure 27a. Slotted stator static pressure distribution at 110% speed.

Symbol	Streamline from tip (%)	In. Hg abs			
		P _{t2}	P _{t core}	P slot 1	P slot 2
X	10	38.02	31.56	28.06	27.96
.	50	38.10	32.16	24.87	27.37
+	90	37.59	31.36	25.41	26.46

M _{2m} = 0.78	i _{2m} = -3.47°	N/√θ = 110%
------------------------	--------------------------	-------------

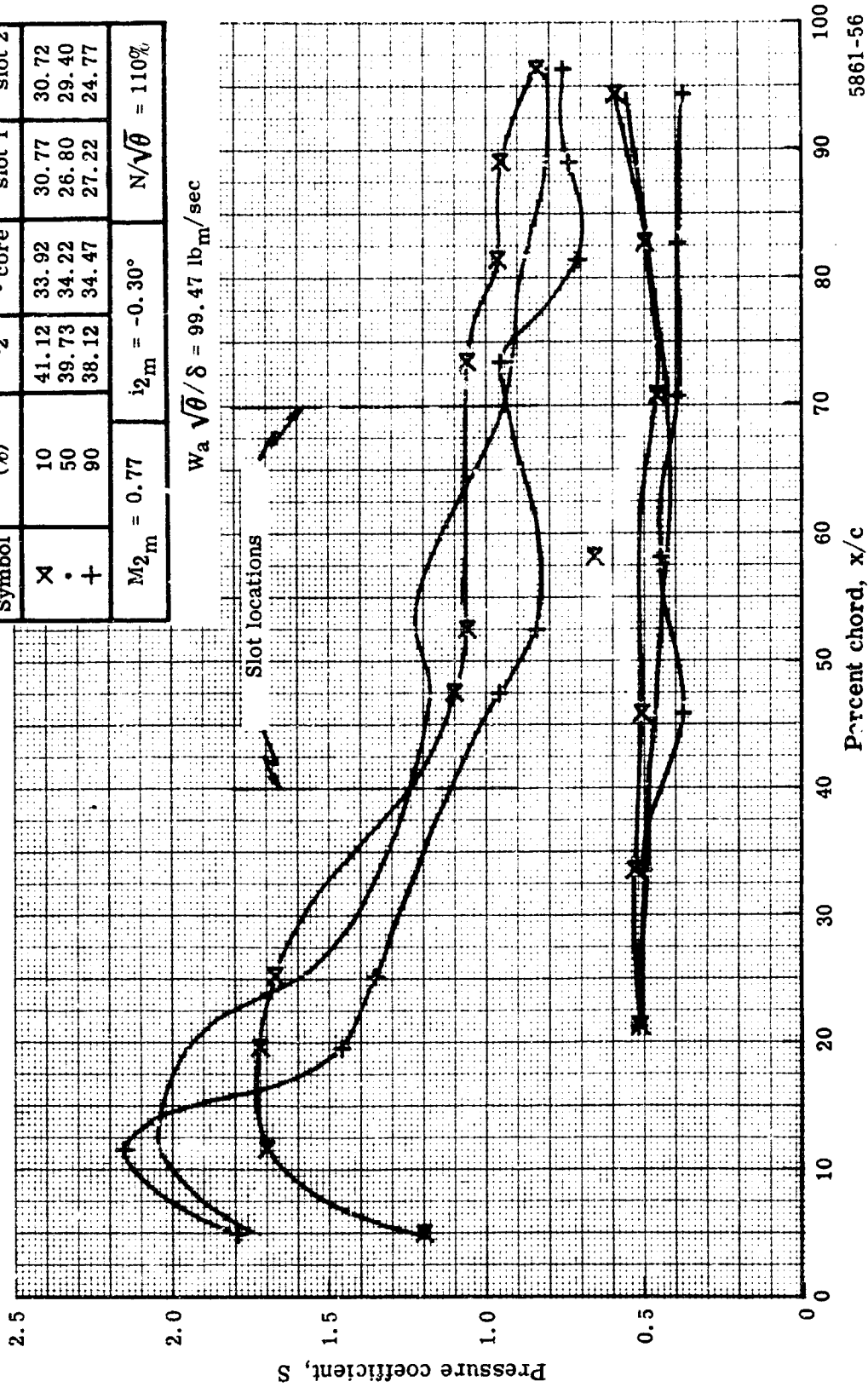
$w_a \sqrt{\theta} / \delta = 99.74 \text{ lb}_m/\text{sec}$



5861-55

Figuer 27b. Slotted stator static pressure distribution at 110% speed.

Symbol	Streamline from tip (%)	In. Hg abs			
		P_{t2}	$P_{t \text{ core}}$	$P_{\text{slot 1}}$	$P_{\text{slot 2}}$
x	10	41.12	33.92	30.77	30.72
.	50	39.73	34.22	26.80	29.40
+	90	38.12	34.47	27.22	24.77
$M_{2m} = 0.77$		$i_{2m} = -0.30^\circ$		$N/\sqrt{\theta} = 110\%$	

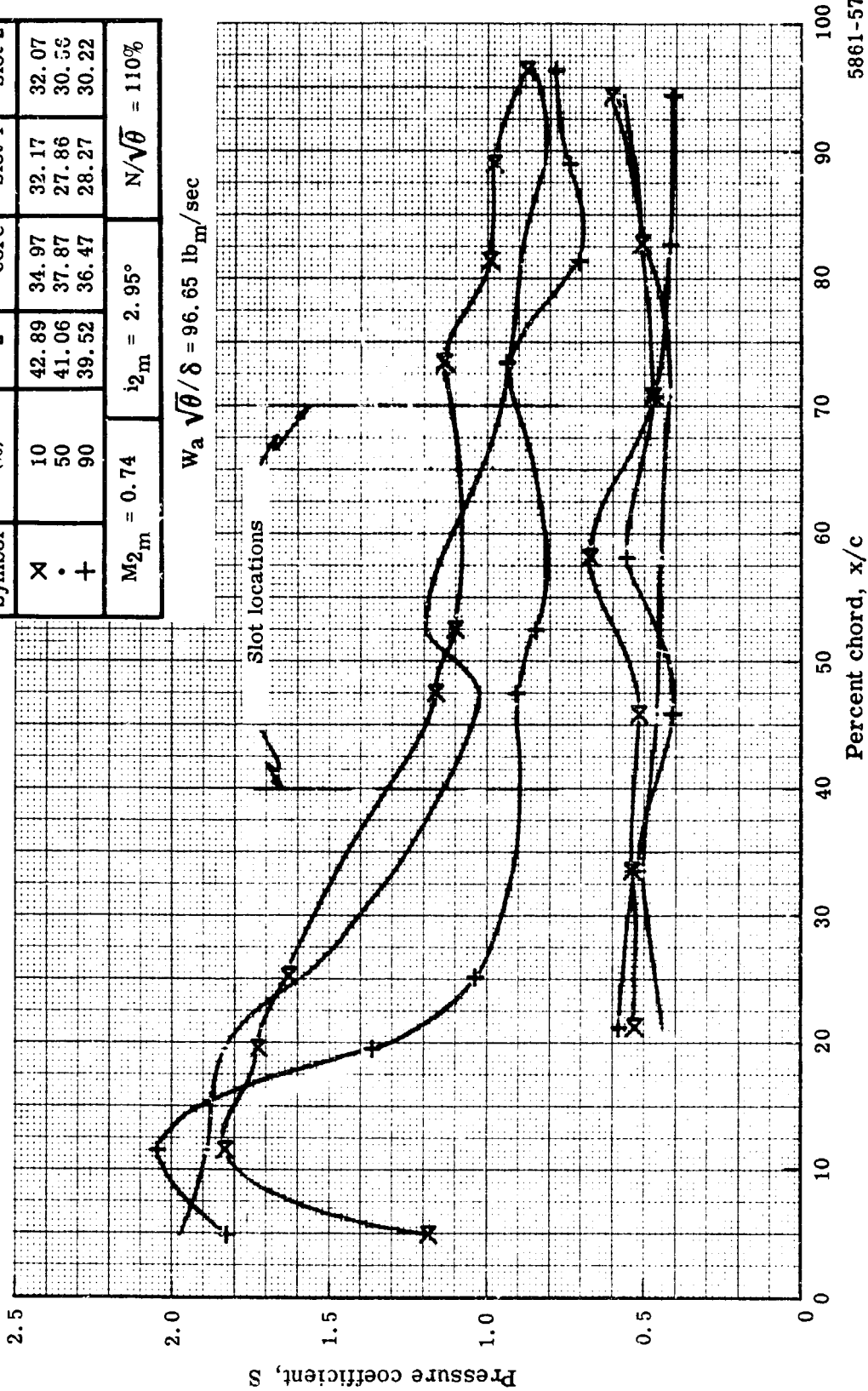


5861-56

Figure 27c. Slotted stator static pressure distribution at 110% speed.

Symbol	Streamline from tip (%)	In. Hg abs			
		P _{t2}	P _{t core}	P slot 1	P slot 2
X	10	42.89	34.97	32.17	32.07
•	50	41.06	37.87	27.86	30.55
+	90	39.52	36.47	28.27	30.22
M _{2m} = 0.74		l _{2m} = 2.95°		N/√θ = 110%	

$W_a \sqrt{\theta} / \delta = 96.65 \text{ lb}_m/\text{sec}$

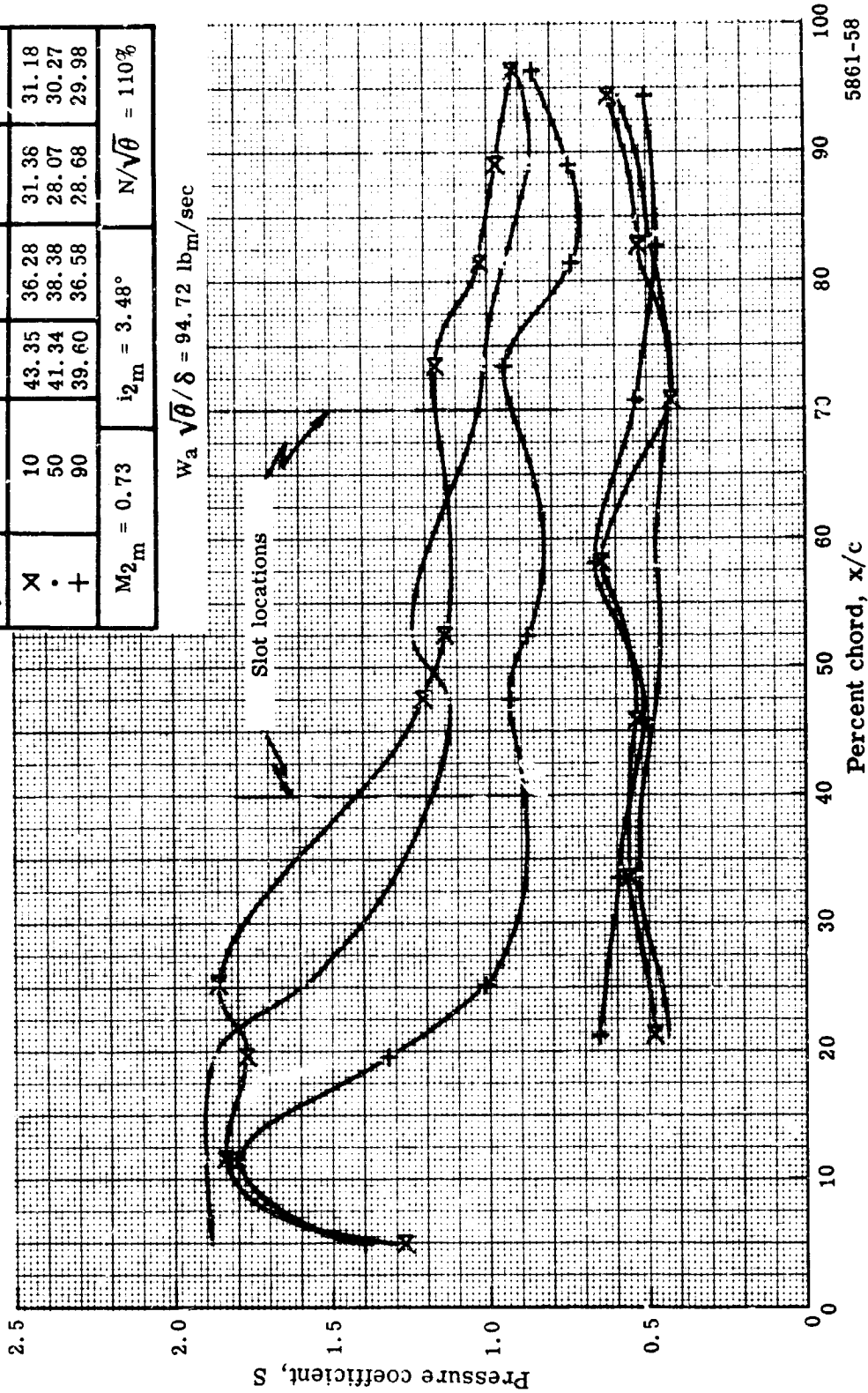


5861-57

Figure 27d. Slotted stator static pressure distribution at 110% speed.

Symbol	Streamline from tip (%)	In. Hg abs			
		P_{t2}	$P_{t \text{ core}}$	$P \text{ slot 1}$	$P \text{ slot 2}$
X	10	43.35	36.28	31.36	31.18
.	50	41.34	38.38	28.07	30.27
+	90	39.60	36.58	28.68	29.98
$M_{2m} = 0.73$		$i_{2m} = 3.48^\circ$		$N/\sqrt{\theta} = 110\%$	

$W_a \sqrt{\theta} / \delta = 94.72 \text{ lb}_m/\text{sec}$

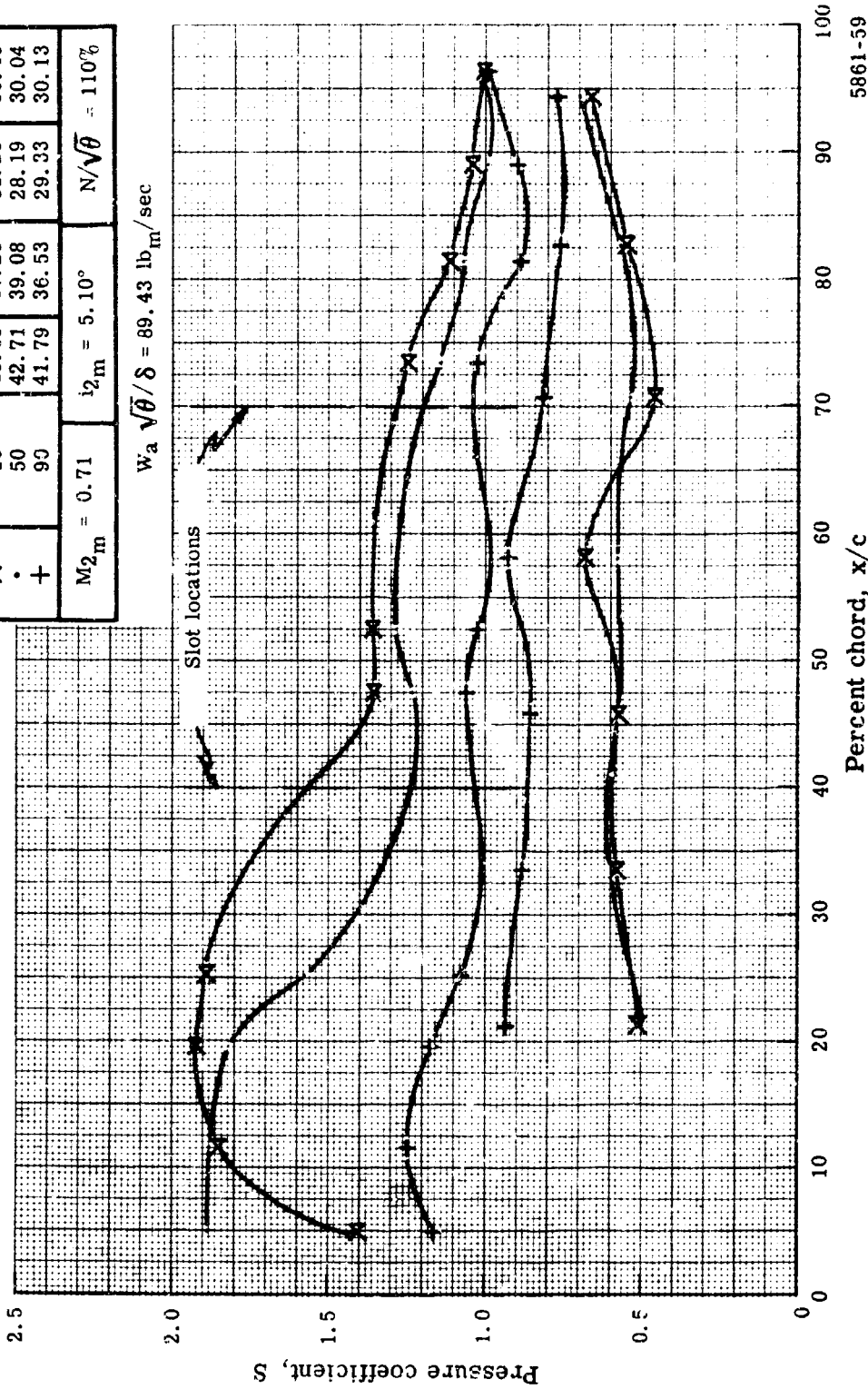


5861-58

Figure 27e. Slotted stator static pressure distribution at 110% speed.

Symbol	Streamline from tip (%)	In. Hg abs			
		P_{t2}	$P_{t \text{ core}}$	$p \text{ slot 1}$	$p \text{ slot 2}$
X	10	45.09	37.28	31.28	30.48
.	50	42.71	39.08	28.19	30.04
+	90	41.79	36.53	29.33	30.13
$M_{2m} = 0.71$		$i_{2m} = 5.10^\circ$		$N/\sqrt{\theta} = 110\%$	

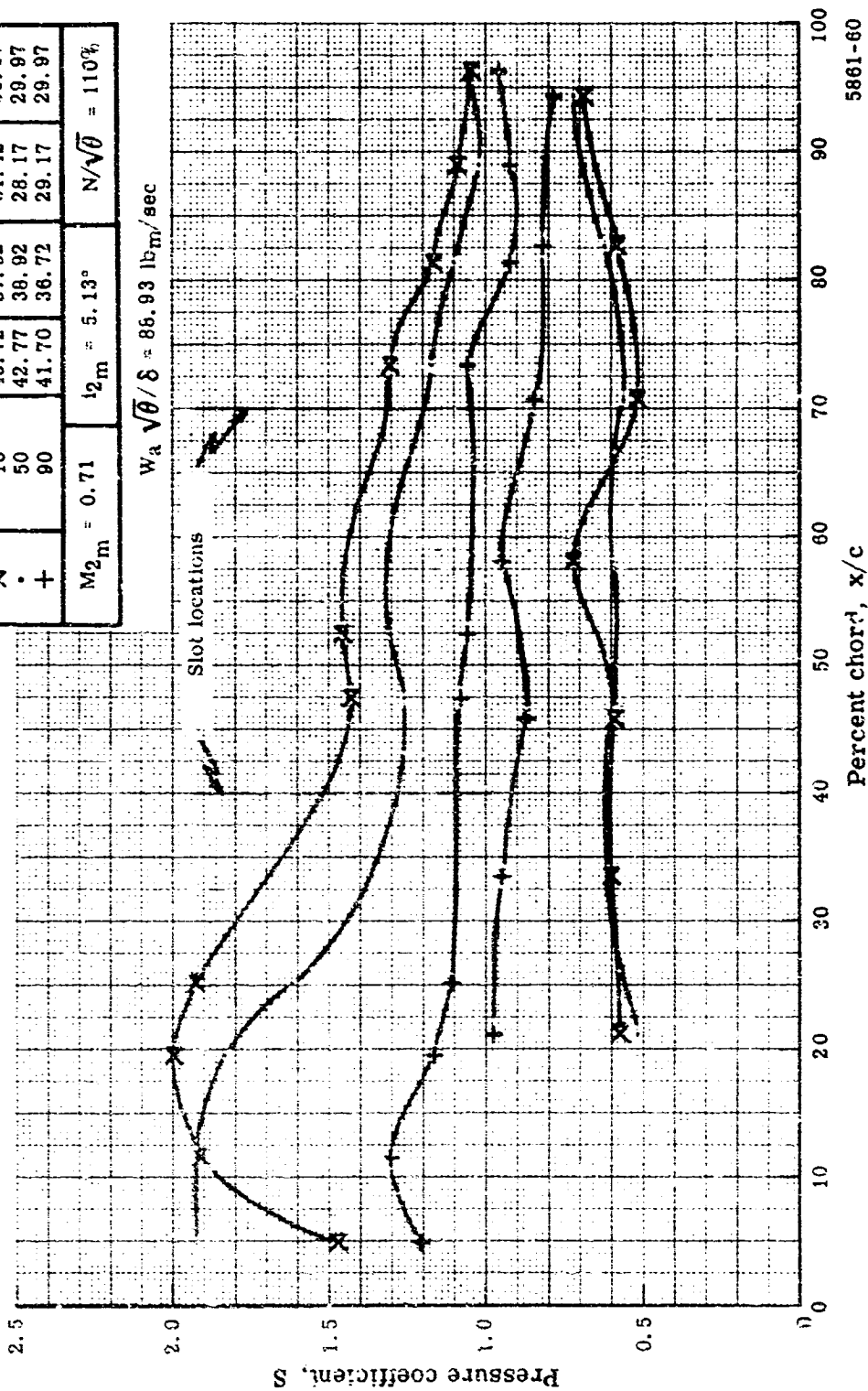
$W_a \sqrt{\theta} / \delta = 89.43 \text{ lb}_m/\text{sec}$



5861-59

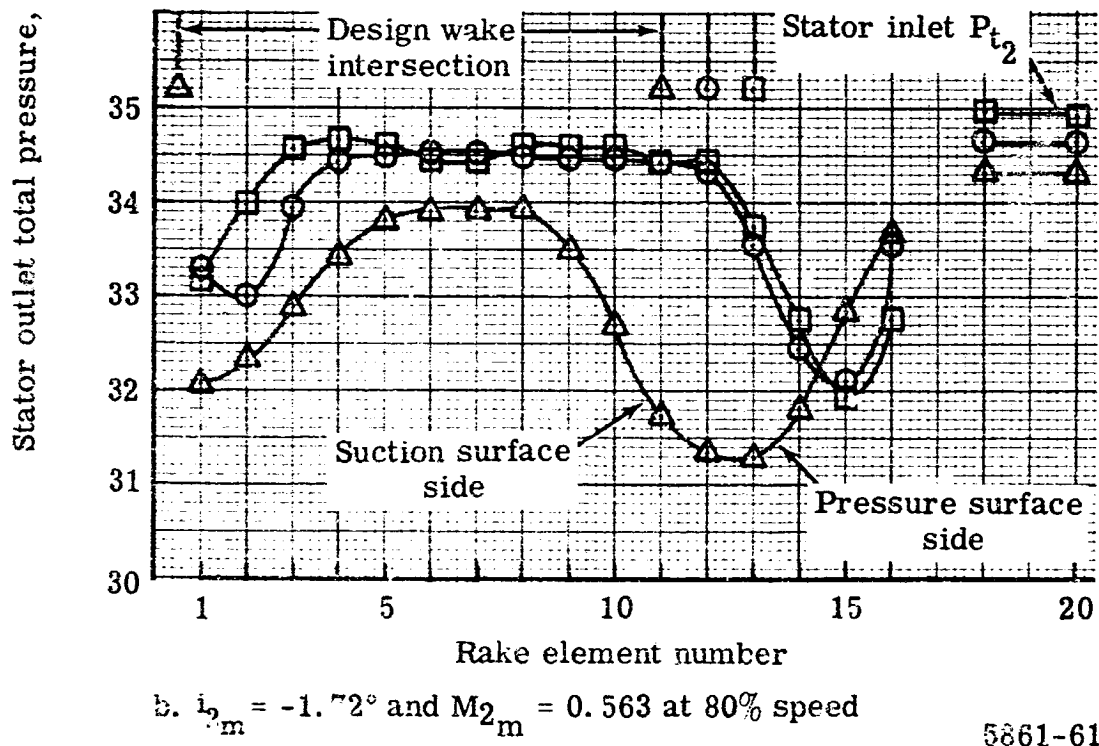
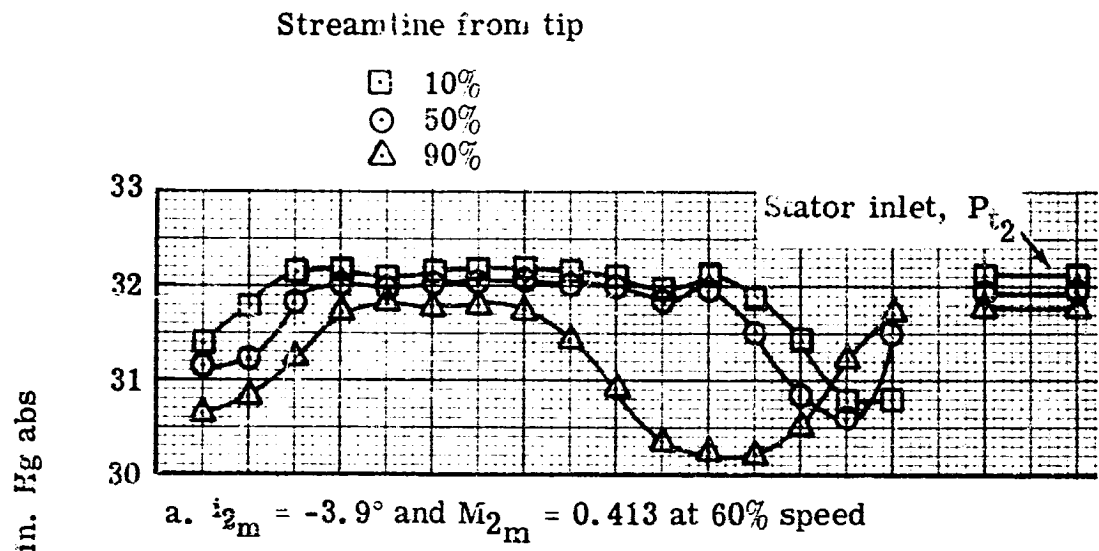
Figure 2/f. Slotted stator static pressure distribution at 110% speed.

Symbol	Streamline from tip (%)	In. Hg abs			
		P _{t2}	P _{t core}	P slot 1	P slot 2
X	10	45.72	37.52	31.42	30.17
.	50	42.77	38.92	28.17	29.97
+	90	41.70	36.72	29.17	29.97
M _{2m} = 0.71		t _{2m} = 5.13°		N/√θ = 110%	



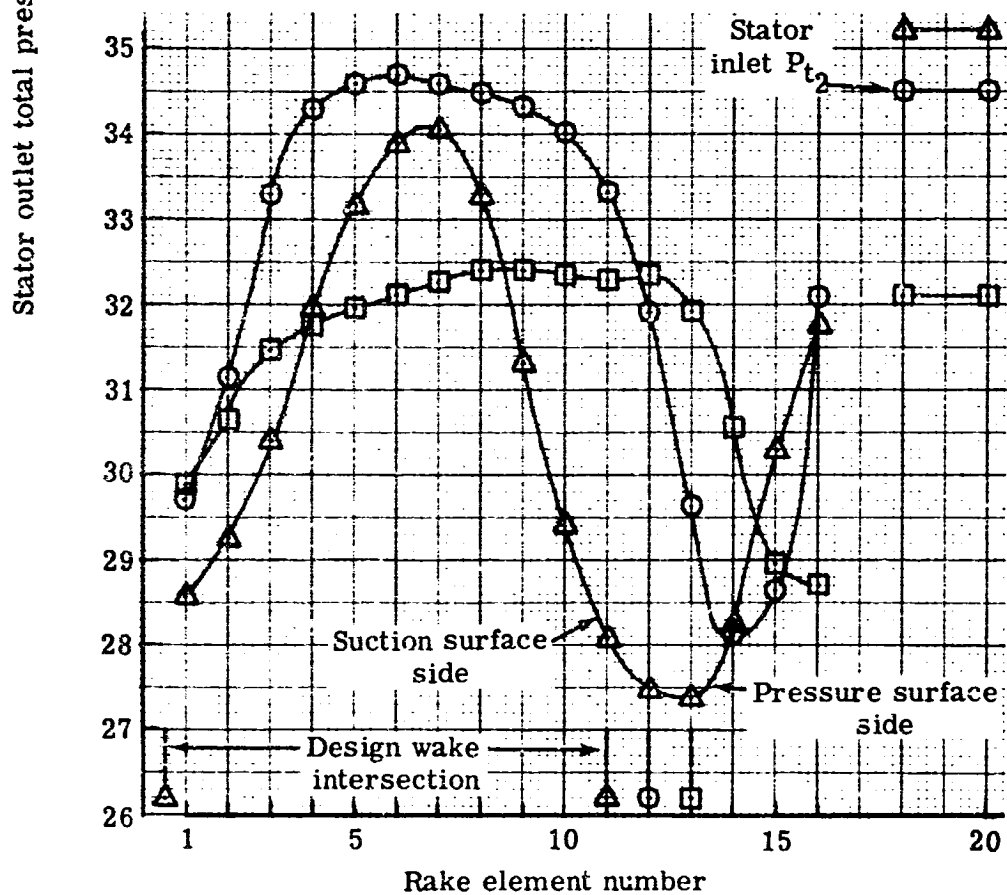
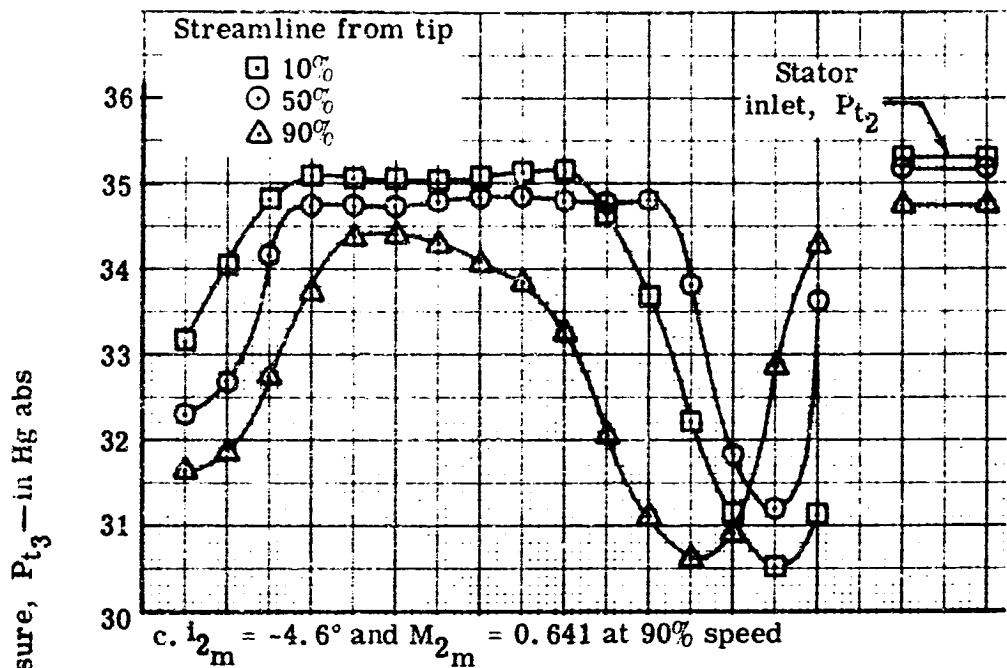
5861-60

Figure 27g. Slotted stator static pressure distribution at 110% speed.



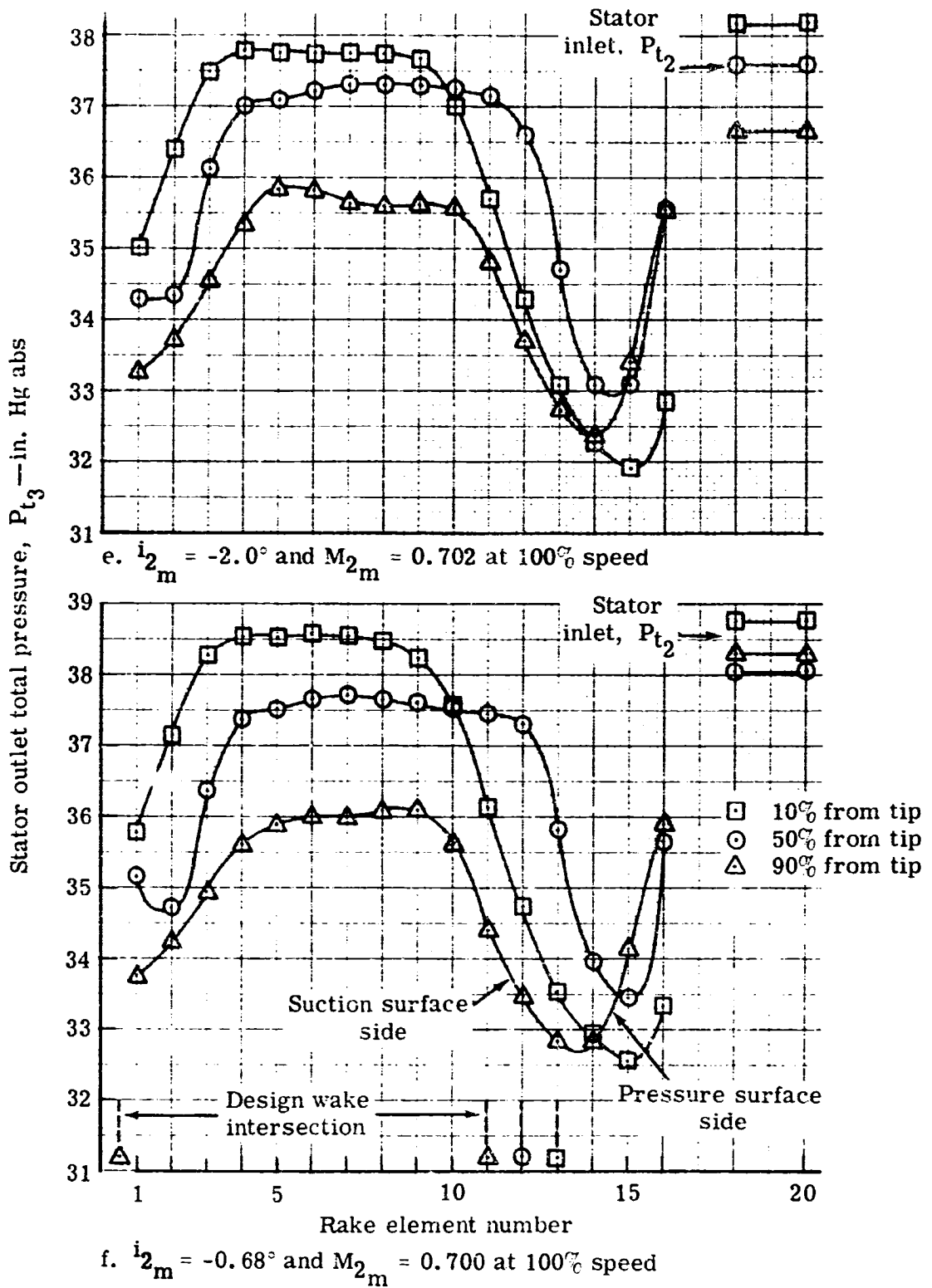
5861-61

Figure 28. Double slotted stator wake surveys.



5861-62

Figure 28. Double slotted stator wake surveys.



5861-63

Figure 28. Double slotted stator wake surveys.

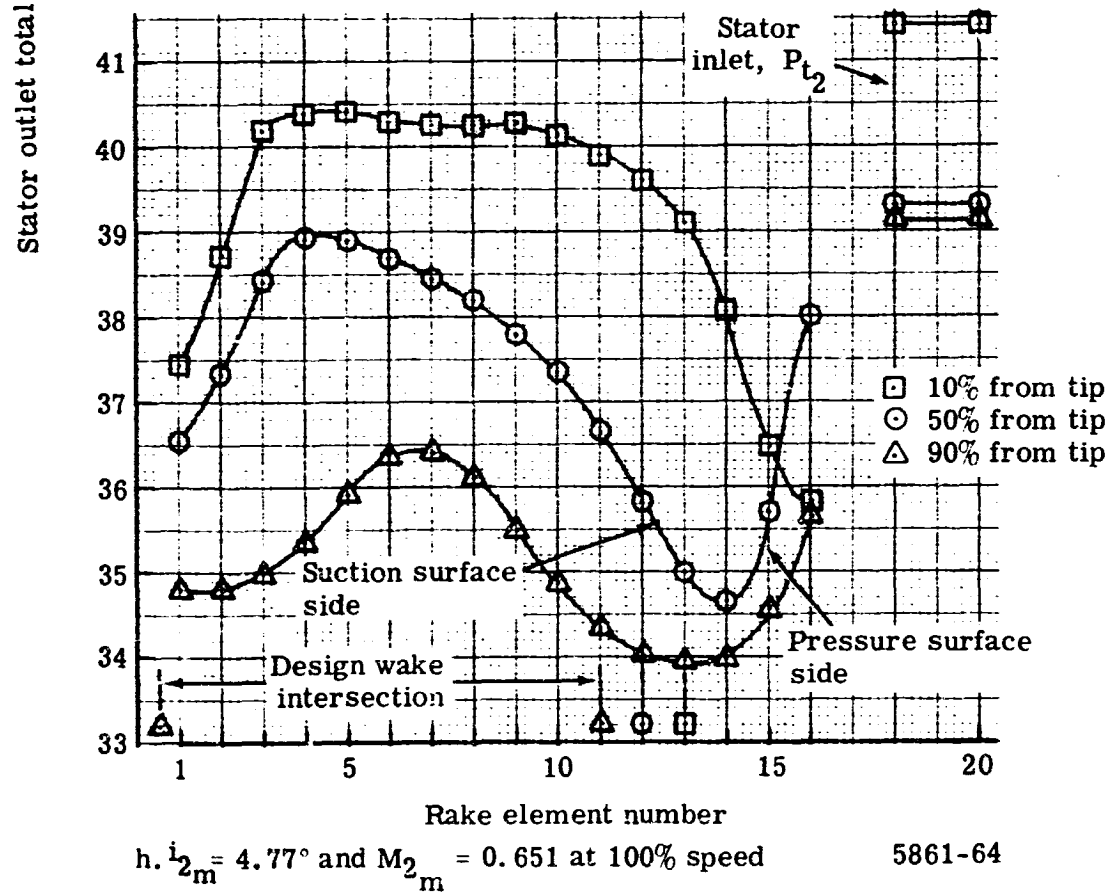
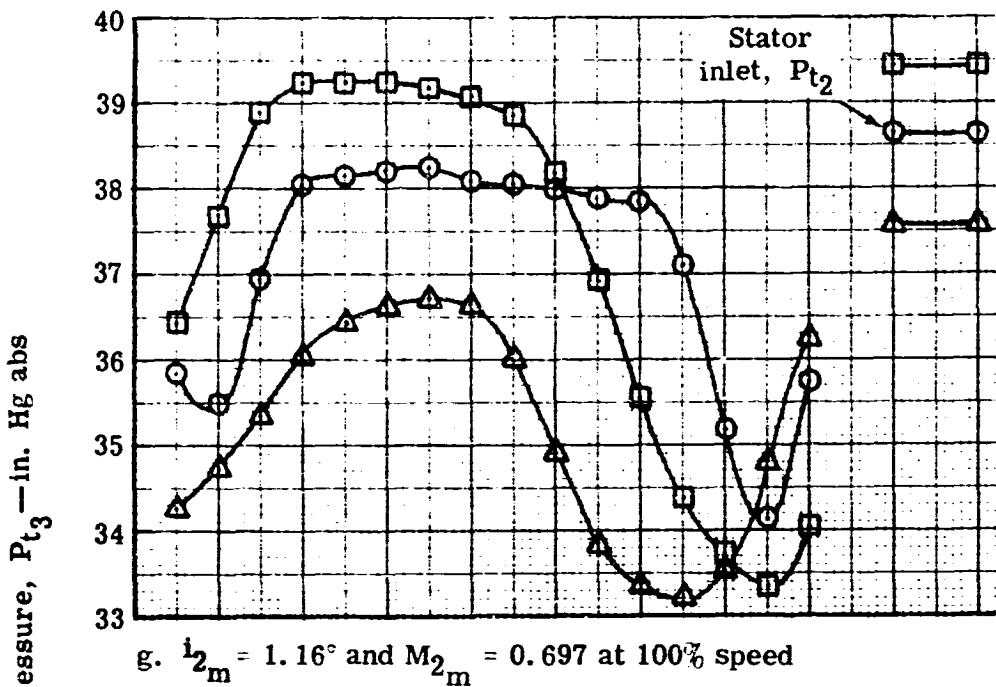
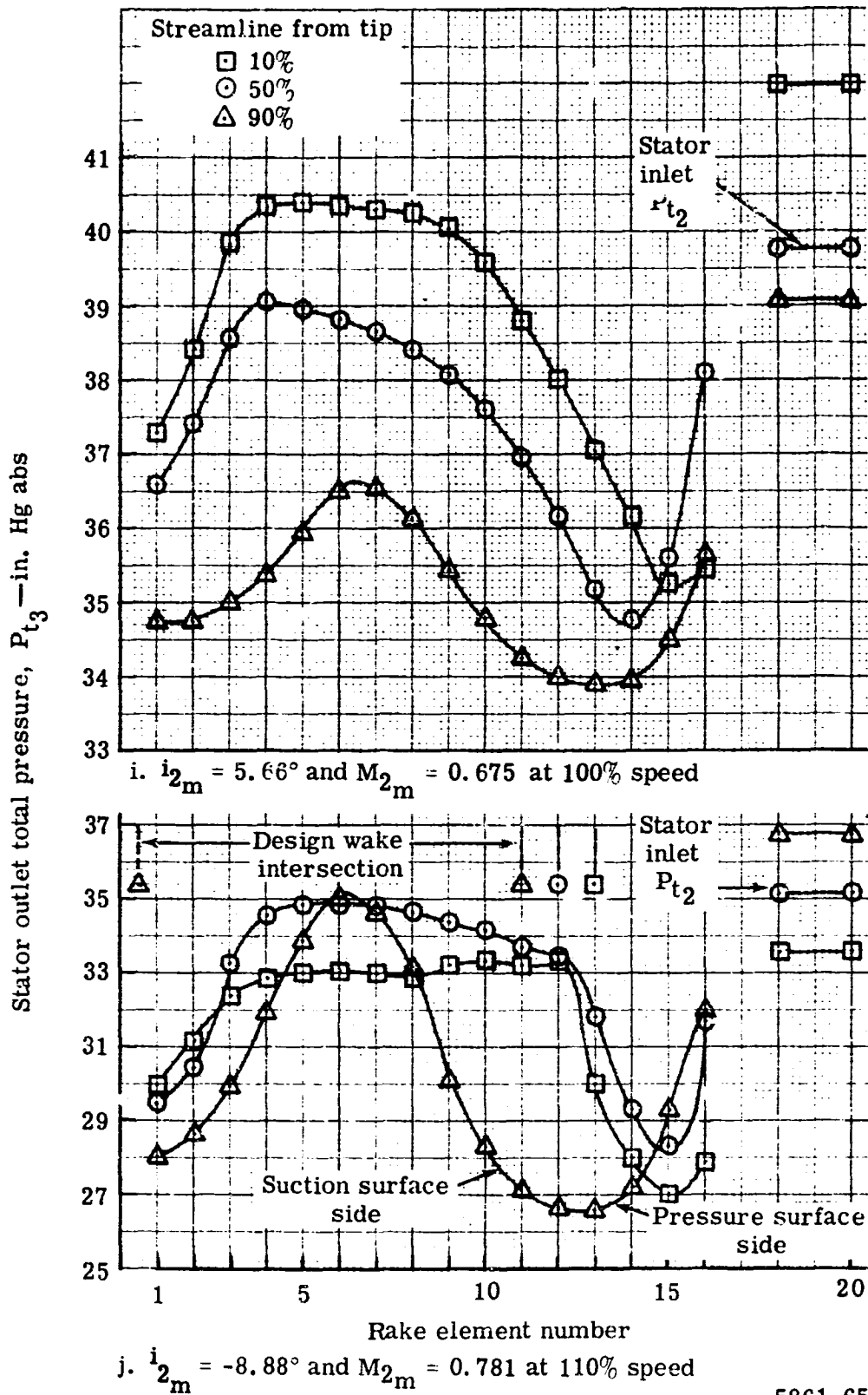
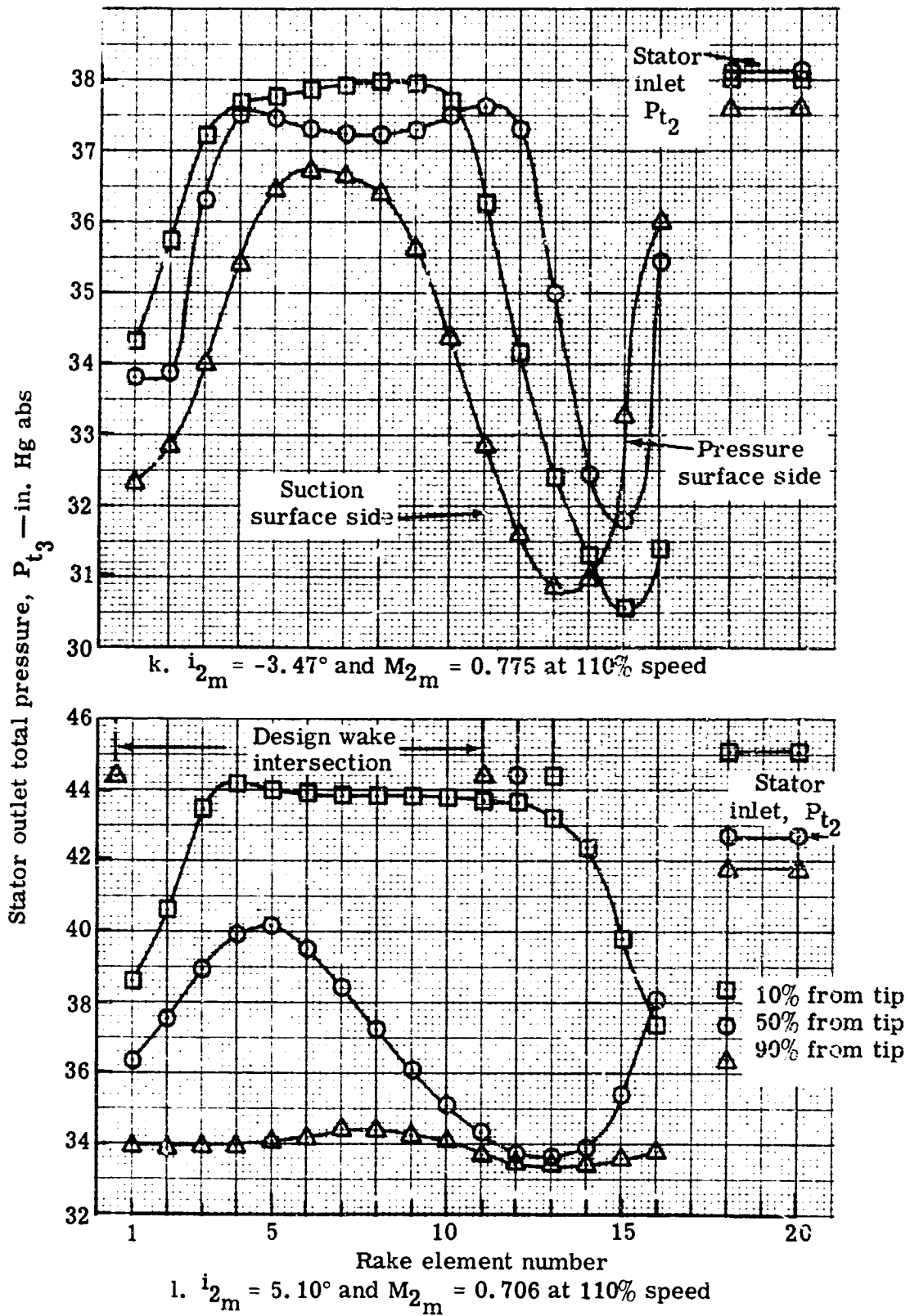


Figure 28. Double slotted stator wake surveys.



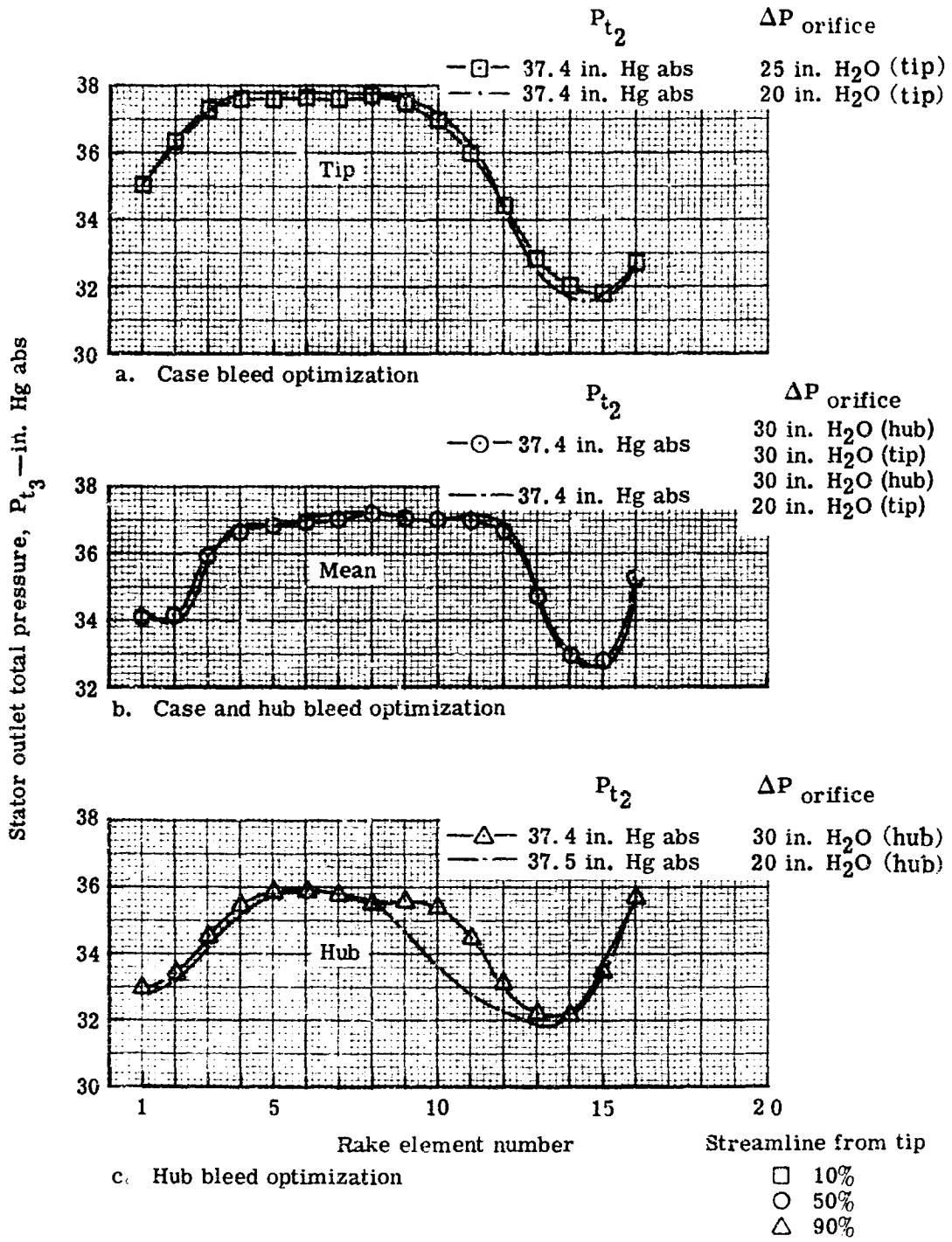
5861-65

Figure 28. Double slotted stator wake surveys.



5861-66

Figure 28. Double slotted stator wake surveys.



5861-67

Figure 29. Variation in stator wake at 10, 50, and 90% streamlines from tip during wall bleed optimization.

Table I.

Blade and vane geometry summary.

Blade row	Exit radius (in.) *	κ_1 (degrees)	κ_2 (degrees)	ϕ ($\kappa_1 - \kappa_2$)	c (in.)	$\bar{\sigma}$	t/c	δ°	i_{des} (degrees)	α des (degrees)	n
Design inlet guide vane (63-006 Series)	10.49	—	—	—	2.733	1.41	0.06	—	—	17.80	34
	11.51	—	—	—	2.733	1.29	0.06	—	—	16.25	
	12.53	—	—	—	2.733	1.18	0.06	—	—	15.16	
	13.54	—	—	—	2.733	1.09	0.06	—	—	14.36	
	14.58	—	—	—	2.733	1.02	0.06	—	—	13.30	
Rotor blade (double-circular arc)	10.97	43.1	9.1	34.0	2.875	1.89	0.078	7.81	0	—	45
	11.86	49.2	21.0	28.2	2.875	1.74	0.052	7.38	0	—	
	12.76	53.4	31.2	22.2	2.875	1.61	0.039	6.34	0	—	
	13.65	56.7	39.1	17.6	2.875	1.51	0.033	5.52	0	—	
	14.54	59.6	44.4	15.2	2.875	1.42	0.032	4.85	0	—	
Stator blade 0.75 L _f H (65 Series - circular arc meanline)	11.02	56.16	-17.80	73.96	3.0	1.65	0.10	17.82	-3	—	38
	11.94	54.15	-17.70	71.85	3.0	1.52	0.10	17.70	-3	—	
	12.84	52.14	-17.75	70.49	3.0	1.41	0.10	17.74	-3	—	
	13.71	52.12	-18.05	70.17	3.0	1.32	0.10	18.06	-3	—	
	14.58	50.09	-18.96	69.05	3.0	1.24	0.10	19.03	-3	—	

*Radii listed represent those for instrumentation (see Figure 6)

Table II.

Rotor incidence at minimum and maximum
flow for flow generation rotor and
slotted stator stage tests.

		Flow generation rotor test		Slotted stator stage test	
Corrected speed (percent)	Streamline from tip (percent)	i_{max} (stall) (degrees)	i_{min} (choke) (degrees)	i_{max} (stall) (degrees)	i_{min} (choke) (degrees)
60	10	6.2	- 8.0	7.4	-3.1
	50	6.0	-12.0	8.0	-4.5
	90	7.6	-13.0	14.8	-3.0
80	10	5.4	- 8.0	5.9	-3.5
	50	5.4	- 7.5	6.3	-4.5
	90	8.0	- 8.0	8.3	-5.2
100	10	4.0	- 3.0	3.1	-2.5
	50	4.0	- 4.3	3.4	-4.2
	90	4.7	- 5.0	5.3	-4.8

Table III.

Rotating stall results for the double slotted stator stage test.

Corrected speed (percent)	Corrected airflow (lb/sec)	Number of stall cells at streamline from tip			Rotative cell speed in (percent rpm)	Stall cell frequency (cps)	Comment
		10%	90%	90%			
60	46.85	1	1	27	23	Abrupt stall at first hysteresis point; stress = 13,600 psi.	
60	46.37	1	1	27	23	Abrupt stall; maximum stress = 12,800 psi.	
80	64.03	1	1	36	50	Abrupt stall; maximum stress = 14,800 psi.	
90	72.43	1	1	43	56	Abrupt stall with maximum stress = 16,800 psi	
100	84.00	1	1			Intermittent stall with no specific pattern; stress = 14,800 psi.	
100	81.00	2	2	35	100	Intermittent stall; maximum stress of 18,000 psi peaks exceed the transient limit.	
110	94.70					Stall cells appearing without a definite pattern; maximum stress = 6,950 psi.	
110	89.50					Intermittent stall with no definite pattern; stress = 10,150 psi.	
110	83.20					No data recorded; stall is abrupt and the maximum stress is considerably higher than the transient stress limit.	

Table IVa.
 BLADE ELEMENT PERFORMANCE - SLOTTED STATOR STAGE

		STATION 1 - STATION 2				STATION 2 - STATION 3					
		10	30	50	70	90	10	30	50	70	90
PERCENT DESIGN SPEED = 59.57											
CORRECTED WEIGHT FLOW = 69.07											
CORRECTED ROTOR SPEED = 5017.26											
PRESSURE RATIO = 1.0917											
ADIABATIC EFFICIENCY = 80.5005											
		ROTOR 1									
		STATION 1 - STATION 2									
		29.150	27.080	25.060	23.020	20.989					
U/A 1		29.088	27.302	25.516	23.730	21.944					
U/A 2		10.620	20.512	22.134	21.280	20.200					
U/A 3		37.632	39.359	41.714	43.807	45.944					
U/A (PR) 1		50.494	52.881	49.255	45.756	41.935					
U/A (PR) 2		47.749	40.800	32.925	23.617	14.533					
V 1		572.77	381.79	386.30	390.53	395.39					
V 2		459.29	409.01	497.27	527.17	546.53					
VZ 1		553.25	357.58	357.83	363.90	371.07					
VZ 2		347.70	393.10	371.20	380.44	380.03					
V-THEIA 1		119.02	133.78	149.55	141.73	136.53					
V-THEIA 2		258.23	297.82	333.69	364.92	392.77					
V(PK) 1		539.69	592.5	548.3	521.6	498.8					
V(PK) 2		517.4	479.7	442.2	415.2	392.6					
V-THEIA PR1		533.0	472.5	415.5	373.6	333.4					
V-THEIA PR2		383.0	313.4	240.4	166.3	98.5					
U 1		622.61	506.27	501.05	515.37	469.88					
U 2		651.22	511.24	571.25	531.27	491.28					
U 3		0.3302	0.3384	0.3425	0.3463	0.3507					
U 4		0.3847	0.4122	0.4372	0.4644	0.4819					
W(PK) 1		0.5669	0.5252	0.4661	0.4625	0.4425					
W(PK) 2		0.4531	0.4210	0.3888	0.3657	0.3462					
LOSS COEF.		0.745	12.081	16.340	22.139	27.402					
LOSS COEF.		0.0993	0.0655	0.0743	0.0521	0.0706					
DFAC		0.2744	0.2791	0.2715	0.3168	0.3356					
EFFP		0.8165	0.8052	0.8984	0.9376	0.9243					
EFF		0.8140	0.8534	0.8970	0.9366	0.9232					
LOSS PARA.		0.0237	0.0209	0.0191	0.0136	0.0178					
INCID		-3.11	-4.02	-4.44	-4.04	-3.06					
DEV		2.049	2.000	2.125	2.917	5.835					
		CORRECTED WEIGHT FLOW									
		UPSTREAM OF ROTOR									
		65.07									
		UPSTREAM OF STATOR									
		65.07									
		DOWNSTREAM OF STATOR									
		61.61									

Table IVb.
 BLADE ELEMENT PERFORMANCE -- SLOTTED STATOR STAGE

		STATION 1 -- STATION 2			
		ROTOR 1			
		10	30	50	90
PERCENT DESIGN SPEED =	59.9%				
CORRECTED WEIGHT FLOW =	59.52				
CORRECTED ROTOR SPEED =	2017.09				
PRESSURE RATIO =	1.1190				
AERODYNAMIC EFFICIENCY =	90.3040				
STATION 1					
		10	30	50	90
U/A 1		29.150	27.050	25.060	23.020
U/A 2		29.080	27.302	25.516	23.730
BETA 1		20.421	20.422	22.766	23.844
BETA 2		42.124	44.670	47.023	51.086
ALFA(PK) 1		59.206	56.758	52.686	45.449
ALFA(PK) 2		40.851	41.499	33.257	23.977
V 1		339.59	346.00	351.29	352.34
V 2		445.36	460.26	464.56	420.73
VZ 1		316.25	324.25	321.99	322.27
VZ 2		330.32	327.32	330.33	330.48
V-THETA 1		118.49	120.73	135.23	142.91
V-THETA 2		278.72	323.57	354.52	384.15
V(PK) 1		621.0	583.8	534.4	492.3
V(PK) 2		483.0	435.7	395.0	351.7
V-THETA PK1		534.0	485.4	425.0	372.4
V-THETA PK2		352.4	287.5	216.5	147.0
U 1		652.49	606.15	560.94	515.27
U 2		651.10	611.12	571.14	531.17
M 1		0.3005	0.3081	0.3109	0.3117
M 2		0.3887	0.4023	0.4243	0.4448
M(PK) 1		0.5497	0.5164	0.4729	0.4353
M(PK) 2		0.4215	0.3808	0.3459	0.3175
TURB(PK)		12.356	14.959	19.429	25.172
LOSS COEFF.		0.0706	0.0825	0.0780	0.0321
DFAC		0.3261	0.3655	0.3804	0.3953
EFFP		0.9028	0.8760	0.9158	0.9499
LEFF		0.9011	0.8942	0.9144	0.9335
LOSS PARA.		0.0170	0.0205	0.0200	0.0083
INCID		-0.39	-0.64	-1.01	-0.65
DEV		1.751	2.499	2.457	3.277
CORRECTED WEIGHT FLOW					
UPSTREAM CF ROTOR				59.52	
UPSTREAM OF STATOR				59.52	
DOWNSTREAM OF STATOR				55.85	
STATION 2					
		10	30	50	90
U/A 3		27.524	25.672	23.674	21.634
BETA 2		44.670	47.023	49.250	51.086
BETA 3		0.001	-0.134	-1.657	-5.635
V 2		460.69	464.59	460.77	529.75
V 3		328.59	320.54	320.45	312.07
VZ 2		327.52	330.33	335.56	327.09
VZ 3		324.59	328.01	320.29	309.96
V-THETA 2		323.57	334.54	364.19	409.18
V-THETA 3		0.01	-4.61	-9.20	-30.06
M 2		0.4023	0.4243	0.4448	0.4574
M 3		0.2655	0.2655	0.2761	0.2707
TURB		44.665	47.177	50.559	57.721
LOSS COEFF.		0.0319	0.0319	0.0765	0.0725
DFAC		0.5310	0.5271	0.6215	0.6567
LOSS PARA.		0.0152	0.0101	0.0250	0.0218
INCID		-1.047	-1.049	-1.470	-1.489
DEV		10.091	17.046	10.623	11.195

Table IVc.
 BLADE ELEMENT PERFORMANCE - SLOTTED STATOR STAGE

ROTOR 1

STATION 1 - STATION 2

	10	30	50	70	90
DIA 1	29.150	27.080	25.060	23.020	20.988
DIA 2	29.088	27.302	25.516	23.730	21.944
BETA 1	19.304	20.905	22.434	23.630	23.928
BETA 2	43.290	45.916	48.781	51.189	52.815
BETA(PRI) 1	60.407	57.465	54.525	51.017	46.539
BETA(PK) 2	47.311	41.909	34.723	25.617	15.964
V 1	328.77	334.13	335.46	337.46	344.22
V 2	443.20	456.90	474.31	493.86	508.57
VZ 1	310.28	312.13	310.07	309.16	314.64
VZ 2	322.60	317.87	312.54	309.53	307.38
V-THETA 1	108.68	119.23	126.02	135.26	139.61
V-THETA 2	303.90	326.20	356.77	384.82	405.17
V(PRI) 1	628.3	580.4	534.3	491.4	451.4
V(PRI) 2	475.8	427.1	380.3	343.3	319.7
V-THETA PRI	546.3	489.3	435.1	382.0	332.0
V-THETA PR2	349.7	285.3	216.6	148.4	87.9
U 1	655.03	608.52	563.12	517.28	471.62
U 2	653.64	613.50	573.37	533.24	493.10
M 1	0.2893	0.2941	0.2953	0.2970	0.3031
M 2	0.3842	0.3969	0.4127	0.4303	0.4436
M(PRI) 1	0.5528	0.5108	0.4702	0.4326	0.4028
M(PRI) 2	0.4125	0.3710	0.3309	0.2991	0.2788
TURN(PRI)	13.096	15.556	19.803	25.401	30.575
LUS3 COEF.	0.0884	0.0856	0.0832	0.0973	0.1614
DFAC	0.3531	0.3800	0.4137	0.4365	0.4400
EFFP	0.8874	0.9011	0.9157	0.9155	0.8776
EFF	0.8852	0.8993	0.9141	0.9140	0.8755
LOSS PARA.	0.0211	0.0210	0.0210	0.0249	0.0405
INCLD	0.81	0.56	0.83	1.22	1.54
DEV	2.211	3.109	3.923	4.917	7.264

PERCENT DESIGN SPEED = 59.93
 CORRECTED WEIGHT FLOW = 56.47
 CORRECTED ROTOR SPEED = 5014.31
 PRESSURE RATIO = 1.1308
 ADIABATIC EFFICIENCY = 90.4677

STATOR 1

STATION 2 - STATION 3

	10	30	50	70	90
DIA 3	20.164	27.422	45.672	23.874	22.034
DIA 4	43.290	45.916	48.781	51.189	52.815
BETA 3	-1.287	-0.250	-0.918	-2.770	-9.298
V 4	543.20	456.90	474.31	493.86	508.57
V 3	328.77	325.03	319.23	307.44	276.83
VZ 2	322.60	317.87	312.54	309.53	307.38
VZ 1	310.28	312.13	310.07	309.16	314.64
V-THETA 4	203.90	248.20	326.77	384.82	405.17
V-THETA 3	-7.45	-3.12	-5.14	-14.88	-44.73
M 2	0.2893	0.2969	0.2970	0.2970	0.3031
M 3	0.2893	0.2969	0.2970	0.2970	0.3031
TURN COEF.	0.0142	0.0174	0.0421	0.0891	0.0891
DFAC	0.5242	0.5551	0.6411	0.6411	0.7229
LOSS PARA.	0.0121	0.0054	0.0061	0.0137	0.0266
INCLD	-8.79	-6.24	-3.92	-2.81	-3.14
DEV	17.675	17.490	16.332	14.910	14.502

CORRECTED WEIGHT FLOW

UPSTREAM OF ROTOR

UPSTREAM OF STATOR

DOWNSTREAM OF STATOR

56.47
 56.47
 52.84

Table IVd.
BLADE ELEMENT PERFORMANCE - SLOTTED STATOR STAGE

ROTOR 1

STATION 1 - STATION 2

	10	30	50	70	90
DIA 1	29.150	27.080	25.060	23.020	20.988
DIA 2	29.088	27.302	25.516	23.730	21.944
BETA 1	20.634	20.510	22.377	23.372	23.747
BETA 2	48.847	51.406	55.861	58.200	59.677
BETA(PK) 1	64.051	61.755	58.571	55.090	51.938
BETA(PK) 2	48.020	42.642	34.335	24.774	12.956
V 1	287.97	290.74	297.46	302.26	303.41
V 2	440.53	452.60	473.65	488.02	503.70
V 1	269.50	272.31	275.06	277.46	277.72
V 2	289.90	282.33	265.81	257.17	254.30
V-THETA 1	101.48	101.86	113.24	119.90	122.18
V-THETA 2	331.70	353.74	392.03	414.76	434.79
V(PK) 1	615.9	575.4	527.5	484.8	446.5
V(PK) 2	433.4	383.8	321.9	283.2	260.9
V-THETA PK1	553.8	506.9	450.1	397.6	349.6
V-THETA PK2	322.2	260.0	181.6	118.7	58.5
U 1	655.28	608.75	563.34	517.48	471.80
U 2	653.89	613.74	573.59	533.44	493.30
M 1	0.2528	0.2552	0.2612	0.2655	0.2665
M 2	0.3813	0.3922	0.4111	0.4240	0.4381
M(PK) 1	0.5406	0.5051	0.4632	0.4258	0.3922
M(PK) 2	0.3752	0.3326	0.2794	0.2461	0.2269
TURN(PK)	16.031	19.112	24.236	30.316	38.982
LOSS COEF.	0.0327	0.0490	0.0669	0.1066	0.1532
DFAC	0.4289	0.4746	0.5459	0.5792	0.5856
EFFP	0.9624	0.9490	0.9404	0.9182	0.8985
EFF	0.9616	0.9480	0.9392	0.9166	0.8965
LUSS PARA.	0.0077	0.0119	0.0170	0.0275	0.0394
INCID	4.45	4.85	4.87	5.29	6.54
DEV	2.920	3.842	3.535	4.074	4.256

STATION 2 - STATION 3

	10	30	50	70	90
PERCENT DESIGN SPEED	59.93				
CORRECTED WEIGHT FLOW	51.32				
CORRECTED ROTOR SPEED	5014.24				
PRESSURE RATIO	1.1470				
ADIABATIC EFFICIENCY	89.0706				

STATOR 1

	10	30	50	70	90
DIA 3	29.164	27.422	25.672	23.874	22.034
BETA 4	59.847	51.406	55.861	58.200	59.677
BETA 3	-4.128	-0.734	-2.027	-4.075	-11.924
V 2	440.53	452.60	473.65	488.02	503.70
V 3	303.34	295.98	290.12	273.28	253.27
V 4	289.90	282.33	265.81	257.17	254.30
V 1	303.07	295.96	289.94	272.59	258.23
V-THETA 2	331.70	353.74	392.03	414.76	434.79
V-THETA 3	-12.69	-3.79	-10.26	-19.42	-48.20
M 2	0.3813	0.3922	0.4111	0.4240	0.4381
M 3	0.2600	0.2542	0.2492	0.2348	0.2001
TURN	51.245	52.140	57.889	62.275	71.602
LOSS COEF.	0.0307	0.0077	0.0286	0.0455	0.1057
DFAC	0.6254	0.6437	0.6861	0.7310	0.8266
LUSS PARA.	0.0123	0.0029	0.0100	0.0148	0.0312
INCID	-3.23	-0.73	3.16	4.20	3.73
DEV	16.562	17.306	15.723	13.605	5.876

STATION 4 - STATION 5

	10	30	50	70	90
UPSTREAM OF ROTOR					51.32
UPSTREAM OF STATOR					51.32
DOWNSTREAM OF STATOR					47.61

CORRECTED WEIGHT FLOW

	10	30	50	70	90
UPSTREAM OF ROTOR					51.32
UPSTREAM OF STATOR					51.32
DOWNSTREAM OF STATOR					47.61

Table IVf.
BLADE ELEMENT PERFORMANCE - SLOTTED STATOR STAGE

ROTOR 1
 STATION 1 - STATION 2

	10	30	50	70	90
DIA 1	29.150	27.080	25.060	23.020	20.980
U/A 1	29.088	27.302	25.516	23.730	21.944
BETA 1	18.940	20.740	21.820	23.800	24.340
BETA 2	37.860	40.364	42.495	44.370	46.435
BETA(PK) 1	56.162	52.545	49.180	44.444	39.821
BETA(PK) 2	46.726	39.684	32.215	23.158	14.492
V 1	501.56	513.46	517.34	528.40	534.82
V 2	598.08	637.00	668.29	705.04	725.88
VZ 1	474.41	480.19	480.28	483.46	487.29
VZ 2	472.19	485.36	492.76	503.99	500.26
V-THETA 1	162.80	181.83	192.29	213.23	220.43
V-THETA 2	307.06	412.54	451.44	493.03	525.96
V(PK) 1	852.0	789.6	734.7	677.2	634.4
V(PK) 2	688.8	630.7	582.4	548.2	516.7
VTHETA PK1	707.7	626.8	556.0	474.2	406.3
VTHETA PR2	501.5	402.7	310.5	215.6	129.3
U 1	870.45	808.63	748.32	687.40	626.72
U 2	868.60	815.26	761.93	708.60	655.27
M 1	0.4480	0.4590	0.4627	0.4730	0.4790
M 2	0.5240	0.5602	0.5890	0.6232	0.6428
M(PK) 1	0.7609	0.7059	0.6571	0.6062	0.5682
M(PK) 2	0.6035	0.5546	0.5134	0.4845	0.4575
TURN(PK)	9.436	12.861	16.965	21.286	25.329
LCSS COEF.	0.0801	0.0612	0.0568	0.0551	0.0765
DFAC	0.2768	0.2949	0.3098	0.2990	0.2993
EFFP	0.8604	0.9067	0.9258	0.9399	0.9267
EFF	0.8573	0.9045	0.9239	0.9383	0.9247
LCSS PARA.	0.0194	0.0155	0.0147	0.0144	0.0193
INCID	-3.44	-4.36	-4.52	-5.36	-5.18
UEV	1.626	0.884	1.415	2.458	5.792

CORRECTED WEIGHT FLOW

UPSTREAM OF ROTOR	83.92
UPSTREAM OF STATOR	83.92
DOWNSTREAM OF STATOR	80.71

PERCENT DESIGN SPEED = 79.93
 CORRECTED WEIGHT FLOW = 83.92
 CORRECTED ROTOR SPEED = 6687.66
 PRESSURE RATIO = 1.1632
 ADIABATIC EFFICIENCY = 81.8163

STATION 1

STATION 2 - STATION 3

	10	30	50	70	90
DIA 3	25.164	27.422	25.672	23.874	22.034
BETA 2	37.860	40.364	42.495	44.370	46.435
BETA 3	-1.472	-1.472	-1.657	-2.398	-12.272
V 2	548.08	637.00	668.29	705.04	725.88
V 3	485.00	485.29	503.17	501.85	467.17
VZ 2	474.19	485.36	492.70	503.99	500.26
VZ 3	484.84	485.19	505.96	501.41	456.50
V-THETA 2	507.06	412.54	451.44	493.03	525.96
V-THETA 3	-12.46	-12.47	-14.04	-21.00	-99.30
M 3	0.5240	0.5602	0.5890	0.6232	0.6428
M 2	0.4209	0.4216	0.4402	0.4362	0.4042
TURN	39.332	41.836	44.151	46.768	53.707
LCSS COEF.	0.0584	0.1015	0.0707	0.1151	0.1183
DFAC	0.4439	0.4850	0.4878	0.5266	0.6166
LCSS PARA.	0.0234	0.0362	0.0249	0.0376	0.0526
INCID	-14.22	-11.78	-10.21	-9.63	-9.52
UEV	17.488	16.568	16.093	15.282	5.528

Table IVg.
BLADE ELEMENT PERFORMANCE - SLOTTED STATOR STAGE

		STATION 1 - STATION 2			
		10	30	50	90
PERCENT DESIGN SPEED = 79.92					
CORRECTED WEIGHT FLOW = 77.55					
CORRECTED ROTOR SPEED = 6687.15					
PRESSURE RATIO = 1.2224					
ADIABATIC EFFICIENCY = 90.5257					
ROTOR 1					
		23.150	27.060	25.060	23.020
DIA 1		29.088	27.302	25.516	23.730
DIA 2		13.610	20.421	23.124	25.014
BETA 1		43.387	45.707	48.406	50.511
BETA 2		59.407	56.396	52.843	48.827
BETA(PR) 1		46.122	40.672	32.952	23.695
BETA(PR) 2		450.88	459.25	465.48	470.74
V 1		601.54	619.03	646.13	673.73
V 2		424.73	430.38	428.08	429.65
VZ 1		437.15	432.29	428.94	428.44
VZ 2		151.32	160.24	182.80	199.05
V-THETA 1		413.21	443.09	483.22	519.95
V-THETA 2		334.5	777.6	708.7	648.0
V(PR) 1		630.7	570.0	511.2	467.9
V(PR) 2		718.4	647.7	564.9	487.7
VHILTA PR1		454.6	371.5	278.0	188.0
VHILTA PR2		869.68	807.93	747.66	686.80
U 1		867.83	814.55	761.26	707.98
U 2		0.4015	0.4092	0.4149	0.4198
M 1		0.5232	0.5403	0.5655	0.5922
M 2		0.7431	0.6929	0.6318	0.5778
M(PR) 1		0.5480	0.4975	0.4474	0.4113
M(PR) 2		13.285	15.724	19.891	25.131
TURN(PR)		0.0471	0.0390	0.0452	-0.0037
LUSS COEF.		0.3557	0.3843	0.4029	0.4093
DFAC		0.9401	0.9540	0.9543	1.0044
EFFP		0.9381	0.9526	0.9529	1.0046
EFF		0.0115	0.0098	0.0116	-0.0010
LOSS PARA.		-0.19	-0.50	-0.86	-0.97
INCID		1.022	1.872	2.152	2.995
DEV					
CORRECTED WEIGHT FLOW					
UPSTREAM OF ROTOR				77.55	
UPSTREAM OF STATOR				77.55	
DOWNSTREAM OF STATOR				73.87	
STATION 2 - STATION 3					
		30	50	70	90
DIA 3		27.164	27.422	25.672	23.874
BETA 2		43.387	45.707	48.406	50.511
BETA 3		-4.075	-0.916	-1.287	-3.142
V 2		601.54	619.03	646.13	673.73
V 3		442.21	440.47	433.83	419.43
VZ 2		437.15	432.29	428.94	428.44
VZ 3		441.10	440.41	433.72	418.80
V-THETA 2		412.21	443.09	483.22	519.95
V-THETA 3		-21.42	-7.00	-9.75	-22.99
M 2		0.5232	0.5403	0.5655	0.5922
M 3		0.7431	0.6929	0.6318	0.5778
TURN		47.462	46.625	45.653	44.179
LOSS COEF.		0.0871	0.0520	0.0603	0.0894
DFAC		0.5617	0.5624	0.5768	0.6410
LOSS PARA.		0.0549	0.0190	0.0212	0.0286
INCID		-6.69	-6.43	-4.29	-3.49
DEV		14.885	17.122	16.463	14.538
					22.034
					52.428
					-11.750
					691.48
					391.73
					421.63
					383.53
					548.06
					-79.78
					0.6080
					0.3368
					64.179
					0.1087
					0.7078
					0.0322
					-3.52
					6.050

Table IVh.
 BLADE ELEMENT PERFORMANCE - SLOTTED STATOR STAGE

		STATION 1 - STATION 2					STATION 2 - STATION 3		
		10	30	50	70	90	30	50	70
PERCENT DESIGN SPEED = 80.00									
CORRECTED WEIGHT FLOW = 75.13									
CORRECTED ROTOR SPEED = 6693.20									
PRESSURE RATIO = 1.2379									
ADIABATIC EFFICIENCY = 90.6545									
ROTOR 1									
		29.150	27.080	25.060	23.020	20.986			
DIA 1		29.088	27.302	25.516	23.730	21.944			
DIA 2		19.160	20.331	22.944	24.204	23.214			
BETA 1		45.375	48.677	50.978	52.728	54.934			
BETA 2		60.576	57.591	54.305	50.517	47.030			
BETA(PK) 1		45.899	40.273	32.701	24.151	13.208			
BETA(PK) 2		433.63	442.23	446.68	452.10	452.91			
V 1		603.30	620.76	643.68	662.45	685.84			
V 2		409.61	414.68	411.34	412.36	416.24			
VZ 1		423.80	409.89	405.27	401.18	394.02			
VZ 2		142.32	153.65	174.13	185.36	178.52			
V-THETA 1		429.38	466.20	500.08	527.16	561.36			
V-THETA 2		833.8	773.7	705.0	648.5	610.7			
V(PR) 1		609.0	537.2	481.6	439.7	404.7			
V(PR) 2		726.2	653.2	572.5	500.5	446.8			
VTHETA PR1		437.3	347.3	260.2	179.9	92.5			
VTHETA PR2		868.54	806.86	746.67	685.89	625.35			
U 1		866.69	813.48	760.26	707.05	653.83			
U 2		0.3866	0.3945	0.3986	0.4035	0.4043			
M 1		0.5243	0.5416	0.5633	0.5814	0.6027			
M 2		0.7433	0.6901	0.6290	0.5789	0.5451			
M(PR) 1		0.5292	0.4687	0.4215	0.3859	0.3556			
M(PR) 2		14.677	17.318	21.604	26.366	33.822			
TURN(PK)		0.0713	0.0521	0.0493	0.0511	0.1033			
LOSS COEF.		0.3918	0.4362	0.4528	0.4625	0.4803			
DFAC		0.9164	0.9433	0.9535	0.9572	0.9237			
EFFP		0.9135	0.9414	0.9519	0.9558	0.9212			
EFF		0.0175	0.0131	0.0127	0.0132	0.0262			
LOSS PARA.		0.98	0.69	0.60	0.72	2.03			
INCID		0.799	1.473	1.901	3.451	4.508			
DEV									
CORRECTED WEIGHT FLOW									
UPSTREAM OF ROTOR						75.13			
UPSTREAM OF STATOR							75.13		
DOWNSTREAM OF STATOR								71.35	
STATOR 1									
		25.874	25.874	25.874	25.874	22.034			
DIA 3		45.375	48.677	50.978	52.728	54.934			
BETA 2		-1.472	-1.472	-1.105	-4.637	-14.355			
BETA 3		42.075	42.075	42.075	42.075	42.075			
V 2		416.44	420.12	412.27	391.54	341.39			
V 3		425.80	405.89	405.27	401.18	394.02			
VZ 2		415.28	419.90	412.20	390.26	330.73			
VZ 3		425.30	406.20	500.08	527.16	561.36			
V-THETA 2		-33.68	-10.75	-7.93	-31.65	-84.64			
V-THETA 3		0.5243	0.5416	0.5633	0.5814	0.6027			
M 2		0.5243	0.5416	0.5633	0.5814	0.6027			
M 3		50.012	50.145	52.081	52.368	54.289			
TURN		0.1036	0.0925	0.0869	0.0691	0.1342			
LOSS COEF.		0.6177	0.6127	0.6370	0.6648	0.787			
DFAC		0.0415	0.0213	0.0200	0.0225	0.0395			
LOSS PARA.		-6.70	-3.46	-1.72	-1.27	-1.02			
INCID		14.523	16.508	18.047	19.043	3.445			
DEV									

Table IVi.
 BLADE ELEMENT PERFORMANCE - SLOTTED STATOR STAGE

		STATION 1 - STATION 2				
		10	30	50	70	90
PERCENT DESIGN SPEED = 79.90		29.150	27.080	25.060	23.020	20.988
CORRECTED WEIGHT FLOW = 70.16		29.088	27.302	25.516	23.730	21.944
CORRECTED ROTOR SPEED = 6685.44		18.350	21.052	22.764	23.664	23.484
PRESSURE RATIO = 1.2621		50.122	53.031	56.082	57.942	60.502
ADIABATIC EFFICIENCY = 88.4093		63.263	60.414	57.140	54.065	50.588
		45.849	40.618	33.765	23.189	11.872
		394.68	402.54	411.21	411.63	412.57
		606.54	618.28	631.56	657.31	670.87
		374.61	375.68	379.18	377.02	378.40
		388.89	371.82	352.41	348.88	330.34
		124.25	144.60	159.11	165.22	164.41
		465.46	493.99	524.10	557.08	583.91
		832.7	760.9	698.8	642.4	596.0
		558.3	489.8	423.9	379.5	337.6
		743.5	661.7	587.0	520.2	460.5
		500.6	318.9	235.6	149.5	69.4
		867.90	806.27	746.13	685.39	624.89
		866.06	812.88	759.70	706.53	653.35
		0.3508	0.3579	0.3659	0.3662	0.3671
		0.5242	0.5369	0.5502	0.5742	0.5870
		0.7401	0.6766	0.6218	0.5716	0.5303
		0.4825	0.4254	0.3693	0.3315	0.2954
		17.414	19.795	23.375	30.876	38.716
		0.0906	0.0534	0.0523	0.0523	0.0925
		0.4748	0.5049	0.5476	0.5731	0.6045
		0.9067	0.9493	0.9551	0.9613	0.9389
		0.9030	0.9474	0.9535	0.9599	0.9368
		0.0223	0.0134	0.0133	0.0136	0.0236
		3.66	3.51	3.44	4.27	5.59
		0.749	1.818	2.965	2.489	3.172
		CORRECTED WEIGHT FLOW				
UPSTREAM OF ROTOR		70.16				
UPSTREAM OF STATOR		70.16				
DOWNSTREAM OF STATOR		66.21				

	STATION 1			STATION 2		
	10	30	50	70	90	90
UIA 3	29.064	27.422	25.672	23.874	22.034	20.202
BETA 2	50.122	50.631	50.062	47.942	45.502	43.062
BETA 3	18.414	18.472	18.537	17.526	16.807	16.087
V 2	66.34	61.26	56.186	51.106	47.027	42.947
V 3	384.72	385.56	374.85	355.71	337.55	319.39
VZ 2	506.85	471.82	432.41	390.88	350.34	310.80
VZ 3	386.58	386.45	372.75	352.32	327.18	302.04
V-THETA 2	465.46	493.59	524.10	557.08	583.91	610.74
V-THETA 3	560.29	550.79	540.76	530.73	520.70	510.67
M 2	0.2242	0.2269	0.2296	0.2322	0.2348	0.2374
M 3	0.2276	0.2322	0.2368	0.2414	0.2460	0.2506
TURN	58.35	54.35	50.35	46.35	42.35	38.35
LUSS COEFF.	0.1333	0.1333	0.1333	0.1333	0.1333	0.1333
DFAC	0.7112	0.6787	0.6462	0.6137	0.5812	0.5487
LUSS PARA.	0.0223	0.0223	0.0223	0.0223	0.0223	0.0223
INCID	1.50	1.50	1.50	1.50	1.50	1.50
DEV	10.546	10.546	10.546	10.546	10.546	10.546

Table IVj.
BLADE ELEMENT PERFORMANCE - SLOTTED STATOR STAGE

		STATION 1 - STATION 2					STATION 2 - STATION 3				
		10	30	50	70	90	10	30	50	70	90
MOTOR 1											
DIA 1		29.150	27.080	25.060	23.020	20.988	22.054	20.974	19.938	18.902	17.866
DIA 2		29.088	27.302	25.516	23.730	21.944	20.158	18.372	16.586	14.800	
BETA 1		18.260	20.421	20.963	22.504	23.034	24.575	26.116	27.657	29.198	
BETA 2		54.355	56.503	59.175	60.232	60.845	61.458	62.071	62.684	63.297	
BETA(PK) 1		65.457	63.335	60.043	56.881	53.313	50.151	47.089	44.027	41.065	
BETA(PK) 2		45.169	40.348	32.415	23.591	10.886	0.000	0.000	0.000	0.000	
V 1		363.69	365.01	378.27	382.07	365.26	348.52	331.78	315.04	298.30	
V 2		620.85	625.71	633.37	654.32	677.54	690.79	704.04	717.29	730.54	
VZ 1		345.38	342.07	353.23	353.00	354.55	365.71	376.87	388.03	399.19	
VZ 2		361.80	345.33	329.67	324.86	330.08	341.24	352.40	363.56	374.72	
V-THETA 1		113.95	127.36	135.33	146.18	150.75	161.60	172.45	183.30	194.15	
V-THETA 2		504.53	521.79	552.49	567.98	591.69	615.40	639.11	662.82	686.53	
V(PR) 1		831.5	762.2	707.4	646.1	593.4	532.6	471.8	411.0	350.2	
V(PR) 2		513.2	453.1	390.5	336.1	281.7	227.3	172.9	118.5	64.1	
V-THETA PR1		756.4	681.2	612.9	541.1	475.9	404.1	332.3	260.5	188.7	
V-THETA PR2		363.9	293.4	209.3	140.5	63.5	0.000	0.000	0.000	0.000	
U 1		870.32	808.52	748.21	687.30	626.63	565.96	505.29	444.62	383.95	
U 2		808.47	815.14	761.82	708.50	655.17	601.84	548.51	495.18	441.85	
M 1		0.3219	0.3231	0.3351	0.3386	0.3415	0.3444	0.3473	0.3502	0.3531	
M 2		0.5329	0.5407	0.5579	0.5689	0.5904	0.6014	0.6124	0.6234	0.6344	
M(PR) 1		0.7361	0.6748	0.6267	0.5725	0.5260	0.4718	0.4176	0.3634	0.3092	
M(PR) 2		0.4405	0.3916	0.3386	0.3078	0.2929	0.2879	0.2829	0.2779	0.2729	
TURN(PR)		20.289	22.987	27.628	33.491	42.427	51.363	60.299	69.235	78.171	
LUSS COEF.		0.1381	0.0441	0.0401	0.0412	0.0629	0.0629	0.0629	0.0629	0.0629	
DFAC		0.5492	0.5735	0.6229	0.6283	0.6146	0.6000	0.5854	0.5708	0.5562	
EFFP		0.8743	0.9618	0.9683	0.9712	0.9620	0.9524	0.9428	0.9332	0.9236	
EFF		0.8689	0.9602	0.9671	0.9701	0.9605	0.9509	0.9413	0.9317	0.9221	
LCSS PARA.		0.0343	0.0111	0.0104	0.0107	0.0161	0.0161	0.0161	0.0161	0.0161	
INCID		5.86	6.43	6.34	7.08	8.31	9.54	10.77	12.00	13.23	
DEV		0.069	1.548	1.615	2.691	2.186	1.671	1.156	0.641	0.126	
CORRECTED WEIGHT FLOW											
UPSTREAM OF ROTOR		65.14									
UPSTREAM OF STATOR		65.14									
DOWNSTREAM OF STATOR		61.11									
PERCENT DESIGN SPEED =		79.96									
CORRECTED WEIGHT FLOW =		65.14									
CORRECTED ROTOR SPEED =		6089.98									
PRESSURE RATIO =		1.2695									
ADIABATIC EFFICIENCY =		82.6022									
STATOR 1											
STATION 2 - STATION 3											
DIA 3		29.164	27.422	25.672	23.922	22.172	20.422	18.672	16.922	15.172	
BETA 2		54.355	56.503	59.175	60.232	60.845	61.458	62.071	62.684	63.297	
BETA 3		-11.228	-2.770	-4.398	-10.002	-25.639	-41.278	-56.917	-72.556	-88.195	
V 2		626.85	625.71	645.37	654.32	677.54	686.49	709.71	718.66	741.88	
V 3		378.75	369.36	367.01	294.61	256.13	183.73	111.33	38.93	-33.47	
VZ 2		361.80	345.33	329.67	324.86	330.08	341.24	352.40	363.56	374.72	
VZ 3		371.51	368.91	366.69	290.14	230.91	161.68	92.45	23.22	-46.01	
V-THETA 2		504.53	521.79	552.49	567.98	591.69	615.40	639.11	662.82	686.53	
V-THETA 3		-73.75	-16.81	-15.36	-51.17	-110.83	-170.49	-229.14	-287.79	-346.44	
M 2		0.5329	0.5407	0.5579	0.5689	0.5904	0.6014	0.6124	0.6234	0.6344	
M 3		0.5200	0.5316	0.5423	0.5501	0.5571	0.5641	0.5711	0.5781	0.5851	
TURN		65.583	59.272	61.575	70.234	86.484	102.733	118.982	135.231	151.480	
LCSS COEF.		0.2178	0.1252	0.1408	0.2014	0.2298	0.2582	0.2866	0.3150	0.3434	
DFAC		0.7640	0.7053	0.7399	0.8592	0.9352	1.0112	1.0872	1.1632	1.2392	
LUSS PARA.		0.0658	0.0486	0.0494	0.0649	0.0626	0.0603	0.0580	0.0557	0.0534	
INCID		2.28	4.56	6.48	6.23	4.89	3.55	2.21	0.87	-0.48	
DEV		7.732	15.270	15.352	7.678	-7.839	-15.698	-23.557	-31.416	-39.275	

Table IVk.
BLADE ELEMENT PERFORMANCE - SLOTTED STATOR STAGE

		STATION 1 - STATION 2				STATION 2 - STATION 3			
		10	30	50	70	10	30	50	70
PERCENT DESIGN SPEED =		89.91							
CORRECTED WEIGHT FLOW =		91.50							
CORRECTED ROTOR SPEED =		7522.68							
PRESSURE RATIO =		1.2006							
ADIABATIC EFFICIENCY =		77.2261							
ROTOR 1									
		29.150	27.080	25.060	23.020	20.988			
U/A 1		29.088	27.302	25.516	23.730	21.944			
U/A 2		20.330	21.682	23.373	25.013	25.013			
BETA 1		39.039	40.801	43.087	44.362	45.906			
BETA 2		55.905	52.595	48.510	44.010	39.933			
BETA(PK) 1		46.637	40.077	32.534	24.017	15.572			
BETA(PK) 2		563.03	571.91	582.75	592.00	594.54			
V 1		670.31	708.11	743.21	780.30	805.14			
V 2		527.96	531.45	532.64	534.89	538.78			
VZ 1		520.64	536.03	542.78	557.87	560.25			
VZ 2		195.61	211.30	236.41	253.68	251.38			
V-THETA 1		422.20	462.70	507.69	545.58	578.26			
V-THETA 2		941.8	874.9	804.0	743.7	702.6			
V(PK) 1		758.3	700.5	643.8	610.7	581.6			
V(PK) 2		779.9	695.0	602.3	516.7	451.0			
VHETA PR1		551.3	451.0	346.2	248.6	156.1			
VHETA PR2		975.55	906.27	838.67	770.40	702.39			
U 1		973.47	913.70	853.93	794.16	734.39			
U 2		0.5075	0.5159	0.5262	0.5350	0.5375			
M 1		0.5884	0.6248	0.6583	0.6937	0.7181			
M 2		0.8489	0.7892	0.7260	0.6722	0.6352			
M(PK) 1		0.6657	0.6181	0.5702	0.5429	0.5187			
M(PK) 2		9.268	12.518	15.977	19.993	24.360			
TURN(PK)		0.1115	0.0768	0.0716	0.0608	0.0377			
LCSS COEF.		0.2805	0.2913	0.2969	0.2812	0.2616			
DFAC		0.8244	0.8905	0.9119	0.9361	0.9644			
EFFP		0.8193	0.8871	0.9092	0.9340	0.9632			
EFF		0.0270	0.0194	0.0185	0.0158	0.0095			
LUSS PARA.		-3.70	-4.31	-5.19	-5.79	-5.07			
INCID		1.537	1.277	1.734	3.317	6.872			
DEV									
CORRECTED WEIGHT FLOW									
UPSTREAM OF ROTOR		91.50							
UPSTREAM OF STATOR		91.50							
DOWNSTREAM OF STATOR		88.45							
ROTOR 2									
		25.034	25.072	25.074	22.034				
DIA 3		40.801	43.087	44.362	45.906				
BETA 2		-1.842	-1.842	-4.824	-13.656				
BETA 3		703.11	743.21	780.30	805.14				
V 2		548.40	569.77	554.86	516.81				
V 3		556.03	542.78	557.87	560.25				
VZ 2		548.12	569.48	552.89	502.20				
VZ 3		462.70	507.07	515.58	578.26				
V-THETA 2		-17.63	-18.31	-46.66	-122.01				
V-THETA 3		6.6248	0.6583	0.6537	0.7181				
M 2		0.4779	0.4964	0.4827	0.4475				
M 3		47.045	43.525	49.186	59.562				
TURN		0.0710	0.0837	0.1439	0.2116				
LCSS COEF.		0.4510	0.4822	0.5371	0.6209				
DFAC		0.0285	0.0405	0.0469	0.0621				
LUSS PARA.		-12.04	-11.54	-9.64	-10.04				
INCID		15.632	16.198	15.908	12.856				
DEV									

Table IVI.
BLADE ELEMENT PERFORMANCE - SLOTTED STATOR STAGE

ROTOR 1
STATION 1 - STATION 2

	10	30	50	70	90
DIA 1	29.150	27.080	25.060	23.020	20.988
DIA 2	29.088	27.302	25.516	23.730	21.944
BETA 1	19.502	21.303	23.137	24.768	26.159
BETA 2	43.324	46.103	48.015	49.821	52.068
BETA(PK) 1	58.135	54.884	51.360	47.221	42.456
BETA(PK) 2	45.911	40.506	32.495	23.655	14.499
V 1	528.13	537.62	544.38	551.13	557.49
V 2	678.53	697.12	731.47	760.06	776.22
VZ 1	497.83	500.66	500.59	500.43	500.38
VZ 2	495.62	483.36	489.31	490.37	477.16
V-THETA 1	176.31	195.84	213.90	230.89	245.78
V-THETA 2	465.56	502.34	543.72	580.71	612.24
V(PK) 1	743.0	870.4	801.7	736.8	678.2
V(PK) 2	709.9	635.7	580.1	535.3	492.9
V-THETA PK1	800.9	712.0	626.2	540.8	457.8
V-THETA PK2	509.6	412.9	311.7	214.8	123.4
U 1	977.20	907.81	840.09	771.70	703.58
U 2	975.12	915.25	855.38	795.51	735.63
M 1	0.4725	0.4814	0.4877	0.4941	0.5001
M 2	0.5882	0.6079	0.6407	0.6685	0.6854
M(PK) 1	0.8437	0.7794	0.7183	0.6605	0.6083
M(PK) 2	0.6150	0.5543	0.5082	0.4708	0.4344
TURN(PK)	12.224	14.378	18.865	23.566	27.957
LOSS COEF.	0.0719	0.0328	0.0101	-0.0036	0.0419
UFAC	0.3566	0.3830	0.3967	0.3991	0.4017
EFFP	0.9109	0.9018	0.9903	1.0043	0.9666
EFF	0.9074	0.9603	0.9900	1.0045	0.9654
LOSS PARA.	0.0176	0.0082	0.0026	-0.0009	0.0106
INCID	-1.46	-2.02	-2.34	-2.58	-2.54
DEV	0.811	1.706	1.695	2.955	5.799

CORRECTED WEIGHT FLOW

UPSTREAM OF ROTOR	87.07
UPSTREAM OF STATOR	87.07
DOWNSTREAM OF STATOR	85.52

PERCENT DESIGN SPEED = 89.69
CORRECTED WEIGHT FLOW = 87.07
CORRECTED ROTOR SPEED = 7004.44
PRESSURE RATIO = 1.2745
ADIABATIC EFFICIENCY = 87.9062

STATOR 1

STATION 2 - STATION 3

	10	30	50	70	90
DIA 3	29.164	27.422	25.672	23.874	22.034
BETA 2	43.324	46.103	48.015	49.821	52.068
BETA 3	-9.474	-2.212	-1.842	-4.824	-14.887
V 1	678.53	697.12	731.47	760.06	776.22
V 3	496.39	501.61	492.34	467.68	431.20
VZ 2	493.62	483.36	489.31	490.37	477.16
VZ 3	485.62	501.43	492.08	466.02	416.73
V-THETA 2	465.56	502.34	543.72	580.71	612.24
V-THETA 3	-81.71	-19.37	-15.82	-39.33	-110.78
M 2	0.5882	0.6079	0.6407	0.6685	0.6841
M 3	0.4241	0.4300	0.4221	0.4002	0.3685
TURN	52.798	46.316	45.857	54.646	66.956
LOSS COEF.	0.1133	0.0662	0.0861	0.1153	0.1305
UFAC	0.5923	0.5622	0.5959	0.6514	0.7259
LOSS PARA.	0.0449	0.0249	0.0303	0.0376	0.0381
INCID	-6.76	-6.04	-4.68	-4.18	-3.88
DEV	9.486	15.828	15.908	12.856	2.913

Table IVm.
BLADE ELEMENT PERFORMANCE - SLOTTED STATOR STAGE

		STATION 1 - STATION 2				
		10	30	50	70	90
ROTOR 1						
DIA 1		29.150	27.000	25.060	23.020	20.980
DIA 2		29.088	27.302	25.516	23.730	21.944
BETA 1		19.315	21.254	22.913	24.704	24.441
BETA 2		47.121	50.289	53.384	54.895	56.026
BETA(PRI) 1		60.613	57.694	54.437	50.149	46.603
BETA(PRI) 2		45.662	40.366	32.759	22.637	13.472
V 1		487.97	495.30	501.74	513.31	512.12
V 2		683.64	698.76	722.37	753.42	761.36
VZ 1		460.51	461.61	462.15	466.33	466.22
VZ 2		465.18	446.45	430.86	433.28	416.60
V-THETA 1		161.40	179.55	195.34	214.53	211.89
V-THETA 2		500.96	537.54	579.82	616.38	637.27
V(PRI) 1		938.5	863.7	794.6	727.7	678.6
V(PRI) 2		665.6	585.9	512.3	469.4	428.4
V-THETA PRI		817.7	730.0	646.4	558.7	493.1
V-THETA PRI 2		476.1	379.5	277.2	180.7	99.8
U 1		979.11	909.58	841.73	773.21	704.96
U 2		977.03	917.04	857.05	797.06	737.07
M 1		0.4355	0.4423	0.4483	0.4590	0.4579
M 2		0.5895	0.6057	0.6265	0.6583	0.6665
M(PRI) 1		0.8376	0.7713	0.7099	0.6508	0.6068
M(PRI) 2		0.5739	0.5079	0.4458	0.4102	0.3750
TURN(PRI)		14.951	17.329	21.678	27.512	33.131
LOSS COEF.		0.0852	0.0596	0.0615	0.0666	0.1118
DFAC		0.4191	0.4555	0.4977	0.5025	0.5196
EFFP		0.9086	0.9406	0.9452	0.9482	0.9205
EFF		0.9044	0.9380	0.9429	0.9460	0.9173
LUSS PARA.		0.0210	0.0150	0.0159	0.0175	0.0283
INCID		1.01	0.79	0.74	0.35	1.60
DEV		0.562	1.566	1.959	1.937	4.772
CORRECTED WEIGHT FLOW						
UPSTREAM OF ROTOR				82.27		
UPSTREAM OF STATOR				82.27		
DOWNSTREAM OF STATOR				78.46		
STATION 2 - STATION 3						
		10	30	50	70	90
DIA 3		29.164	27.422	25.072	23.874	22.034
BETA 2		47.121	50.289	53.384	54.895	56.826
BETA 3		-11.053	-1.842	-1.842	-0.992	-18.450
V 2		683.64	698.76	722.37	753.42	761.36
V 1		453.38	446.30	441.31	423.25	360.81
VZ 2		465.18	456.45	430.66	435.28	416.60
VZ 3		444.97	458.06	441.08	420.10	342.26
V-THETA 2		500.96	537.54	579.82	616.38	637.27
V-THETA 3		-86.92	-14.73	-14.18	-51.52	-14.19
M 2		0.5895	0.6057	0.6265	0.6583	0.6665
M 3		0.3839	0.3898	0.3758	0.3605	0.3064
TURN		58.174	52.131	55.226	61.887	75.276
LOSS COEF.		0.1214	0.0690	0.0753	0.1025	0.1245
DFAC		0.6822	0.6419	0.6782	0.7281	0.8243
LUSS PARA.		0.0478	0.0260	0.0264	0.0333	0.0357
INCID		-4.96	-1.65	0.68	0.90	0.88
DEV		7.907	16.196	15.908	10.688	-0.050

Table IVn.
BLADE ELEMENT PERFORMANCE - SLOTTED STATOR STAGE

ROTOR 1

STATION 1 - STATION 2

	10	30	50	70	90
DIA 1	29.180	27.080	25.060	23.020	20.998
DIA 2	29.088	27.302	25.516	23.730	21.944
BETA 1	19.499	21.311	22.636	24.307	27.116
BETA 2	50.943	54.444	56.315	58.005	58.796
BETA(PR) 1	62.379	59.566	56.464	53.017	48.887
BETA(PR) 2	45.313	40.239	33.280	23.500	11.355
Y 1	458.12	466.22	473.14	476.33	481.78
Y 2	690.57	701.73	715.85	738.58	767.59
YZ 1	431.85	434.33	436.69	434.11	426.22
YZ 2	435.12	408.06	397.03	391.23	397.67
V-THEIA 1	152.92	169.44	182.10	196.07	204.49
V-THEIA 2	536.24	570.89	595.66	626.22	656.54
V(IPR) 1	931.5	857.5	790.4	721.6	643.4
V(IPR) 2	618.7	534.6	474.9	426.6	405.6
V-THEIA PR1	825.2	739.2	658.9	574.4	499.8
V-THEIA PR2	439.9	345.3	260.6	170.1	79.9
U 1	978.22	908.75	849.97	772.51	704.52
U 2	976.14	916.20	856.27	796.33	736.40
M 1	0.4983	0.4157	0.4221	0.4251	0.4301
M 2	0.5937	0.6065	0.6211	0.6434	0.6704
M(IPR) 1	0.8201	0.7846	0.7052	0.6440	0.5922
M(IPR) 2	0.5320	0.4621	0.4121	0.3717	0.3543
TURN(PR)	17.066	15.327	13.183	11.517	10.532
LUSS COEF.	0.0924	0.0672	0.0713	0.0571	0.1081
DFAC	0.4616	0.5282	0.5537	0.5688	0.5335
EFFP	0.9095	0.9303	0.9406	0.9581	0.9319
EFF	0.9821	0.9356	0.9379	0.9363	0.9289
LUSS PARA.	0.0229	0.0169	0.0163	0.0149	0.0276
INCID	2.78	2.67	2.76	3.22	3.89
DEV	0.213	1.439	2.480	2.800	2.655

CORRECTED WEIGHT FLOW

UPSTREAM OF ROTOR	78.64
UPSTREAM OF STATOR	78.64
DOWNSTREAM OF STATOR	74.71

STATOR 1

STATION 2 - STATION 3

	10	30	50	70	90
DIA 3	29.164	27.422	25.672	23.874	22.034
BETA 2	50.943	54.444	56.315	58.005	58.796
BETA 3	-13.483	-2.627	-8.545	-21.136	-31.136
Y 2	690.57	701.73	715.85	738.58	767.59
Y 3	432.38	441.83	426.47	371.17	316.27
YZ 2	435.12	408.06	397.03	391.23	397.67
YZ 3	420.46	447.55	422.83	372.58	294.94
V-THEIA 2	536.24	570.89	595.66	626.22	656.54
V-THEIA 3	-100.81	-15.84	-23.47	-58.64	-113.04
M 2	0.5937	0.6065	0.6211	0.6434	0.6704
M 3	0.3643	0.2798	0.3621	0.3198	0.2671
TURN	64.426	56.571	57.957	54.950	79.932
LUSS COEF.	0.1794	0.0986	0.0817	0.1346	0.1978
DFAC	0.7449	0.6169	0.7083	0.7725	0.8913
LUSS PARA.	0.0701	0.0344	0.0297	0.0435	0.0558
INCID	-1.14	2.20	3.62	4.01	2.85
DEV	5.477	16.013	14.608	8.735	-3.136

Table IVc.
BLADE ELEMENT PERFORMANCE - SLOTTED STATOR STAGE

ROTOR 1

STATION 1 - STATION 2

	10	30	50	70	90
U1A 1	29.150	27.080	25.060	23.020	20.988
U1A 2	29.088	27.302	25.516	23.730	21.944
BETA 1	18.973	20.445	22.756	23.996	23.022
BETA 2	53.187	55.785	59.258	60.199	60.835
BETA(PK) 1	63.739	60.890	58.364	54.786	51.773
BETA(PK) 2	46.157	41.858	34.563	24.138	12.533
V 1	433.58	444.36	443.61	451.24	448.74
V 2	680.88	684.12	702.20	725.27	745.44
VZ 1	410.02	516.37	409.08	412.24	413.00
VZ 2	407.99	394.68	358.95	358.30	363.27
V-THETA 1	140.96	155.22	171.60	183.51	175.50
V-THETA 2	545.11	565.72	603.53	630.70	650.94
V(PK) 1	926.7	855.8	779.9	714.9	667.5
V(PK) 2	589.0	516.5	435.9	392.6	372.1
V-THETA PK1	831.0	747.7	664.0	584.1	524.2
V-THETA PK2	424.8	344.6	267.3	160.6	80.8
U 1	971.98	902.96	835.61	767.58	699.83
U 2	969.92	910.36	850.81	791.26	731.71
M 1	0.3879	0.3978	0.3971	0.4042	0.4019
M 2	0.5858	0.5929	0.6100	0.6326	0.6514
M(PK) 1	0.6289	0.7662	0.6982	0.6403	0.5971
M(PK) 2	0.5067	0.4476	0.3767	0.3424	0.3252
TURN(PK)	17.581	19.032	23.800	30.647	39.238
LOSS COEF.	0.1327	0.0705	0.0921	0.0946	0.1297
UFAC	0.5190	0.5520	0.6050	0.6191	0.6155
EFFP	0.8777	0.9365	0.9284	0.9351	0.9210
EFF	0.8745	0.9334	0.9250	0.9321	0.9171
LOSS PARA.	0.0124	0.0174	0.0233	0.0245	0.0330
INC10	4.14	3.99	4.66	4.99	6.77
DEV	1.057	3.058	3.763	3.438	3.835

CORRECTED WEIGHT FLOW

UPSTREAM OF ROTOR	74.74
UPSTREAM OF STATOR	74.74
DOWNSTREAM OF STATOR	70.63

STATOR 1

STATION 2 - STATION 3

	10	30	50	70	90
U1A 3	29.164	27.422	25.672	23.874	22.034
BETA 2	53.187	55.785	59.258	60.199	60.835
BETA 3	20.060	22.170	24.824	27.128	27.631
V 2	680.88	684.12	702.20	725.27	745.44
V 3	475.78	455.22	402.84	314.53	264.03
VZ 2	407.99	384.68	358.95	358.30	363.27
VZ 3	471.08	454.69	401.41	306.30	233.91
V-THETA 2	545.11	565.72	603.53	630.70	650.94
V-THETA 3	56.71	22.00	32.88	71.49	122.45
M 2	0.5858	0.5929	0.6100	0.6326	0.6514
M 3	0.4028	0.2875	0.2427	0.2664	0.2234
TURN	61.247	58.555	64.082	73.537	84.467
LOSS COEF.	0.1326	0.0572	0.1549	0.2541	0.2762
UFAC	0.6621	0.6583	0.7455	0.8829	0.9593
LOSS PARA.	0.0527	0.0466	0.0523	0.0809	0.0739
INC10	1.11	3.65	6.56	6.40	4.89
DEV	10.900	15.270	14.926	4.562	4.831

Table IVp.
BLADE ELEMENT PERFORMANCE - SLOTTED STATOR STAGE

		STATION 1 - STATION 2			
		10	30	50	70
ROTOR 1					
PERCENT DESIGN SPEED = 100.10					
CORRECTED WEIGHT FLOW = 96.21					
CORRECTED ROTOR SPEED = 3379.15					
PRESSURE RATIO = 1.2265					
ADIABATIC EFFICIENCY = 68.3840					
		STATION 1			
		10	30	50	70
DIA 1		29.150	27.080	25.060	23.020
DIA 2		29.088	27.302	25.516	23.730
BETA 1		22.034	24.912	27.600	28.919
BETA 2		39.802	41.762	44.370	45.167
BETA(PRI) 1		57.152	53.569	49.451	44.856
BETA(PRI) 2		50.805	40.987	32.337	24.203
V 1		601.24	613.02	624.39	634.79
V 2		686.65	775.99	827.42	863.82
VZ 1		557.33	555.98	553.34	555.64
VZ 2		527.53	578.82	591.47	609.04
V-THETA 1		229.56	258.22	289.28	306.97
V-THETA 2		439.55	516.83	578.61	612.59
V(PRI) 1		1027.5	936.2	851.2	783.6
V(PRI) 2		834.7	760.8	700.0	667.7
VTHETA PRI 1		863.2	753.3	646.7	552.9
VTHETA PRI 2		646.9	502.9	374.5	273.8
U 1		1088.79	1011.47	936.02	859.83
U 2		1086.47	1019.77	953.06	886.35
M 1		0.5425	0.5537	0.5647	0.5747
M 2		0.5981	0.6821	0.7313	0.7660
M(PRI) 1		0.9271	0.8457	0.797	0.7096
M(PRI) 2		0.7270	0.6740	0.6107	0.5921
TURN(PRI)		0.347	12.582	17.113	20.653
LOSS COEF.		0.2156	0.1438	0.1205	0.1352
DFAC		0.2618	0.2692	0.2757	0.2493
EFFP		0.6658	0.8145	0.8700	0.8766
EFF		0.6566	0.8081	0.8651	0.8717
LUSS PARA.		0.0480	0.0358	0.0312	0.0350
INCID		-2.45	-3.33	-4.25	-4.94
DEV		5.705	2.187	1.537	3.503
		CORRECTED WEIGHT FLOW			
UPSTREAM OF ROTOR		96.21			
UPSTREAM OF STATOR		96.21			
DOWNSTREAM OF STATOR		93.29			
		STATION 2 - STATION 3			
		10	30	50	70
DIA 3		29.164	27.422	25.672	23.874
BETA 2		39.804	41.762	44.370	45.167
BETA 3		57.098	53.472	49.777	45.277
V 1		686.65	775.99	827.42	863.82
V 2		602.31	602.30	602.30	610.95
VZ 1		527.53	578.82	591.47	609.04
VZ 2		549.20	601.53	633.42	607.28
V-THETA 1		439.55	516.82	578.61	612.59
V-THETA 2		1027.5	936.2	851.2	783.6
M 1		0.5981	0.7313	0.797	0.8457
M 2		0.4725	0.5200	0.5475	0.5277
TURN		45.300	45.374	45.842	45.444
LOSS COEF.		0.0377	0.0322	0.0348	0.0321
DFAC		0.4942	0.4000	0.4270	0.3499
LUSS PARA.		0.0150	0.0351	0.0333	0.0327
INCID		-14.28	-10.38	-9.33	-8.83
DEV		12.562	15.626	16.276	11.403
		CORRECTED WEIGHT FLOW			
UPSTREAM OF ROTOR		96.21			
UPSTREAM OF STATOR		96.21			
DOWNSTREAM OF STATOR		93.29			

Table IVq.
 BLADE ELEMENT PERFORMANCE - SLOTTED STATOR STAGE

		STATION 1 - STATION 2					STATION 2 - STATION 3					
		10	30	50	70	90	10	30	50	70	90	
PERCENT DESIGN SPEED = 100.06												
CORRECTED WEIGHT FLOW = 93.63												
CORRECTED ROTOR SPEED = 0371.61												
PRESSURE RATIO = 1.3621												
ADIABATIC EFFICIENCY = 06.9142												
ROTOR 1 STATION 1 - STATION 2												
DIA 1		29.150	27.080	25.060	23.020	20.988	DIA 3	29.154	27.422	25.072	22.034	
DIA 2		29.088	27.302	25.516	23.730	21.944	BETA 2	48.127	48.759	50.090	52.011	55.576
BETA 1		21.041	23.926	25.813	27.000	26.466	BETA 3	-11.402	-2.027	-1.074	-7.520	0.000
BETA 2		46.127	48.799	50.680	52.611	55.576	V 2	755.39	776.29	804.07	830.85	841.81
BETA(PK) 1		58.073	54.824	51.181	47.196	43.121	V 3	315.77	328.90	340.15	347.70	344.13
BETA(PK) 2		45.988	40.456	32.972	24.170	14.767	VZ 2	523.07	514.28	509.09	504.51	475.88
V 1		586.48	594.26	602.35	607.35	610.60	VZ 3	505.01	528.13	509.87	483.50	424.13
V 2		755.59	776.19	804.67	830.85	841.81	V-THETA 2	544.08	564.00	622.51	600.14	694.39
VZ 1		547.37	543.20	542.25	541.15	546.69	V-THETA 3	-101.97	-18.09	-10.40	-63.68	0.000
VZ 2		523.67	511.28	509.88	504.51	475.88	M 2	0.6523	0.6743	0.6743	0.6743	0.6743
V-THETA 1		241.00	241.00	262.28	275.73	272.16	M(PK) 1	0.9319	0.8495	0.8495	0.8495	0.8495
V-THETA 2		544.68	584.00	622.51	660.14	694.39	M(PK) 2	0.6506	0.5838	0.5838	0.5838	0.5838
V(PK) 1		1035.1	942.9	865.0	796.4	749.0	TURN(PK)	12.085	14.367	18.209	23.026	28.354
V(PK) 2		753.7	671.9	607.8	553.0	492.1	LOSS COEF.	0.0759	0.0471	0.0450	0.0316	0.0015
V-THETA PR1		878.5	770.7	674.0	584.3	512.0	UFAC	0.3864	0.4045	0.4191	0.4333	0.4773
V-THETA PR2		542.0	436.0	330.8	226.4	125.4	EFFP	0.9159	0.9523	0.9595	0.9747	0.9365
U 1		1084.05	1011.71	936.24	860.03	784.11	EFF	0.9115	0.9499	0.9575	0.9735	0.9357
U 2		1086.73	1020.00	953.28	886.55	819.83	LOSS PARA.	0.0186	0.0118	0.0116	0.0082	0.0205
M 1		0.5280	0.5354	0.5431	0.5479	0.5511	INCID	-1.53	-2.08	-2.52	-2.60	-1.88
M 2		0.6523	0.6743	0.6743	0.6743	0.6743	DEV	0.888	1.656	2.172	3.470	0.067
M(PK) 1		0.9319	0.8495	0.8495	0.8495	0.8495	CORRECTED WEIGHT FLOW					
M(PK) 2		0.6506	0.5838	0.5838	0.5838	0.5838	UPSTREAM OF ROTOR			93.63		
TURN(PK)		12.085	14.367	18.209	23.026	28.354	UPSTREAM OF STATOR			93.63		
LOSS COEF.		0.0759	0.0471	0.0450	0.0316	0.0015	DOWNSTREAM OF STATOR			89.86		
UFAC		0.3864	0.4045	0.4191	0.4333	0.4773						
EFFP		0.9159	0.9523	0.9595	0.9747	0.9365						
EFF		0.9115	0.9499	0.9575	0.9735	0.9357						
LOSS PARA.		0.0186	0.0118	0.0116	0.0082	0.0205						
INCID		-1.53	-2.08	-2.52	-2.60	-1.88						
DEV		0.888	1.656	2.172	3.470	0.067						
STATION 2 - STATION 3												
DIA 3		29.154	27.422	25.072	22.034	20.034						
BETA 2		48.127	48.759	50.090	52.011	55.576						
BETA 3		-11.402	-2.027	-1.074	-7.520	0.000						
V 2		755.39	776.29	804.07	830.85	841.81						
V 3		315.77	328.90	340.15	347.70	344.13						
VZ 2		523.07	514.28	509.09	504.51	475.88						
VZ 3		505.01	528.13	509.87	483.50	424.13						
V-THETA 2		544.08	564.00	622.51	600.14	694.39						
V-THETA 3		-101.97	-18.09	-10.40	-63.68	0.000						
M 2		0.6523	0.6743	0.6743	0.6743	0.6743						
M 3		0.9319	0.8495	0.8495	0.8495	0.8495						
TURN		12.085	14.367	18.209	23.026	28.354						
LOSS COEF.		0.0759	0.0471	0.0450	0.0316	0.0015						
UFAC		0.3864	0.4045	0.4191	0.4333	0.4773						
LOSS PARA.		0.0186	0.0118	0.0116	0.0082	0.0205						
INCID		-1.53	-2.08	-2.52	-2.60	-1.88						
DEV		0.888	1.656	2.172	3.470	0.067						

Table IVr.

BLADE ELEMENT PERFORMANCE - SLOTTED STATOR STAGE

ROTOR 1

STATION 1 - STATION 2

	10	30	50	70	90
U1A 1	29.150	27.080	25.060	23.020	20.988
U1A 2	29.088	27.302	25.516	23.730	21.944
BETA 1	22.345	23.386	24.736	26.352	25.902
BETA 2	47.299	49.807	52.020	54.136	56.229
DELTA(PK) 1	58.576	55.529	52.076	47.876	44.186
BETA(PK) 2	45.652	40.168	32.822	24.278	10.428
V 1	574.86	583.37	590.88	599.27	597.89
V 2	700.47	779.26	804.17	824.77	877.97
VZ 1	531.69	535.45	536.66	537.00	537.83
VZ 2	515.73	502.90	494.88	483.20	468.04
V-THETA 1	218.55	231.55	247.25	266.01	261.18
V-THETA 2	558.88	595.26	633.86	668.40	729.82
V(PK) 1	1019.8	946.0	873.2	800.6	750.0
V(PK) 2	737.8	658.1	588.9	530.1	496.2
VTHETA PK1	870.2	779.9	688.8	593.8	522.8
VTHETA PK2	527.6	424.5	319.2	217.9	89.8
U 1	1088.79	1011.47	936.02	859.83	783.93
U 2	1086.47	1019.77	953.06	886.35	819.64
M 1	0.5168	0.5249	0.5321	0.5400	0.5387
M 2	0.6546	0.6753	0.7002	0.7211	0.7331
M(PK) 1	0.9169	0.8512	0.7862	0.7215	0.6758
M(PK) 2	0.6351	0.5703	0.5128	0.4634	0.4370
TURN(PK)	12.924	15.361	19.254	23.599	33.758
LOSS COEF.	0.0819	0.0503	0.0474	0.0687	-0.0158
UFAC	0.3950	0.4283	0.4554	0.4713	0.4887
EFFP	0.9154	0.9211	0.9583	0.9458	1.0123
EFF	0.9108	0.9485	0.9561	0.9431	1.0129
LOSS PARA.	0.0202	0.0127	0.0122	0.0178	-0.0040
INC1U	-1.02	-1.37	-1.62	-1.92	-0.81
DEV	0.552	1.368	2.022	3.578	1.728

CORRECTED WEIGHT FLOW

UPSTREAM OF ROTOR	92.31
UPSTREAM OF STATOR	92.31
DOWNSTREAM OF STATOR	88.44

U1A 1 DESIGN SPEED = 100.00

CORRECTED WEIGHT FLOW = 92.31

CORRECTED ROTOR SPEED = 8367.39

PRESSURE RATIO = 1.3433

ADIABATIC EFFICIENCY = 87.6662

STATOR 1

STATION 2 - STATION 3

	10	30	50	70	90
U1A 3	29.104	27.422	25.872	23.674	22.034
BETA 4	47.299	49.807	52.020	54.135	56.229
BETA 5	-12.272	-1.472	-2.212	-8.591	-20.598
V 2	766.47	775.26	804.17	824.77	877.97
V 3	513.21	521.17	455.32	465.79	398.32
VZ 2	515.73	502.90	454.88	483.20	488.04
VZ 3	501.48	521.00	454.95	480.57	372.86
V-THETA 2	558.88	595.26	633.86	668.40	729.82
V-THETA 3	-105.08	-13.39	-19.12	-69.58	-140.13
M 2	0.6546	0.6753	0.7002	0.7211	0.7331
M 3	0.4319	0.4411	0.4193	0.3542	0.3361
TURN	59.571	51.279	54.252	62.727	76.827
LOSS COEF.	0.1258	0.0745	0.0886	0.0535	0.2226
DFAC	0.6779	0.6255	0.6696	0.7273	0.8457
LOSS PARA.	0.0480	0.0281	0.0311	0.0302	0.0629
INC1U	-4.78	-6.33	-0.68	0.14	0.28
DEV	6.688	16.508	15.558	9.089	-2.798

Table IVs.
 BLADE ELEMENT PERFORMANCE - SLOTTED STATOR STAGE

ROTOR 1

STATION 1 - STATION 2

	10	30	50	70	90
DIA 1	29.150	27.080	25.060	23.020	20.988
DIA 2	29.088	27.302	25.516	23.730	21.944
BETA 1	19.997	23.116	24.736	26.353	24.916
BETA 2	48.591	51.207	53.863	56.467	58.585
DELTA(PK) 1	59.727	50.558	53.250	49.086	45.868
DELTA(PK) 2	45.642	34.964	32.711	24.594	13.154
V 1	557.89	506.65	572.65	581.87	578.13
V 2	751.76	781.85	803.44	815.94	840.56
VZ 1	524.26	521.16	520.11	521.40	524.33
VZ 2	503.85	489.84	473.80	450.74	438.13
V-THETA 1	170.78	222.46	239.62	258.29	243.56
V-THETA 2	571.33	809.39	848.86	680.14	717.34
V(PK) 1	1039.9	945.7	869.3	796.1	753.0
V(PK) 2	720.7	639.1	563.1	495.7	449.9
V(META) PK1	898.1	789.1	696.5	601.6	540.5
V(META) PK2	515.3	410.5	304.3	206.3	102.4
U 1	1086.92	1011.59	936.13	859.93	784.02
U 2	1086.00	1019.88	953.17	886.45	819.73
M 1	0.5002	0.5085	0.5141	0.5228	0.5193
M 2	0.6536	0.6752	0.6970	0.7107	0.7347
M(PK) 1	0.9324	0.8486	0.7804	0.7154	0.6764
M(PK) 2	0.6185	0.5519	0.4885	0.4318	0.3933
TURN(PK)	14.085	16.594	20.539	24.492	32.714
LOSS COEFF.	0.0757	0.0559	0.0574	0.0845	0.0981
DFAC	0.4368	0.4563	0.4906	0.5184	0.5540
EFFP	0.9224	0.9480	0.9518	0.9354	0.9312
EFF	0.9181	0.9451	0.9492	0.9321	0.9278
LOSS PARA.	0.0117	0.0141	0.0148	0.0218	0.0249
INCID	0.13	-0.34	-0.45	-0.71	0.87
DEV	0.542	1.164	1.911	3.894	4.454

CORRECTED WEIGHT FLOW

UPSTREAM OF ROTOR	90.40
UPSTREAM OF STATOR	90.40
DOWNSTREAM OF STATOR	86.42

PERCENT DESIGN SPEED = 99.90
 CORRECTED WEIGHT FLOW = 90.40
 CORRECTED ROTOR SPEED = 6358.52
 PRESSURE RATIO = 1.3996
 ADIABATIC EFFICIENCY = 87.2623

STATOR 1

STATION 2 - STATION 3

	30	50	70	90
DIA 3	29.164	25.672	23.874	22.034
DELTA 2	48.591	53.863	56.467	58.585
BETA 3	-12.619	-2.212	-9.474	-21.675
V 2	764.76	805.44	815.94	840.56
V 3	504.91	515.28	448.11	373.45
VZ 2	505.85	489.84	450.74	438.12
VZ 3	492.71	515.07	441.99	347.05
V-THETA 2	571.33	605.35	680.14	717.34
V-THETA 3	-110.31	-14.90	-73.76	-137.93
M 2	0.5538	0.6752	0.6970	0.7107
M 3	0.4231	0.4544	0.4087	0.3134
TURN	0.1258	0.0753	0.0837	0.1475
LOSS COEFF.	0.6963	0.6418	0.6891	0.8231
DFAC	0.0493	0.0264	0.0270	0.0414
LOSS PARA.	-3.49	-0.92	2.47	2.63
INCID	6.341	10.363	8.200	-3.875
DEV				

Table IVu.

BLADE ELEMENT PERFORMANCE - SLOTTED STATOR STAGE

ROTOR 1

STATION 1 - STATION 2

	10	30	50	70	90
U1A 1	29.150	27.080	25.060	23.020	20.988
U1A 2	19.088	27.302	25.516	23.730	21.944
BETA 1	19.552	21.160	22.658	24.094	22.756
BETA 2	50.989	53.750	57.473	60.294	62.025
BETA(PR) 1	2.738	59.926	57.092	53.409	50.289
BETA(PR) 2	5.541	42.144	37.712	26.285	14.488
V 1	59.740	506.04	509.72	517.80	516.47
V 2	757.84	749.75	746.70	785.24	804.92
VZ 1	667.77	471.92	470.38	472.69	476.27
VZ 2	477.04	443.34	401.50	389.12	377.57
V-THETA 1	166.13	182.67	196.36	211.38	199.78
V-THETA 2	588.86	604.63	629.57	682.04	710.87
V(PR) 1	1021.2	941.8	865.8	793.0	745.4
V(PR) 2	678.7	597.9	507.5	434.0	390.0
VTHETA PR1	907.8	815.0	726.9	636.7	573.4
VTHETA PR2	482.8	401.2	310.5	192.2	97.6
U 1	1073.90	997.64	923.23	848.07	773.21
U 2	1071.62	1005.82	940.02	874.23	808.43
M 1	0.4489	0.4580	0.4615	0.4691	0.4679
M 2	0.6539	0.6518	0.6513	0.6890	0.7081
M(PR) 1	0.9236	0.8524	0.7839	0.7184	0.6753
M(PR) 2	0.5857	0.5198	0.4427	0.3808	0.3431
TURN(PR)	17.397	17.783	19.380	27.124	35.801
LOSS C/JEF.	0.1101	0.0614	0.0736	0.0373	0.0586
UFAC	0.4821	0.5101	0.5613	0.6119	0.6431
EFFP	0.9006	0.9460	0.9398	0.9737	0.9621
EFF	0.8944	0.9428	0.9365	0.9722	0.9601
LOSS PARA.	0.0273	0.0150	0.0179	0.0095	0.0148
INCID	3.14	3.03	3.39	3.61	5.29
DEV	0.241	3.344	6.912	5.585	5.788

CORRECTED WEIGHT FLOW

UPSTREAM OF ROTOR	84.82
UPSTREAM OF STATOR	84.82
DOWNSTREAM OF STATOR	80.81

STATOR 1

STATION 2 - STATION 3

	10	30	50	70	90
DIA 3	29.154	27.422	25.672	23.874	22.034
BETA 2	50.989	53.750	57.473	60.294	62.025
BETA 3	-8.945	-2.398	-6.098	-13.656	-31.452
V 2	757.84	749.75	746.70	785.24	804.92
V 3	542.65	515.63	442.24	324.14	276.58
VZ 2	477.04	443.34	401.50	389.12	377.57
VZ 3	536.05	515.18	439.74	314.98	235.94
V-THETA 2	588.86	604.63	629.57	682.04	710.87
V-THETA 3	-84.37	-21.57	-46.98	-76.53	-144.32
M 2	0.6539	0.6518	0.6513	0.6890	0.7081
M 3	0.4588	0.4363	0.3750	0.2739	0.2333
TURN	59.933	56.148	63.571	73.950	93.478
LOSS COEF.	0.1626	0.1123	0.1464	0.3112	0.3196
UFAC	0.6407	0.6270	0.7263	0.9031	0.9774
LOSS PARA.	0.0645	0.0423	0.0512	0.0589	0.0824
INCID	-1.09	1.61	4.77	6.29	6.08
DEV	10.015	15.642	11.652	4.024	-13.652

Table IVv.
BLADE ELEMENT PERFORMANCE - SLOTTED STATOR STAGE

ROTOR 1

STATION 1 - STATION 2

	10	30	50	70	90
DIA 1	29.150	27.080	25.060	23.020	20.988
DIA 2	29.088	27.302	25.516	23.730	21.944
BETA 1	19.256	21.191	22.949	24.267	24.025
BETA 2	39.931	41.436	43.816	45.744	47.524
BETA(PR) 1	58.439	55.033	51.398	47.332	43.298
BETA(PR) 2	49.438	42.688	34.111	26.833	14.890
V 1	639.66	654.54	665.09	673.50	678.10
V 2	774.82	811.62	884.92	909.06	980.09
VZ 1	603.87	610.28	612.45	613.99	619.36
VZ 2	594.15	608.46	638.53	634.40	661.83
V-THETA 1	210.95	236.60	259.33	276.80	276.08
V-THETA 2	497.34	537.12	612.67	651.09	722.88
V(PR) 1	1153.7	1064.9	981.6	905.9	851.0
V(PR) 2	913.7	841.4	771.2	711.0	664.8
VTHETA PRA	983.1	872.6	767.2	666.1	583.6
VTHETA PR2	694.4	581.2	432.5	320.9	176.0
U 1	1194.02	1109.23	1026.49	942.93	859.69
U 2	1191.48	1118.32	1045.16	972.01	898.85
M 1	0.5802	0.5947	0.6049	0.6132	0.6177
M 2	0.6752	0.7129	0.7807	0.8060	0.8765
M(PR) 1	1.0465	0.9674	0.8929	0.8248	0.7752
M(PR) 2	0.7962	0.7391	0.6803	0.6303	0.6124
TURN(PR)	9.000	11.345	17.288	20.499	28.408
LOSS COEF.	0.2064	0.1772	0.1902	0.1900	0.0987
DFAC	0.2964	0.3001	0.3139	0.3235	0.3200
EFFP	0.6960	0.7553	0.7884	0.8089	0.9152
EFF	0.6850	0.7464	0.7795	0.8009	0.9111
LOSS PARA.	0.0473	0.0423	0.0483	0.0482	0.0248
INCID	-1.16	-1.87	-2.30	-2.47	-1.70
DEV	4.338	4.888	3.311	6.133	6.190

CORRECTED WEIGHT FLOW

UPSTREAM OF ROTOR	99.90
UPSTREAM OF STATOR	99.90
DOWNSTREAM OF STATOR	97.28

STATOR 1

STATION 2 - STATION 3

	10	30	50	70	90
DIA 3	29.164	27.422	25.672	23.874	22.034
BETA 2	39.931	41.436	43.816	45.744	47.524
BETA 3	-10.703	-4.262	-3.328	-5.200	-20.777
V 2	774.82	811.62	884.92	909.06	980.09
V 3	607.67	626.15	674.93	665.15	578.04
VZ 2	594.15	608.46	638.53	634.40	661.83
VZ 3	597.10	624.41	673.79	662.41	540.45
V-THETA 2	497.34	537.12	612.67	651.09	722.88
V-THETA 3	-112.86	-46.53	-39.18	-60.28	-205.05
M 2	0.6752	0.7129	0.7807	0.8060	0.8765
M 3	0.5207	0.5390	0.5812	0.5717	0.4917
TURN	50.635	45.698	47.144	50.544	68.302
LOSS COEF.	0.1385	0.1179	0.1202	0.1256	0.3291
DFAC	0.5320	0.4955	0.4963	0.5242	0.6963
LOSS PARA.	0.0546	0.0443	0.0422	0.0409	0.0929
INCID	-12.15	-10.70	-8.88	-8.26	-8.43
DEV	6.257	13.778	14.422	12.490	-2.977

Table IVw.
BLADE ELEMENT PERFORMANCE - SLOTTED STATOR STAGE

		STATION 1 - STATION 2				
		10	30	50	70	90
PERCENT DESIGN SPEED = 109.87						
CORRECTED WEIGHT FLOW = 99.74						
CORRECTED ROTOR SPEED = 9192.88						
PRESSURE RATIO = 1.3905						
ADIABATIC EFFICIENCY = 80.3394						
ROTOR 1						
		29.150	27.080	25.060	23.020	20.988
DIA 1		29.086	27.302	25.516	23.730	21.944
DIA 2		20.570	21.960	23.763	24.647	24.747
BETA 1		46.043	47.943	49.231	50.522	51.773
BETA(PR) 1		58.157	54.810	51.283	47.178	42.829
BETA(PR) 2		46.736	41.126	32.805	23.462	15.460
V 1		643.45	657.78	665.68	675.73	683.22
V 2		818.94	843.94	868.54	929.24	941.14
VZ 1		602.43	610.06	609.23	614.16	620.48
VZ 2		568.44	565.33	580.23	590.79	582.36
V-THETA 1		226.08	245.99	268.24	281.80	286.01
V-THETA 2		569.53	626.60	672.94	717.25	739.32
V(IPR) 1		1141.8	1058.6	974.1	903.6	846.0
V(IPR) 2		829.4	750.5	690.3	644.0	604.2
V(HEIA) PK1		970.0	865.1	760.0	662.7	575.2
V(HEIA) PR2		604.0	493.6	374.0	256.4	161.1
U 1		1196.05	1111.12	1028.24	944.53	861.16
U 2		1193.51	1120.23	1046.95	973.67	900.38
M 1		0.5825	0.5964	0.6041	0.6139	0.6212
M 2		0.7048	0.7317	0.7753	0.8161	0.8298
M(IPR) 1		1.0237	0.9599	0.8840	0.8209	0.7693
M(IPR) 2		0.7138	0.6507	0.6023	0.5656	0.5327
TURN(PR)		11.420	13.684	18.477	23.717	27.369
LOSS COEF.		0.1626	0.1477	0.1374	0.1243	0.1582
DFAC		0.3866	0.4069	0.4128	0.4150	0.4133
EFFP		0.8172	0.8432	0.8711	0.8957	0.8759
EFF		0.8074	0.8350	0.8642	0.8900	0.8695
LOSS PARA.		0.0393	0.0367	0.0354	0.0324	0.0397
INCID		-1.44	-2.09	-2.42	-2.62	-2.17
DEV		1.636	2.326	2.005	2.762	6.760
CORRECTED WEIGHT FLOW						
UPSTREAM OF ROTOR				99.74		
UPSTREAM OF STATOR					99.74	
DOWNSTREAM OF STATOR						96.29
STATOR 1						
		29.164	27.422	25.672	23.674	22.034
DIA 3		46.043	47.943	49.231	50.522	51.773
BETA 3		-11.828	-2.956	-1.842	-9.650	-20.777
V 2		816.94	843.94	888.54	929.24	941.14
V 3		586.53	613.58	592.95	562.42	511.05
VZ 2		568.44	565.33	580.23	590.79	582.36
VZ 3		569.53	612.76	592.65	554.46	477.82
V-THETA 2		589.53	626.60	672.94	717.25	739.32
V-THETA 3		-140.18	-31.64	-19.06	-94.28	-181.29
M 2		0.7048	0.7317	0.7753	0.8161	0.8298
M 3		0.4944	0.5205	0.5029	0.4764	0.4316
TURN		29.871	20.698	21.073	60.172	72.550
LOSS COEF.		0.1153	0.0456	0.1001	0.1486	0.1651
DFAC		0.6416	0.5668	0.6065	0.6803	0.7525
LOSS PARA.		0.0450	0.0472	0.0352	0.0479	0.0466
INCID		-6.94	-4.20	-3.47	-3.48	-4.18
DEV		5.132	15.084	15.908	8.030	-2.977

Table IVx.
BLADE ELEMENT PERFORMANCE - SLOTTED STATOR STAGE

ROTOR 1

STATION 1 - STATION 2

	10	30	50	70	90
UIA 1	29.150	27.080	25.060	23.020	20.988
UIA 2	29.088	27.302	25.516	23.730	21.944
BETA 1	20.278	21.617	22.924	24.534	24.177
BETA 2	48.560	51.218	52.402	53.447	55.824
BETA(PR) 1	58.192	55.228	51.647	47.521	43.542
BETA(PR) 2	44.321	39.137	32.509	23.534	15.242
V 1	642.23	649.58	660.69	669.27	673.37
V 2	853.42	867.33	884.79	914.57	916.74
VZ 1	602.42	603.89	608.51	608.84	614.31
VZ 2	564.82	543.26	539.83	544.69	514.96
V-THETA 1	222.58	239.31	257.34	277.90	275.78
V-THETA 2	639.77	676.12	701.03	734.68	758.44
V(PR) 1	1143.0	1058.9	980.7	901.6	847.5
V(PR) 2	789.5	700.4	640.1	594.1	533.7
VTHETA PR1	971.3	869.8	769.0	664.9	583.8
VTHETA PR2	551.6	442.1	344.0	237.2	140.3
U 1	1193.89	1109.11	1026.38	942.83	859.60
U 2	1191.35	1118.20	1045.05	971.90	898.76
M 1	0.5824	0.5895	0.6003	0.6087	0.6127
M 2	0.7325	0.7504	0.7706	0.8017	0.8053
M(PR) 1	1.0364	0.9609	0.8910	0.8199	0.7711
M(PR) 2	0.6777	0.6060	0.5575	0.5208	0.4689
TURN(PR)	13.871	16.091	19.138	23.987	28.301
LOSS COEF.	0.1285	0.0965	0.0883	0.0782	0.1479
DFAC	0.4388	0.4719	0.4802	0.4758	0.5065
EFFP	0.8723	0.9084	0.9211	0.9370	0.8872
EFF	0.8640	0.9027	0.9164	0.9333	0.8811
LOSS PARA.	0.0324	0.0247	0.0229	0.0204	0.0372
INCLD	-1.41	-1.67	-2.05	-2.28	-1.48
DEV	-0.779	0.337	1.709	2.834	6.542

CORRECTED WEIGHT FLOW

UPSTREAM OF ROTOR	99.47
UPSTREAM OF STATOR	99.47
DOWNSTREAM OF STATOR	95.74

STATOR 1

STATION 2 - STATION 3

	10	30	50	70	90
UIA 3	29.164	27.422	25.672	23.874	22.034
UIA 2	48.560	51.218	52.402	53.447	55.824
BETA 3	-15.420	-1.472	-2.398	-10.177	-24.736
V 2	653.42	667.33	684.79	914.57	916.74
V 3	556.42	574.50	542.51	502.37	433.51
VZ 4	564.82	543.26	539.83	544.69	514.96
VZ 3	536.39	574.31	542.03	494.46	393.74
V-THETA 2	639.77	676.12	701.03	734.68	758.44
V-THETA 3	-147.95	-14.76	-22.70	-88.77	-181.60
M 2	0.7325	0.7504	0.7706	0.8017	0.8053
M 3	0.4846	0.4842	0.4580	0.4238	0.3642
TURN	63.580	52.690	54.800	63.624	80.560
LOSS COEF.	0.1980	0.1174	0.1129	0.1423	0.1415
DFAC	0.7187	0.6378	0.6745	0.7451	0.8368
LOSS PARA.	0.0767	0.0442	0.0396	0.0458	0.0388
INCLD	-3.92	-0.92	-0.30	-0.55	-0.13
DEV	3.540	16.568	15.352	7.503	-6.936

Table IVy.
 BLADE ELEMENT PERFORMANCE - SLOTTED STATOR STAGE

ROTOR 1

STATION 1 - STATION 2

	10	30	50	70	90
DIA 1	29.150	27.080	25.060	23.020	20.988
DIA 2	29.088	27.302	25.516	23.730	21.944
BETA 1	20.041	21.601	23.042	25.140	24.662
BETA 2	51.366	52.586	55.649	58.274	60.314
BETA(PRI) 1	59.721	56.750	53.472	49.529	45.572
BETA(PRI) 2	45.021	39.720	34.602	27.125	15.923
V 1	610.67	619.85	627.17	633.46	638.31
V 2	845.92	859.33	858.75	866.33	868.31
VZ 1	573.69	576.32	577.14	573.45	580.08
VZ 2	528.15	522.10	484.56	455.56	439.93
V-THETA 1	209.27	228.19	245.48	269.11	266.35
V-THETA 2	660.79	682.53	708.98	736.88	771.72
V(PRI) 1	1137.8	1051.1	969.6	883.5	828.7
V(PRI) 2	747.2	678.8	588.7	511.9	457.5
VHETA PRI	982.6	879.0	779.2	672.1	591.8
VHETA PR2	528.5	433.8	334.3	233.4	125.5
U 1	1191.85	1107.22	1024.63	941.22	858.14
U 2	1189.32	1116.30	1043.27	970.25	897.22
M 1	0.5529	0.5617	0.5688	0.5749	0.5796
M 2	0.7231	0.7417	0.7448	0.7545	0.7760
M(PRI) 1	1.0301	0.9525	0.8793	0.8018	0.7524
M(PRI) 2	0.6387	0.5859	0.5105	0.4458	0.3996
TURN(PRI)	14.700	17.030	18.870	22.404	29.650
LOSS COEF.	0.1136	0.0505	0.0563	0.0759	0.1255
UFAC	0.4840	0.4940	0.5336	0.5617	0.5945
EFFP	0.8951	0.9555	0.9531	0.9424	0.9130
EFF	0.8877	0.9524	0.9501	0.9389	0.9079
LOSS PARA.	0.0283	0.0128	0.0142	0.0192	0.0314
INCID	0.12	-0.15	-0.23	-0.27	0.57
DEV	-0.079	0.920	3.802	6.425	7.223

CORRECTED WEIGHT FLOW

UPSTREAM OF ROTOR	96.65
UPSTREAM OF STATOR	96.65
DOWNSTREAM OF STATOR	92.78

PERCENT DESIGN SPEED = 109.84
 CORRECTED WEIGHT FLOW = 96.65
 CORRECTED ROTOR SPEED = 9190.02
 PRESSURE RATIO = 1.4723
 ADIABATIC EFFICIENCY = 83.6033

STATOR 1

STATION 2 - STATION 3

	10	30	50	70	90
DIA 3	29.164	27.422	25.672	23.874	22.034
BETA 2	51.366	52.586	55.649	58.274	60.314
BETA 3	-14.355	-0.250	-3.514	-11.750	-27.813
V 2	845.92	859.33	858.75	866.33	868.31
V 3	542.74	564.93	521.75	402.93	348.65
VZ 2	528.15	522.10	484.56	455.56	439.93
VZ 3	525.80	504.91	520.77	394.49	308.36
V-THETA 2	660.79	682.53	708.98	736.88	771.72
V-THETA 3	-134.56	-5.42	-31.58	-82.06	-162.67
M 2	0.7231	0.7417	0.7448	0.7545	0.7760
M 3	0.4517	0.4752	0.4394	0.3375	0.2409
TURN	65.721	53.136	55.164	70.025	68.126
LOSS COEF.	0.2400	0.1606	0.1394	0.2246	0.2372
UFAC	0.7300	0.6442	0.6958	0.6440	0.9253
LOSS PARA.	0.0434	0.0605	0.0491	0.0719	0.0634
INCID	-0.71	0.45	2.95	4.27	4.36
DEV	4.605	17.490	14.236	5.930	-10.013

Table IVz.
BLADE ELEMENT PERFORMANCE - SLOTTED STATOR STAGE

NOTOR 1

STATION 1 - STATION 2

	10	30	50	70	90
DIA 1	29.150	27.080	25.060	23.020	20.988
DIA 2	29.088	27.302	25.516	23.730	21.944
BETA 1	20.444	21.766	22.924	24.068	22.924
BETA 2	51.655	52.721	56.184	59.317	62.273
BETA(PRI) 1	60.292	57.126	54.181	50.581	47.022
BETA(PRI) 2	45.723	41.015	36.658	28.350	19.321
V 1	593.73	607.63	610.30	614.88	617.84
V 2	830.61	837.41	831.23	847.83	849.12
VZ 1	556.33	564.31	562.10	561.42	569.05
VZ 2	515.30	507.22	462.61	432.64	395.07
V-THETA 1	207.39	225.32	237.72	250.76	240.65
V-THETA 2	651.44	666.33	690.61	729.14	751.62
V(PRI) 1	1122.6	1039.6	960.5	884.1	834.7
V(PRI) 2	738.1	672.2	576.7	491.6	418.6
VTHETA PRI	975.1	873.1	778.8	683.0	610.7
VTHETA PR2	528.5	441.2	344.4	233.4	138.5
U 1	1182.44	1098.47	1016.53	933.78	851.36
U 2	1179.92	1107.48	1035.03	962.56	890.14
M 1	0.5412	0.5547	0.5573	0.5617	0.5646
M 2	0.7156	0.7287	0.7264	0.7443	0.7459
M(PRI) 1	1.0234	0.9490	0.8770	0.8077	0.7628
M(PRI) 2	0.6359	0.5850	0.5040	0.4315	0.3677
TURN(PRI)	14.569	10.111	17.512	22.230	27.701
LOSS COEF.	0.0836	0.0116	0.0066	0.0016	0.0803
UFAC	0.4828	0.4905	0.5383	0.5884	0.6456
EFFV	0.9235	0.9904	0.9453	0.9998	0.9424
EFF	0.9179	0.9897	0.9950	0.9997	0.9390
LOSS PARA.	0.0206	0.0729	0.0016	0.0004	0.0197
INCID	0.69	0.23	0.48	0.78	2.02
DEV	0.623	2.215	5.868	7.650	10.621

CORRECTED WEIGHT FLOW

UPSTREAM OF ROTOR	94.72
UPSTREAM OF STATOR	94.72
DOWNSTREAM OF STATOR	90.88

STATOR 1

STATION 2 - STATION 3

	10	30	50	70	90
DIA 3	29.164	27.432	25.672	23.874	22.034
BETA 2	51.655	52.721	56.184	59.317	62.273
BETA 3	-14.532	-0.918	-4.075	-12.272	-30.540
V 2	830.61	837.41	831.23	847.83	849.12
V 3	573.21	601.46	489.44	325.48	237.00
VZ 2	515.30	507.22	462.61	432.64	395.07
VZ 3	554.87	601.39	488.20	318.04	204.12
V-THETA 2	651.44	666.33	650.61	729.14	751.62
V-THETA 3	-143.83	-5.64	-34.78	-69.16	-120.43
M 2	0.7150	0.7287	0.7264	0.7443	0.7459
M 3	0.4800	0.5096	0.4130	0.2725	0.1980
TURN	60.188	53.639	60.259	71.589	92.813
LOSS COEF.	0.2418	0.1350	0.2225	0.3880	0.3694
UFAC	0.6944	0.5855	0.7180	0.9240	1.0312
LOSS PARA.	0.0940	0.0506	0.0780	0.1240	0.0961
INCID	-0.42	0.58	3.48	5.32	6.32
DEV	4.428	17.122	13.675	5.408	-12.740

Table IVaa.
BLADE ELEMENT PERFORMANCE - SLOTTED STATOR STAGE

ROTOR 1

STATION 1 - STATION 2

	10	30	50	70	90
JIA 1	29.150	27.080	25.060	23.020	20.988
JIA 2	29.088	27.302	25.516	23.730	21.944
BETA 1	20.444	21.586	23.366	24.608	24.324
BETA 2	53.263	54.461	57.802	60.914	64.369
BETA(PRI) 1	63.090	60.191	57.156	53.782	50.156
BETA(PRI) 2	45.579	42.735	38.511	29.813	19.198
V 1	518.47	551.62	558.83	563.14	565.99
V 2	835.60	819.71	814.67	835.07	845.78
VZ 1	504.55	512.93	513.00	511.99	515.75
VZ 2	499.84	476.46	434.09	405.90	365.86
V-THETA 1	188.09	202.94	221.63	234.50	233.13
V-THETA 2	669.62	667.02	689.38	729.79	762.55
V(PRI) 1	1114.8	1031.8	945.9	866.5	805.0
V(PRI) 2	714.1	648.7	554.8	467.8	387.4
VTHETA PRI	994.1	895.3	794.7	699.1	618.0
VTHETA PR2	510.0	440.2	345.4	232.6	127.4
U 1	1182.18	1098.24	1016.31	933.58	851.17
U 2	1179.67	1107.24	1054.81	962.38	889.94
M 1	0.4881	0.5006	0.5075	0.5116	0.5143
M 2	0.7133	0.7066	0.7062	0.7276	0.7370
M(PRI) 1	1.0105	0.9364	0.8590	0.7872	0.7315
M(PRI) 2	0.6096	0.5592	0.4809	0.4076	0.3376
TUNNIPRI	17.511	17.454	18.646	23.968	30.958
LOSS CUEF.	0.1421	0.0690	0.0420	0.0129	0.0911
DFAC	0.5125	0.5169	0.5392	0.6131	0.6775
EFFP	0.8826	0.9435	0.9680	0.9919	0.9445
EFF	0.8736	0.9394	0.9659	0.9914	0.9409
LOSS PARA.	0.0351	0.0167	0.0101	0.0032	0.0224
INCID	3.49	3.29	3.46	3.98	5.16
DEV	0.479	3.936	7.711	9.113	10.498

CORRECTED WEIGHT FLOW

UPSTREAM OF ROTOR	89.43
UPSTREAM OF STATOR	89.43
DOWNSTREAM OF STATOR	85.64

STATOR 1

STATION 2 - STATION 3

	10	30	50	70	90
DIA 3	29.164	27.422	25.672	23.874	22.034
BETA 2	53.260	54.461	57.802	60.918	64.369
BETA 3	-3.701	-4.449	-8.414	-23.654	-39.349
V 2	835.60	819.71	814.67	835.07	845.78
V 3	709.17	638.04	472.83	306.74	148.44
VZ 2	495.84	476.46	434.09	405.90	365.86
VZ 3	707.69	636.11	467.74	280.97	114.79
V-THETA 2	669.62	667.02	689.38	729.79	762.55
V-THETA 3	-45.78	-49.50	-69.19	-123.07	-94.12
M 2	0.7133	0.7066	0.7062	0.7276	0.7370
M 3	0.5962	0.5393	0.3962	0.2550	0.1232
TURN	55.962	58.911	66.216	84.572	103.719
LOSS COEF.	0.1431	0.1897	0.3860	0.5627	0.6009
DFAC	0.4951	0.5510	0.7470	0.9667	1.1305
LOSS PARA.	0.0574	0.0712	0.1343	0.1685	0.1404
INCID	1.18	2.32	5.10	6.92	8.42
DEV	15.259	13.591	9.336	-5.574	-21.549

DIA 3
BETA 2
BETA 3
V 2
V 3
VZ 2
VZ 3
V-THETA 2
V-THETA 3
M 2
M 3
TURN
LOSS COEF.
DFAC
LOSS PARA.
INCID
DEV

Table IVbb.
BLADE ELEMENT PERFORMANCE - SLOTTED STATOR STAGE

ROTOR 1

STATION 1 - STATION 2

	10	30	50	70	90
PERCENT DESIGN SPEED =	102.79				
CORRECTED WEIGHT FLOW =	88.93				
CORRECTED ROTOR SPEED =	9186.47				
PRESSURE RATIO =	1.5182				
ADIABATIC EFFICIENCY =	74.0116				
STATION 1 - STATION 2					
DIA 1	29.150	27.080	25.060	23.020	20.988
DIA 2	29.088	27.302	25.516	23.730	21.944
BETA 1	19.916	21.278	23.599	24.966	24.244
BETA 2	53.139	54.256	57.825	60.590	63.978
BETA(PRI) 1	63.033	60.279	57.289	53.687	50.316
BETA(PRI) 2	44.194	43.209	38.329	29.415	19.388
V 1	543.27	593.44	559.40	567.11	567.07
V 2	857.65	818.57	821.13	843.11	849.96
VZ 1	510.78	515.36	512.62	514.12	517.02
VZ 2	514.48	478.18	437.25	410.17	372.88
V-TMETHA 1	185.06	201.74	223.93	239.37	232.88
V-TMETHA 2	686.20	644.38	695.03	736.61	763.80
V(PRI) 1	1126.3	1039.5	948.6	868.1	809.7
V(PRI) 2	717.6	656.1	557.4	470.9	395.3
VIMETHA PRI	1003.9	902.8	798.2	699.5	623.2
VIMETHA PR2	500.2	449.2	345.7	231.3	131.2
U 1	1188.93	1104.50	1022.11	938.91	856.02
U 2	1186.40	1113.55	1040.71	967.87	895.02
M 1	0.4898	0.4994	0.5051	0.5124	0.5124
M 2	0.7280	0.7014	0.7070	0.7291	0.7341
M(PRI) 1	1.0155	0.9281	0.8465	0.7844	0.7316
M(PRI) 2	0.6091	0.5622	0.4999	0.4072	0.3414
TURN(PRI)	16.839	17.070	18.960	24.272	30.929
LOSS COEF.	0.1502	0.0796	0.0670	0.0427	0.1894
DFAC	0.5206	0.5129	0.5587	0.6109	0.6700
EFFP	0.8777	0.9342	0.9494	0.9382	0.8990
EFF	0.8882	0.9296	0.9460	0.9254	0.8925
LOSS PARA.	0.0380	0.0191	0.0161	0.0155	0.0416
INC10	3.43	3.38	3.59	3.89	5.32
DEV	-0.906	4.409	7.529	8.715	10.688

CORRECTED WEIGHT FLOW

UPSTREAM OF ROTOR	88.93
UPSTREAM OF STATOR	88.93
DOWNSTREAM OF STATOR	85.13

STATOR 1

STATION 2 - STATION 3

	10	30	50	70	90
DIA 3	29.164	27.422	25.672	23.874	22.034
BETA 2	53.139	54.256	57.825	60.890	63.978
BETA 3	-2.770	-2.888	-10.177	-32.904	-47.232
V 2	857.65	818.57	821.13	843.11	849.96
V 3	712.12	645.37	477.34	305.43	114.65
VZ 4	514.48	478.18	437.25	410.17	372.88
VZ 5	714.29	643.88	469.83	234.30	77.41
V-TMETHA 2	686.20	664.38	655.03	736.61	763.80
V-TMETHA 3	-34.41	-43.78	-84.24	-192.92	-84.27
M 2	0.7280	0.7014	0.7070	0.7291	0.7341
M 3	0.5947	0.5418	0.5372	0.2520	0.0945
TURN	55.909	58.444	68.003	100.794	114.511
LOSS COEF.	0.1638	0.1709	0.3872	0.5712	0.6134
DFAC	0.5071	0.5375	0.7524	0.9994	1.1667
LOSS PARA.	0.0737	0.0642	0.1340	0.1432	0.1251
INC10	1.06	2.12	5.13	6.89	8.03
DEV	16.190	14.152	7.573	-22.224	-29.732